ISSN 1173-5996

An Investigation of the Effects of Sprinklers on Compartment Fires

M W Radford

Supervised by

Dr Charley Fleischmann

Fire Engineering Research Report 96/6
December 1996

This report was presented as a project report
as part of the M.E.(Fire) degree at the University of Canterbury

School of Engineering
University of Canterbury
Private Bag 4800
Christchurch, New Zealand

Phone 643 366-7001
Fax 643 364-2758

ABSTRACT

The effects of automatic sprinklers on compartment fires has been investigated in this report. The interaction of a sprinkler spray with a buoyant hot upper layer has also been examined.

A model was developed to predict the rate of smoke production and hence the depth of a smoke layer that may be produced, for an uncontrolled growing fire. Flow out of vents was included in this model. The model compared well to the predictions of 'Firecalc'.

An method for the prediction of detector actuation has been used that is valid for growing fires, avoiding the quasi-steady assumption used in 'Firecalc' and 'FPEtool'. This method also includes the transport lag time of the fire signature from the source to the detector.

The interaction of a sprinkler spray with a fire induced hot upper layer is a very complex problem. The combining effects of drag induced on the upper layer and evaporative cooling by the sprinkler spray may cause the layer to fall to a lower level.

The model developed to predict the rate of smoke production, hence smoke layer depth, is only valid for uncontrolled fires. Time constraints prevented the effects of sprinklers on compartment fires to be incorporated into this model, although the theory of the effects is included with this report.

Acknowledgments

First and foremost I would like to thank the New Zealand Fire Service Commission who provided the financial support for the Masters of Fire Engineering course.

Thanks to Dr. Charles Fleischmann who was always prepared to listen and give technical support not only with this report, but the entire course. I would like to thank Associate Professor Andy Buchanan for his perseverance in creating the Fire Engineering Masters course. The well being of all the students was a top priority with Andy and this was recognised and very much appreciated.

Thanks to my fellow classmates, Jason Clement, Tom Kardos, Tony Parkes and Michael Belsham for maintaining the ability to laugh when the going got tough. It was always good to know that at times I wasn't the only one in the computer room when the sun was coming up.

I would like to thank Richard Evans and Jeff Crombie who, over the last five years, have had extremely sensitive rubber arms that could be twisted with ease. I couldn't ask for two better mates.

Thanks to my flatmate Shelley Venning for all of her support and understanding during this course.

Finally I would like to thank my family for all of their love and support they have provided me with over the last 23 years. They were always prepared to listen and give me advice when I needed it.

Table of Contents

List of Figures

List of Tables

Nomenclature

A	area (m^2)
A_0	area of opening in compartment (m^2)
A_D	cross sectional area of water drop (m^2)
A_f	area of fire (m^2)
$A_{H,D}$	$g / (c_p T_\infty \rho_\infty)$
A_T	total area of compartment enclosing surfaces (m^2)
b	plume radius (m)
B	buoyancy flux (m^4/s^3)
B_F	buoyancy force of hot upper layer (N)
c	specific heat of compartment surface (m)
c_p	heat capacity of plume gases (J/kg K)
C	orifice constriction coefficient
C_D	drag coefficient
C_E	empirical coefficient of entrainment
C_m	momentum coefficient for sprinklers
C_p	specific heat of air (kJ/kg.K)
C_{SE}	constant for sprinkler spray envelope
D	diameter (m)
D_{cw}	spray cone diameter (m)
D_F	fractional height of thermal discontinuity (Z_D/H_o)
D_D	drag force on water droplet (N)
D_N	sprinkler nozzle diameter (m)
D_w	diameter of single water droplet (m)
D_{wm}	mean diameter of a water droplet (m)
$\dot{f}_w$	flow rate of water (m^3/s)
g	acceleration due to gravity (m/s^2)
h	depth of smoke layer (m)
h_f	specific molar enthalpy of fluid (kJ/kG)
h_g	specific molar enthalpy of gas (kJ/kG)

h_k	effective heat transfer coefficient of compartment lining materials (kW/m.K)
h_w	heat transfer coefficient of water ($W/m^2°C$)
H	ceiling height above fuel source (m)
H_0	height of opening in compartment (m)
ΔH_c	heat of combustion (kJ/kg)
$\Delta H_{c\,air}$	heat of combustion of air, $\Delta Hc/r$, (kJ/kg)
k	thermal conductivity of compartment surface (kW/m.K)
k_1	experimentally derived constant for determining plume centreline velocity ($m^{4/3}/kW^{1/3}.s$)
k_2	experimentally derived constant for determining plume centreline temperature ($m^{5/3}K/kW^{2/3}$)
k_a	thermal conductivity of air (W/m°C)
k_D	drag constant of proportionality (kg/m)
K_c	centreline emission coefficient (m^{-1})
L	mean flame height (m)
L_v	latent heat of vaporisation (kJ/Kg or Kw/l/s)
m_D	mass of drop (kg)
$\dot{m}_d$	mass rate of water evaporation from a single drop (kg/s)
$\dot{m}_f$	mass burning rate of fuel (kg/s)
$\dot{m}_{air}$	mass burning rate of air (kg/s)
$\dot{m}_{ent}$	mass flow rate entrained into the plume (kg/s)
$\dot{m}_{ent,\,L}$	$\dot{m}_{ent}$ at the mean flame height (kg/s)
$\dot{m}_{out}$	gas mass flow leaving the compartment (kg/s)
$\dot{m}_{vf}$	volatile fuel mass flow (kg/s)
$\dot{m}''$	mass loss rate per unit area ($g/m^2.s$)
$\dot{M}$	mass flow rate of jet gases through a section of a sprinkler spray cone
$\dot{M}_P$	mass flow rate in the plume (kg/s)
N_D	number of drops per unit volume from sprinkler spray
N_F	fractional height above neutral plane at door
Nu	Nusselt number

Pr	Prandtl number
q_d	convective cooling between a water droplet and upper layer gases
$\dot{Q}$	total heat release rate (kW)
$\dot{Q}_c$	convective heat release rate, approximately 0.7Q (kW)
$\dot{Q}_p$	heat energy flow in plume (W)
$\dot{Q}(t - t_{act})$	post sprinkler actuation heat release rate of the fire (kW)
$\dot{Q}(t_{act})$	heat release rate at the time of sprinkler actuation (kW)
$\dot{Q}_{TH}$	theoretical heat release rate (kW)
r	radial distance from the axis of the plume (m)
r_p	drop size parameter of sprinkler ($m\ s^{-2/3}$)
R	half-width of Gaussian distribution (m)
R_D	radial distance of detector from plume axis (m)
Re_d	Reynolds number of water droplets
RTI	response time index, $(mc_p)_{detector}/(hA).U_{jet}^{1/2}$, $(m^{1/2}\text{-}s^{1/2})$
t	time (s)
t_{act}	detector actuation time (s)
t_p	thermal penetration time (s)
T_d	temperature of water droplet (K)
$T_{D,\ activation}$	detector actuation temperature (°C)
$T_{D,t}$	detector temperature at time, t (°C)
T_g	upper gas layer temperature (K)
T_{jet_t}	temperature of jet at time, t (°C)
$T_{jet_{t+\Delta t}}$	same as T_{jet_t} but at next time step (°C)
T_p	temperature in the plume (K)
T_{pc}	plume centreline temperature (K)
T_s	temperature in sprinkler spray envelope (K)
T_∞	ambient temperature (K)
ΔT	$T\text{-}T_\infty$, mean temperature rise above ambient (K)
ΔT_g	upper gas temperature rise above ambient, $T_g\text{-}T_\infty$, (K)
ΔT_m	change in plume centreline temperature (K)

U	axial velocity in the plume (m/s)
U_{jet_t}	ceiling jet velocity at time, t (m/s)
U_m	plume centreline axial velocity (m/s)
U_r	radial velocity of entrainment (m/s)
v_f	specific volume of water in the liquid phase (m^3/kg)
v_g	specific volume of water in the gaseous phase (m^3/kg)
V	volume (m^3)
V_D	velocity of water drop (m/s)
V_{Di}	initial water droplet velocity (m/s)
V_r	velocity of water column (m/s)
V_{smoke}	volume of smoke within a compartment (m^3)
$\dot{V}_{ent}$	volume flow rate entrained into the plume (m^3/s)
$\dot{V}_{Remaining}$	volume flow rate remaining within the compartment (m^3/s)
W_e	weber number.
$\dot{w}''$	sprinkler spray density (mm/s)
x	displacement (m)
x_s	displacement from sprinkler head (m)
Z	height above top of combustible (m)
Z_0	height of virtual origin above top of combustible (m)
Z_D	height of thermal discontinuity deep in compartment (m)

Symbols

α	fire growth constant, $Q = at^n$
α'	entrainment coefficient
δ	thickness of compartment surface (m)
μ	absolute coefficient of viscosity (Ns/m^2)
μ_a	absolute coefficient of viscosity of air (Ns/m^2)
μ_w	viscosity of water (kg/ms)
μ_1	viscosity of free stream of air (kg/ms)
ρ	mean density (kg/m^3)
ρ_a	density of air (kg/m^3)

ρ_c	density of compartment surface (kg/m^3)
ρ_p	density of the plume gases (kg/m^3)
$\rho_{U.L}$	density of upper layer in a compartment (kg/m^3)
ρ_w	density of water (kg/m^3)
ρ_∞	ambient density (kg/m^3)
σ	Stephen-Boltzman's constant, ($5.67e^{-8}$ W/m^2K^4)
$\sigma_{\Delta T}$	plume radius to point where $\Delta T/\Delta T_m = e^{-1}$ (m)
σ_u	plume radius to point where $U/U_m = e^{-1}$ (m)
σ_w	surface tension of water droplet
τ	detector time constant, $(mc_p)_{detector}/(hA)$
τ_1	time constant for sprinkler reduced heat release rate, (s)
ϕ	equivalence ratio

Superscripts

*	dimensionless quantity

Chapter 1
Introduction

1.1 Purpose Of Research

At present, the selection of smoke extraction fan size is based on the fire size at the time of sprinkler activation. When sprinklers activate, there will initially be an increase in the rate of smoke production due to the expansion of water to steam. As time progresses, however, the sprinklers will reduce the heat release rate of the fire, hence the net amount of smoke produced will reduce.

Little work has been performed on the effects of automatic sprinklers on smoke production and movement. The purpose of this report is to provide a basis for investigating the effects of automatic sprinklers on fire severity and smoke production.

Due to the exothermic reactions in fires which increase the temperature of the surroundings, there is generally an initial stage where a buoyant gas stream will rise above the fire source into uncontaminated air. The buoyant gas stream is turbulent and the flow of this along with any flames is called the 'Fire Plume'. The fire plume carries the products of combustion which are diluted by entrained air to the ceiling. When the ceiling is reached, the vertical flow of the fire plume turns horizontally and flows under the ceiling to other parts of the compartment or building. If this horizontal flow is obstructed by walls or beams, then a layer of diluted fire products will begin to form beneath the ceiling. This represents the initiation of the hot smoke layer development.

Smoke may be defined as the gaseous products of burning organic materials in which small solid and liquid particles are also dispersed. The rate of entrainment into the fire plume is therefore important when trying to determine the rate of smoke production,

as the contribution from the combustion products to this is negligible compared to the air entrained into the plume.

Extensive research has been performed by many investigators on the effects of steady state fires, but significantly less data is available for growing fires. In reality a fire will not be steady state, but will grow according to a t^2 relationship until it becomes limited by some factor, such as ventilation or exposed fuel surface control.

Various models have been developed, such as 'FPEtool' and 'Firecalc', which are commonly used to predict the entrainment rate of air into the fire plume, hence the rate of smoke production. An independent quasi-steady state model has been developed to predict the rate of smoke production, the depth of the smoke layer in a compartment for a growing fire and detector actuation. This model therefore provides a basis to examine the effects of sprinkler spray on fire severity and smoke production. The results from this independent model are compared to 'FPEtool' and 'Firecalc'.

The potential of this investigation for practical application is quite significant. If under certain conditions it can be shown that the rate of smoke production is ultimately reduced, the rate at which smoke extraction is required may also be reduced. This would reduce the size of the required extraction fans and thus the overall cost.

1.2 Outline Of Report

As the purpose of this project is to provide a basis for the effects of automatic sprinklers on smoke production and heat release rate, Chapter 2 outlines the fundamentals of fire plume theory. Methods to determine the temperature and velocity of the fire plume are examined, as is the mass flow rate of entrainment.
Correlations proposed by two researchers are investigated and compared to the results predicted by 'Firecalc', for the fire plume temperature, velocity and entrainment.

A quasi-steady state two layer zone model using the correlations from Chapter 2 was produced for growing fires. Chapter 3 details the development of this model and how it is used. An arbitrary fire scenario was selected so that the results of this model could be compared to the one room 'HotLayer' model of 'Firecalc'

Chapter 4 investigates detector actuation. The method for predicting detector actuation in 'FPEtool' and Firecalc is the same and is based on a quasi-steady assumption. Another method for predicting detector actuation is examined and recommended, as it is designed for growing fires and incorporates the transport lag time that the fire signature takes to reach the detector.

Chapter 5 investigates the effects of automatic sprinklers on compartment fires. A method for predicting the reduction in heat release rate is proposed. Two effects of sprinkler spray interaction with a fire induced smoke layer are examined, these being the drag effect and the evaporative cooling of the layer, the combination of which may cause smoke logging.

Finally Chapter 6 details the conclusions and recommendations for this investigation.

Chapter 2

Fire PlumeTheory

2.1 Introduction

Due to the exothermic reactions in fires which increase the surrounding temperature, there is generally an initial stage where a gas stream will rise above the fire source into uncontaminated air. Under a constant pressure process, the heating of the products of combustion will result in a reduction in density of these gases. It is the difference in density between this gas stream and the surrounding air that induce this stream to rise, as buoyancy force will cause a less dense fluid to rise with respect to its surroundings.

The buoyant gas stream is turbulent, and the flow of this along with any flames is called the *'Fire Plume'*. The fire plume contains three distinct regions which are:

- the continuous region, which always has luminous flame present,
- the intermittent region which has luminous flame present some of the time and,
- the buoyant plume region which contains only products of combustion and entrained air.

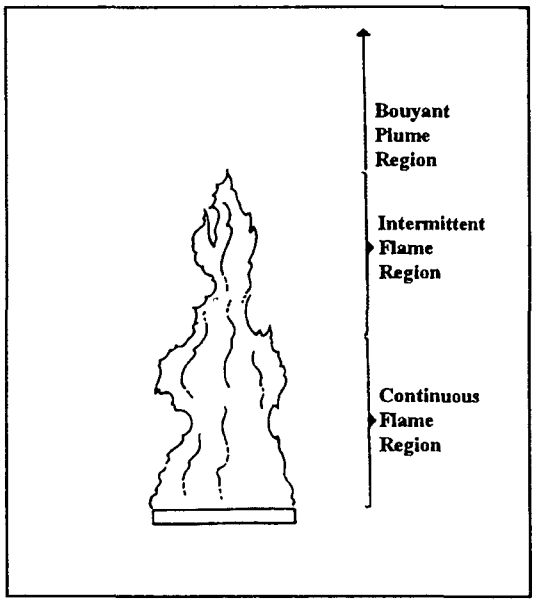

Figure 2.1: Schematic of fire plume regions.

Figure 2.1 shows a schematic diagram of the three distinct regions, adapted from Drysdale (1992). For the remainder of this chapter the buoyant plume will be referred to simply as the 'plume' whereas the 'fire plume' consists of all three regions.

Fire plumes begin at the source of the flame and continue to rise as shown by the dotted lines in Figure 2.2.

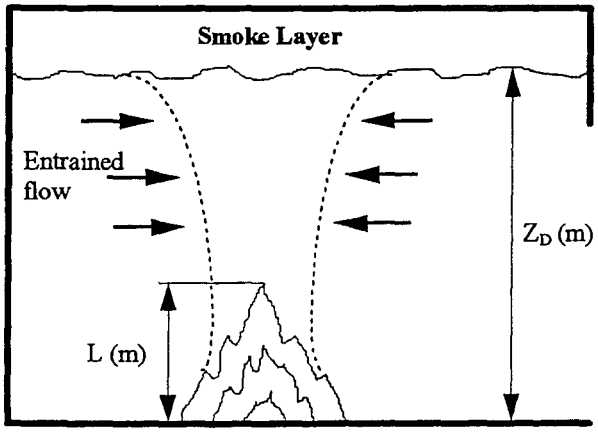

Figure 2.2: Fire in Compartment Showing Entrainment into Plume.

L is the mean flame height and Z_D is the height to the thermal discontinuity where there is a definite separation between a hot upper layer and a cooler lower layer.

As the fire plume rises it entrains air from the surroundings and carries this, as well as the products of combustion to the ceiling. When the ceiling is encountered, which acts as a barrier, a layer of diluted fire products will begin to form, "smoke".

Smoke may be defined as the gaseous products of burning organic materials in which small solid and liquid particles are also dispersed, Gross *et. al.*(1967). The rate of entrainment into the fire plume is therefore important when trying to determine the rate of smoke production. The contribution from the combustion products is negligible compared to the air entrained into the plume, thus the rate of smoke production is a direct function of the air entrained into the fire plume.

The fundamentals of fire plume theory need to be clearly understood before analysis of smoke filling rates can be performed.

This chapter looks at methods for predicting the maximum temperatures and velocities within the fire plume. The entrainment rate of the fire plume for a constant heat release rate is also considered as this provides the basis for smoke production. 'Firecalc' is a common software package used by fire engineers in New Zealand. A model based upon the correlations proposed by Heskestad (1983) and Cox and Chitty (1980 and 1985) has been developed to compare with the predictions of 'Firecalc' for the fire plume temperature, velocity and entrainment.

2.2 Mean Flame Height

The visible flames of a fire represents the region where combustion is occurring.
The mean flame height, L, is defined as the elevation above the source of the fire on the central axis, where the flames appear 50% of the time.
Zukoski *et al.* (1981) performed experiments in which the observations for flame height were photographically recorded. Heskestad (1983) used the results from these to estimate the mean flame height by,

$$L = -1.02D + 0.235\dot{Q}^{2/5} \qquad (2.1)$$

where D is the diameter of the fire (m) and $\dot{Q}$ is the heat release rate (kW).

2.3 Plume Temperature and Velocity

The following section details methods for determining the temperature and velocity within the fire plume.

Plume motion is governed by the equations for conservation of continuity, momentum and buoyancy. If the profiles are assumed to be uniform, Morton *et al.* (1956) showed

these equations to be, respectively,

$$\frac{d}{dz}(b^2u) = 2\alpha' bu \tag{2.2}$$

$$\frac{d}{dz}(b^2u^2) = b^2g\frac{\rho_\infty - \rho}{\rho_\infty} \tag{2.3}$$

$$\frac{d}{dz}\left(b^2ug\frac{\rho_\infty - \rho}{\rho_\infty}\right) = 0 \tag{2.4}$$

direct integration of equation (2.4) gives,

$$\left(b^2ug\frac{\rho_\infty - \rho}{\rho_\infty}\right) = \text{Constant} = B \tag{2.5}$$

Where B is the buoyancy flux within the fire plume and will be constant at all elevations.

The following is the derivation, by the author, to validate equation (2.10) as suggested by Morton *et al.*(1956). From the steady flow energy equation applied to the convective heat in the plume, $\dot{Q}_c$,

$$\dot{Q}_c - \dot{W} = \Delta U + \Delta PE + \Delta KE \tag{2.6}$$

Where U is the internal energy, PE is the Potential Energy and KE is the Kinetic energy.

For systems where the velocity is small and the changes in elevation are negligible, we can ignore the changes in the potential and kinetic energy terms giving:

$$\dot{Q}_c - \dot{W} = \Delta U \tag{2.7}$$

Now for a constant pressure process,

$$W = \int_1^2 PdV = P(V_2 - V_1) \tag{2.8}$$

Thus equation (2.7) becomes,

$$\begin{aligned} \dot{Q}_c &= (U_2 - U_1) + P(V_2 - V_1) \\ &= (U_2 + PV_2) - (U_1 - PV_1) \\ &= H_2 - H_1 \\ &= \Delta H \end{aligned} \tag{2.9}$$

As H=U+PV, where H is the enthalpy.

Knowing that $c_p = \left(\frac{dh}{dT}\right)_p$

gives $\Delta H = \dot{m} c_p \Delta T$

Substituting this into equation (2.9) then yields:

$$\begin{aligned} \dot{Q}_c &= \dot{m} c_p \Delta T \\ &= u\pi b^2 c_p \rho (T - T_\infty) \\ &= u b^2 c_p \pi T_\infty (\rho_\infty - \rho) \end{aligned} \tag{2.10}$$

As $\dot{m} = \rho$ Au and $A=\pi b^2$, where b is the plume radius (m) and from the ideal gas law it can be shown that,

$$\rho(T-T_\infty) = T_\infty(\rho_\infty-\rho) \tag{2.11}$$

When equations (2.5) and(2.10) are combined and re-arranged for the buoyancy flux

the following equation is produced,

$$B = \frac{\dot{Q}_c g}{\rho_\infty \pi c_p T_\infty} \tag{2.12}$$

The conservation equations (2.2) - (2.4), can then be solved to give the centreline velocity and temperature of the plume which have been found to obey the following:

$$U_m = k_1 Z^{-1/3} \dot{Q}^{1/3}$$
$$\Delta T_m = k_2 Z^{-5/3} \dot{Q}^{2/3} \tag{2.13}$$

The value of Z here is the height above the virtual origin to the point of interest, not the actual fuel source, and the constants, k_1 and k_2, have been determined experimentally by various investigators.
A comprehensive list of these constants has been published by Beyler (1986).

Heskestad's correlations for the centreline temperature and velocity of the plume are,

$$\Delta T_m = 9.1\left[\frac{T\infty}{g c_p^2 \rho_\infty^2}\right]^{1/3} \dot{Q}_c^{2/3}(Z - Z_0)^{-5/3} \tag{2.14}$$

$$U_m = 3.4\left[\frac{g}{c_p \rho_\infty T_\infty}\right]^{1/3} \dot{Q}_c^{1/3}(Z - Z_0)^{-1/3} \tag{2.15}$$

Where Z_0 is the height of the virtual origin which will be discussed in the next section. Under normal ambient conditions of $T_\infty = 293K$, $g = 9.81 m/s^2$, $c_p = 1 kJ/Kg.K$ and $\rho_\infty = 1.2\ Kg/m^3$, equations (2.14) and (2.15) simplify to,

$$\Delta T_m = 25\dot{Q}_c^{2/3}(Z - Z_0)^{-5/3} \tag{2.16}$$

$$U_m = 1.03\dot{Q}_c^{1/3}(Z - Z_0)^{-1/3} \tag{2.17}$$

These equations, termed strong plume relations are only valid above the mean flame height and do not hold in the continuous or intermittent flame regions. A strong plume occurs when there is a large temperature increase as a weak plume is defined by $\Delta T/T_\infty << 1$. They also cease to be valid when the plume enters the smoke region, so $Z_{max} = Z_D$. To determine the temperature and velocity within the plume at a location that is not on the centreline the following equations may be used,

$$\Delta T = \Delta T_m \exp\left[-\left(\frac{r}{\sigma_{\Delta T}}\right)^2\right] \tag{2.18}$$

$$U = U_m \exp\left[-\left(\frac{r}{\sigma_u}\right)^2\right] \tag{2.19}$$

where r is the radial distance from the axis of the plume and $\sigma_{\Delta T}$ and σ_u are measurements of the plume width.

An alternative method for determining the centreline temperature and velocity was proposed by Cox and Chitty (1985), who developed correlations for each of the regions shown in Figure 2.1. The conditions that define the three regions of the fire plume are shown Table 2.1.

$\dot{Q}^{2/5}/D$	**Constraint**	**Region**
>10.2	$Z/\dot{Q}^{2/5} > 0.2$	Plume
	$0.08 < Z/\dot{Q}^{2/5} < 0.2$	Intermittent
	$0.03 < Z/\dot{Q}^{2/5} < 0.08$	Continuous
<10.2	$Z/\dot{Q}^{2/5} > 0.12$	Plume
	$0.06 < Z/\dot{Q}^{2/5} < 0.12$	Intermittent
	$0.02 < Z/\dot{Q}^{2/5} < 0.06$	Continuous

Table 2.1: Constraints in determining regions in a fire plume.

Where D is the diameter of the fire (m^2), $\dot{Q}$ is the heat release rate (kW) and Z is the height of the point of interest above the virtual origin (m).

The centreline temperature and velocity correlations for the corresponding regions are:

- *Plume Region*

$$\Delta T_m = 23.9Q^{2/3}(Z - Z_0)^{-5/3} \qquad \text{For } \frac{\dot{Q}^{2/5}}{D} > 10.2 \qquad (2.20)$$

$$U_m = 1.08Q^{1/3}(Z - Z_0)^{-1/3} \qquad \text{For } \frac{\dot{Q}^{2/5}}{D} > 10.2 \qquad (2.21)$$

or

$$\Delta T_m = 20.5Q^{2/3}(Z - Z_0)^{-5/3} \qquad \text{For } \frac{\dot{Q}^{2/5}}{D} < 10.2 \qquad (2.22)$$

$$U_m = 0.89Q^{1/3}(Z - Z_0)^{-1/3} \qquad \text{For } \frac{\dot{Q}^{2/5}}{D} < 10.2 \qquad (2.23)$$

- *Intermittent Region*

$$\Delta T_m = 78Q^{2/5}Z^{-1} \qquad \text{For } \frac{\dot{Q}^{2/5}}{D} > 10.2 \qquad (2.24)$$

$$U_m = 1.85Q^{1/5} \qquad \text{For } \frac{\dot{Q}^{2/5}}{D} > 10.2 \qquad (2.25)$$

or

$$\Delta T_m = 20.5Q^{2/3}(Z - Z_0)^{-5/3} \qquad \text{For } \frac{\dot{Q}^{2/5}}{D} < 10.2 \qquad (2.26)$$

$$U_m = 1.65Q^{1/5} \qquad \text{For } \frac{\dot{Q}^{2/5}}{D} < 10.2 \qquad (2.27)$$

- *Continuous Region*

$$\Delta T_m = 980 \qquad \text{For } \frac{\dot{Q}^{2/5}}{D} > 10.2 \qquad (2.28)$$

$$U_m = 6.83Z^{1/2} \qquad \text{For } \frac{\dot{Q}^{2/5}}{D} > 10.2 \qquad (2.29)$$

or

$$\Delta T_m = 960 \qquad \text{For } \frac{\dot{Q}^{2/5}}{D} < 10.2 \qquad (2.30)$$

$$U_m = 6.83Z^{1/2} \qquad \text{For } \frac{\dot{Q}^{2/5}}{D} < 10.2 \qquad (2.31)$$

Equations (2.16), (2.17) and (2.20-2.31) were used to develop a model for predicting the centreline temperatures and velocities of the fire plume for a given fire size. This model will be discussed later in section 2.7.

2.4 Virtual Origin

The virtual origin, Z_0, is a point source to which the plume at that location will have exactly the same characteristics as the real plume. Figure 2.3 shows a diagrammatical representation for the location of the virtual origin adapted from Drysdale (1992).

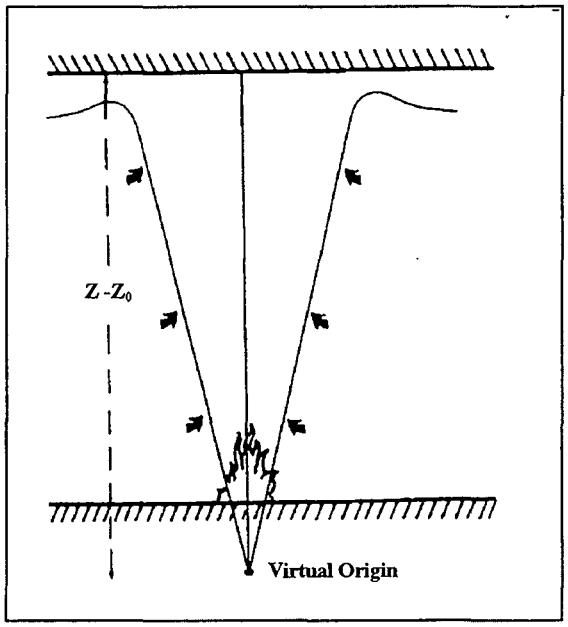

Figure 2.3: Location of the virtual origin

The virtual origin is generally determined from temperature data above the flames along the plume axis. Heskestad (1983) showed that the location of the virtual origin can be approximated by,

$$Z_0 = -1.02D + 0.083\dot{Q}^{2/5} \qquad (2.32)$$

This expression is limited to fire sources that do not have very much in-depth combustion such as high storage racks. For these cases the virtual origin should be taken as the top of the combustible material.

Alternatively, Cox and Chitty (1985) estimate the location of the virtual origin to be,

$$\frac{Z_0}{D} = -0.158\dot{Q}^{2/5} + 15.6\left(0.0607\frac{\dot{Q}^{2/5}}{D}\right)^5 \qquad \text{For } \frac{\dot{Q}^{2/5}}{D} < 10.2 \qquad (2.33)$$

or

$$\frac{Z_0}{D} = 0 \qquad \text{For } \frac{\dot{Q}^{2/5}}{D} > 10.2 \qquad (2.34)$$

Various other correlations derived from experimental data for the location of the virtual origin are available and can again be found in Beyler (1986).

2.5 Entrainment Into The Fire Plume

Once ignition has occurred the fire plume carries the products of combustion that are diluted by entrained air vertically, until an obstacle is encountered such as a ceiling. If the ceiling is confined, a layer will start to form, which will become hotter and thicker with increasing time. This is the formation of the smoke layer.

It should be noted that as the plume rises its temperature will decrease as more, cooler air is entrained.

The mass flow at any given elevation, Z, above the virtual origin, is made up almost entirely of the air that is entrained by the plume from the lower elevations, as the contribution from the products of combustion is negligible.

It can therefore be said that the rate of smoke production is a function of the air entrained into the fire plume. For this reason the measurement of the mass flow rate of entrained air at given elevations is very important.

Heskestad (1983) proposed two correlations for the total mass flow rate of entrainment from experimental data, which are:

- the total mass flow rate of entrainment above the mean flame height, L, is,

$$\dot{m}_{ent} = 0.071\dot{Q}_c^{1/3}(Z - Z_0)^{5/3}.[1 + 0.027\dot{Q}_c^{2/3}(Z - Z_0)^{-5/3}] \qquad (2.35)$$

- the total mass flow rate of entrainment at and below the mean flame height is,

$$\dot{m}_{ent} = 0.0056\dot{Q}_c \frac{Z}{L} \qquad (2.36)$$

where the mean flame height and virtual origin are determined by equations (2.1) and (2.32) respectively.

The entrainment at the mean flame height, L, can be calculated with equation (2.36) by setting Z=L and this is termed $\dot{m}_{ent,L}$.

Equations (2.35) and (2.36) are not valid for elevations where the plume enters the smoke region, therefore the maximum entrainment predicted by these equations will occur at the interface between the upper and lower layer, Z_D.

Alternatively, Cox and Chitty (1980) developed three separate correlations for given conditions to determine the total mass flow rate of entrainment at a given elevation. These are,

- if $(Z/\dot{Q}^{2/5} > 0.2)$,

$$\dot{m}_{ent} = 0.289\dot{Q}\tan^{-1}\left[0.0805\left(\frac{Z}{\dot{Q}^{2/5}}\right)^{-5/3}\right]^{1/2}\cdot\left[\left(\frac{Z}{\dot{Q}^{2/5}}\right)^{5/2} + 0.32\left(\frac{Z}{\dot{Q}^{2/5}}\right)^{3/2} + 0.0256\left(\frac{Z}{\dot{Q}^{2/5}}\right)^{1/2}\right] \quad (2.37)$$

- if $(0.08 < Z/\dot{Q}^{2/5} < 0.2)$,

$$\dot{m}_{ent} = 0.272\dot{Q}\tan^{-1}\left[0.266\left(\frac{Z}{\dot{Q}^{2/5}}\right)^{-1}\right]^{1/2}\cdot\left[\left(\frac{Z}{\dot{Q}^{2/5}}\right)^{5/2} + 0.32\left(\frac{Z}{\dot{Q}^{2/5}}\right)^{3/2} + 0.0256\left(\frac{Z}{\dot{Q}^{2/5}}\right)^{1/2}\right] \quad (2.38)$$

- if $(0.03 < Z/\dot{Q}^{2/5} < 0.08)$

$$\dot{m}_{ent} = 0.284\dot{Q}\tan^{-1}\left[3.34\left(\frac{Z}{\dot{Q}^{2/5}}\right)\right]^{1/2}\cdot\left[\left(\frac{Z}{\dot{Q}^{2/5}}\right)^{5/2} + 0.32\left(\frac{Z}{\dot{Q}^{2/5}}\right)^{3/2} + 0.0256\left(\frac{Z}{\dot{Q}^{2/5}}\right)^{1/2}\right] \quad (2.39)$$

The model developed, (discussed in section 2.7), uses equations (2.35-2.39) to predict the total mass flow rate of entrainment for a given fire size and elevation.

2.6 'Firecalc' Predictions

The computer program 'Firecalc', can be used to predict the temperature, velocity and air entrainment in a fire plume for a given fire size and a specified hot layer height. A sub program called 'PLUME' performs this by using the conservation law equations, except in the flame region where the conservation of energy cannot be used without taking into account chemical reactions.

The flame height with this package is estimated on the basis of the work of McCaffrey (1979) and on experimental data for luminous flame heights measured by

Cetegen *et al.* (1982). Statistical analysis of this data by Cetegen *et al.* led to the following equations which are used in 'PLUME' for determining the flame height,

$$L/D = \left[\frac{3.18\,\dot{Q}}{(\rho_\infty c_p T_\infty g^{1/2} D^{5/2})}\right]^{2/5} \quad \text{for} \quad \frac{\dot{Q}}{(\rho_\infty c_p T_\infty g^{1/2} D^{5/2})} < 0.865$$

$$L/D = \left[\frac{3.3\,\dot{Q}}{(\rho_\infty c_p T_\infty g^{1/2} D^{5/2})}\right]^{0.744} \quad \text{for} \quad \frac{\dot{Q}}{(\rho_\infty c_p T_\infty g^{1/2} D^{5/2})} > 0.865 \qquad (2.40)$$

2.6.1 Derivation of formulae used in 'Firecalc'

The following equations used in the calculation of air entrainment for a given steady state fire and specified hot layer height, have been derived in part by the author to validate the paper by Shestopal and Grubits (1993).

Gaussian profiles for axial temperature and velocity distributions were assumed through the horizontal cross section of the plume. In 'Firecalc' the half-widths of these profiles were assumed to be:

$$U = U_m \exp\left(\frac{-r^2}{R^2}\right)$$

$$T_p - T_\infty = (T_{pc} - T_\infty)\exp\left(\frac{-r^2}{R^2}\right) \qquad (2.41)$$

where r is the radial distance from the axis of the plume, R is the half-width of the Gaussian distribution, T_p is the temperature of the plume and T_{pc} is the centreline temperature in the plume.

Dimensionless parameters of:

$$\psi = (T_{PC} - T_0)/T_0$$

$$\Psi = \ln(1+\psi)/\psi \qquad (2.42)$$

are used to obtain convenient expressions for the results.

An expression for the density of the plume gases is determined using equation (2.41) as shown below.

$$(T_P - T_\infty) = (T_{PC} - T_\infty)\exp\left(\frac{-r^2}{R^2}\right)$$

$$\left(\frac{T_P}{T_\infty}\right)^{-1} = \left[1 + \left(\frac{T_{PC} - T_\infty}{T_\infty}\right)\exp\left(\frac{-r^2}{R^2}\right)\right]^{-1}$$

Now using the ideal gas law, P=ρRT, for a constant pressure process,

$$\rho_P T_P = \rho_\infty T_\infty$$

$$\rho_P = \rho_\infty\left(\frac{T_\infty}{T_P}\right)$$

$$= \rho_\infty\left[\frac{1}{1 + \left(\frac{T_{PC} - T_\infty}{T_\infty}\right)\exp\left(\frac{-r^2}{R^2}\right)}\right]$$

Substitution of equation (2.42) into this gives,

$$\rho_p = \rho_\infty\left[\frac{1}{1 + \psi\exp\left(\frac{-r^2}{R^2}\right)}\right] \qquad (2.43)$$

The expression for the mass flow in the cross section of the plume, from continuity, may then be shown as,

$$\dot{M}_p = \rho_p AU$$

$$= \int \rho_p 2\pi \; r \, U dr$$

$$= 2\pi U_m \rho_\infty \int_0^\infty \frac{\exp\left(\frac{-r^2}{R^2}\right)}{1+\psi \exp\left(\frac{-r^2}{R^2}\right)} r dr \qquad (2.44)$$

now,

$$\frac{d}{dr}\left(1+\psi \exp\left(\frac{-r^2}{R^2}\right)\right) = \frac{-2r}{R^2}\psi \exp\left(\frac{-r^2}{R^2}\right)$$

so

$$\int_0^\infty \frac{\exp\left(\frac{-r^2}{R^2}\right)}{1+\psi \exp\left(\frac{-r^2}{R^2}\right)} r dr = \frac{-R^2}{2\psi} \int_0^\infty \frac{\frac{-2r}{R^2}\psi \exp\left(\frac{-r^2}{R^2}\right)}{1+\psi \exp\left(\frac{-r^2}{R^2}\right)} dr$$

and knowing that,

$$\int_0^\infty \frac{f'(x)}{f(x)} = \ln|f(x)|_0^\infty$$

$$\frac{-R^2}{2\psi} \int_0^\infty \frac{\frac{-2r}{R^2}\psi \exp\left(\frac{-r^2}{R^2}\right)}{1+\psi \exp\left(\frac{-r^2}{R^2}\right)} dr = \frac{-R^2}{2\psi}\left[\ln\left|1+\psi \exp\left(\frac{-r^2}{R^2}\right)\right|\right]_{r=0}^{r=\infty}$$

$$= \frac{-R^2}{2\psi}\left[\ln(1) - \ln(1+\psi)\right]$$

$$= \frac{R^2}{2}\left(\frac{\ln(1+\psi)}{\psi}\right)$$

$$= \frac{R^2 \Psi}{2}$$

Thus the equation for the mass flow in the cross section of the plume becomes,

$$\dot{M}_P = \pi U_m \rho_\infty R^2 \Psi \tag{2.45}$$

The equation for the energy flow in the cross section is given by,

$$\dot{Q}_p = \dot{m} c_p \Delta T \tag{2.46}$$

where,

and $$\dot{m} = \int_0^\infty 2\pi r \rho_p U dr$$

$$\Delta T = T_P - T_\infty$$

$$= (T_{PC} - T_\infty) \exp\left(\frac{-r^2}{R^2}\right)$$

$$= \frac{T_\infty}{T_\infty}(T_{PC} - T_\infty) \exp\left(\frac{-r^2}{R^2}\right)$$

$$= T_\infty \psi \exp\left(\frac{-r^2}{R^2}\right)$$

Therefore equation (2.46) may be expressed as,

$$\dot{Q}_p = \int_0^\infty c_p \rho_p 2\pi r U (T_P - T_\infty)$$

Which after substituting for $(T_P - T_\infty)$, U and ρ_P, from equations (2.41) and (2.43) respectively, becomes,

$$\dot{Q}_p = U_m 2\pi \rho_\infty c_p T_\infty \int_0^\infty \frac{\psi \exp(-r^2/R^2)^2}{1 + \psi \exp(-r^2/R^2)} r dr$$

To solve for the integral in this equation, let $h = \exp(-r^2/R^2)$ so,

$$dh = \frac{-2r}{R^2}\exp(-r^2/R^2)dr$$

$$\text{as } r \to \infty,\ h \to 0$$

$$r \to 0,\ h \to 1$$

so,

$$\int_0^{\infty} \frac{\psi \exp(-r^2/R^2)^2}{1+\psi\exp(-r^2/R^2)} rdr = \frac{-R^2}{2}\int_1^0 \left(\frac{\psi h}{1+\psi h}\right)dh$$

$$= \frac{R^2}{2}\int_0^1 \left(\frac{\psi h + 1 - 1}{1+\psi h}\right)dh$$

$$= \frac{R^2}{2}\int_0^1 \left(1 - \frac{1}{1+\psi h}\right)dh$$

$$= \frac{R^2}{2}\left[h - \frac{1}{\psi}\ln(1+\psi h)\right]_0^1$$

$$= \frac{R^2}{2}\left[\left(1 - \frac{\ln(1+\psi)}{\psi}\right) - 0\right]$$

$$= \frac{R^2}{2}[1-\Psi]$$

The final expression for the energy flow in a cross section of the plume is therefore,

$$\dot{Q}_p = \pi R^2 U_m c_p T_\infty \rho_\infty (1-\Psi) \qquad (2.47)$$

Shestopal and Grubits (1993) misprinted equation (2.47) by not including the heat capacity of the plume gases, c_p, and printing ψ instead of Ψ. This was found to be a typographical error only.

At the flame height, 'Firecalc' assumes the following initial values. The centreline temperature and emission coefficient at the base of the plume are assumed to be equal to that of the flame. R is assumed to be equal to the radius of the fire source and $\dot{Q}_p$ is taken as the source heat release less the radiation losses from the flame, Shestopal and Grubits.

Grouping the common variables in equations (2.43) and (2.45) gives,

$$\pi R^2 U_m \rho_\infty = \frac{\dot{M}_P}{\Psi}$$

$$= \frac{\dot{Q}_p}{T_\infty c_p (1 - \Psi)}$$

which results in an expression for the mass flow rate in the plume as a function of the energy in the plume,

$$\dot{M}_P = \frac{\dot{Q}_p \Psi}{T_\infty c_p (1 - \Psi)} \qquad (2.48)$$

These initial parameters are computed by 'Firecalc' and are then followed by the integration of the following plume equations.

With equation (2.47), the energy conservation law, is,

$$\frac{d}{dz}\left[R^2 U_m (1 - \Psi) = \frac{-2\sigma T_\infty^3 R}{c_p \rho_\infty} \right] f(K_c R, \Psi) \qquad (2.49)$$

where the dimensionless function $f(K_c R, \Psi)$ describes the radiation losses from a medium with a Gaussian temperature distribution. The derivation of this may be found in the appendix of the paper written by Shestopal and Grubits, but noting that the first equation (A1) in this paper has been misprinted and does not include the half-width of the Gaussian distribution, R. The equation should read,

$$K = K_c R \exp\left(\frac{-r^2}{R^2}\right) \tag{2.50}$$

Again this is a typographical error as the remainder of the analysis follows with equation (2.50)

Cetegen *et al.* (1982) showed the momentum equation to be,

$$\frac{d}{dz}\int_0^\infty \rho_p U^2 r dr = g\int_0^\infty (\rho_\infty - \rho_p)\, r dr$$

if viscous forces are neglected and temperature differences are small.

When the momentum equation is integrated and equations (2.41) and (2.47) are substituted, this simplifies to,

$$\frac{d}{dz}\left(\frac{U_m{}^2 R^2 (1-\Psi)}{\psi}\right) = gR^2 \Psi \psi \tag{2.51}$$

To use the mass conservation law, an assumption regarding the rate of entrainment needs to be made. The relation of radial entrainment velocity to the axial velocity by the entrainment coefficient, C_E, and the density ratio, is described by the equation,

$$\lim_{r \to \infty}(rU_r) = C_E U_m R\left(\frac{\rho_p}{\rho_\infty}\right)^{1/2}$$

thus the mass conservation equation then becomes,

$$\frac{d}{dz}(R^2 U_m \Psi) = 2C_E R U_m \tag{2.52}$$

Equations (2.49), (2.51) and (2.52) can then be used for integration if the entrainment coefficient is known, C_E. Attempts to use a constant value of C_E did not give satisfactory results as a much better fit to the experiments performed by Cetegen *et al.* (1982), has been obtained with a variable entrainment coefficient. It was assumed with this model that C_E depends on the dimensionless parameter,

$$q^* = \frac{T_{PC} - T_\infty}{T_\infty} \frac{U_m}{\sqrt{2gR}}$$

which is proportional to the Froude number and represents a local normalised heat flow. An algebraic equation was determined from the best fit to the results of the experimental data obtained by Cetegen *et al.* (1982). The temperatures from these results were measured in the hot layer, not the plume, so the heat losses from the hot layer were estimated to compute the plume temperatures at the interface height. The resulting expression for the entrainment parameter is,

$$C_E = \frac{q^*(81.5 - 24.5q^* + 30.8q^{*2})}{(1 + 531q^* - 468q^{*2} + 580q^{*3} - 1.537q^{*4} + 0.816q^{*5})}$$

2.6.2 Steps Used In 'Firecalc' For Plume Analysis.

The computation starts by estimating the radiation losses from the flame to the flame height. Equations (2.49), (2.51) and (2.52) are then numerically integrated with respect to z, to give three variables, R, U_m and ψ. Equation (2.42) is then used to determine the temperature. The maximum temperature will be seen in the plume centreline, T_{PC}, and the average temperature is computed as,

$$T_{av} = \frac{\dot{Q}_p}{c_p \dot{M}_P} + T_\infty \qquad (2.53)$$

This is the temperature of the hot layer, due to subsequent mixing of the smoke. The test measurements are often made along the centreline of the plume, so the centreline

temperature values are included in the output for comparison, Shestopal and Grubits. The layout for the output of the program 'PLUME' is shown in Table 2.2.

Program PLUME					
Heat Release 'x' kW Plume height 'x' m Area of fire 'x' m^2 Flame temperature 'x' °C Room temperature 'x' °C Optical density of smoke at the source 1 1/m					
Height m	**Average radius m**	**Average temperature °C**	**Maximum temperature °C**	**Max. axial velocity m/s**	**Flow kg/s**
'y'	'y'	'y'	'y'	'y'	'y'
Temperature at plume height 'y' °C Flow of hot gases, 'y' kg/s, 'y' m^3/s					

Table 2.2: Layout of 'Plume' output in 'Firecalc'.

In Table 2.2 'x' represents inputs from the user and 'y' represents the calculated outputs. It should be noted that only one row of calculated values for the height, radius, temperatures, velocity and flow rate has been shown here, but the output of 'Plume' will always display 16 rows of calculations.

2.7 Comparison Of 'Firecalc' With Fire Plume Correlations

A model was developed so that the correlations for predicting the temperature, velocity and entrainment in the fire plume for a steady state fire, discussed in sections 2.3 and 2.5, could be compared to the output of 'Firecalc', section 2.6.

An arbitrary steady state fire can be input by the user into the model, as can the area of the fire, the height of the plume and the ambient temperature of the room.

The flame temperature used for the 'Firecalc' analysis was based on the correlation

developed by Cox & Chitty (1985), for the continuous flaming region, equations (2.28) and (2.30)

Figures 2.4-2.6 show the comparison of the results from the correlations and the 'Firecalc' output for a steady state heat release rate of 1000kW, a plume height of 10m, a fire area of $5m^2$ and an ambient compartment temperature of 26°C. Sample calculations and a full summary of the output for this example from the model and 'Firecalc' are provided in Appendix A. Two other sample runs with different conditions are also provided in this Appendix.

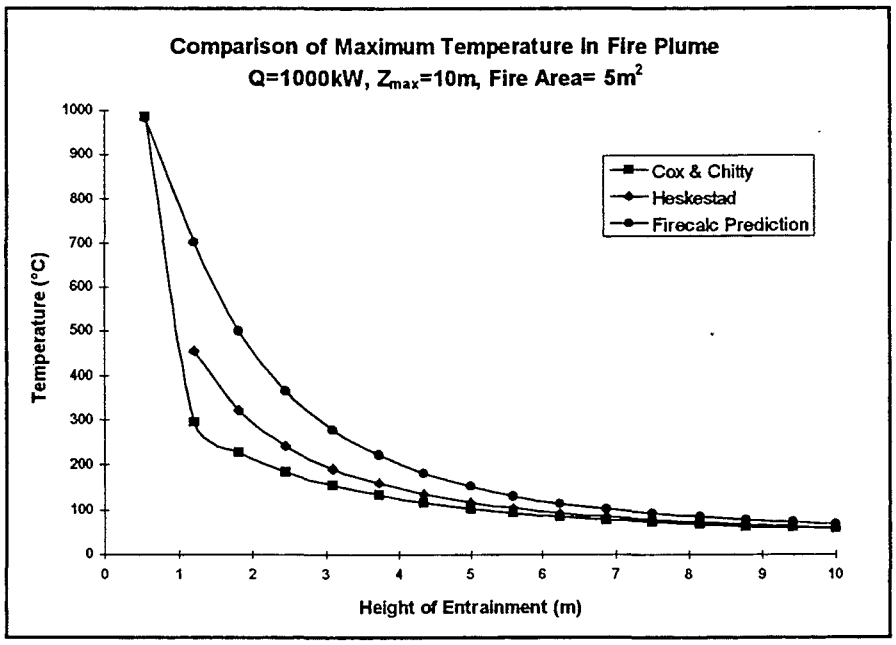

Figure 2.4: Comparison of different methods for determining the maximum temperature in the fire plume.

Figure 2.4 shows the differences between the models for the maximum temperature in the fire plume. A definite relationship is seen with all three predictions for the reduction in temperature of the fire plume with increasing elevation. At lower elevations there is a significant difference with the results of the correlations, but at higher elevations the results converge. The other sample runs provided in Appendix 1 compliment these findings.

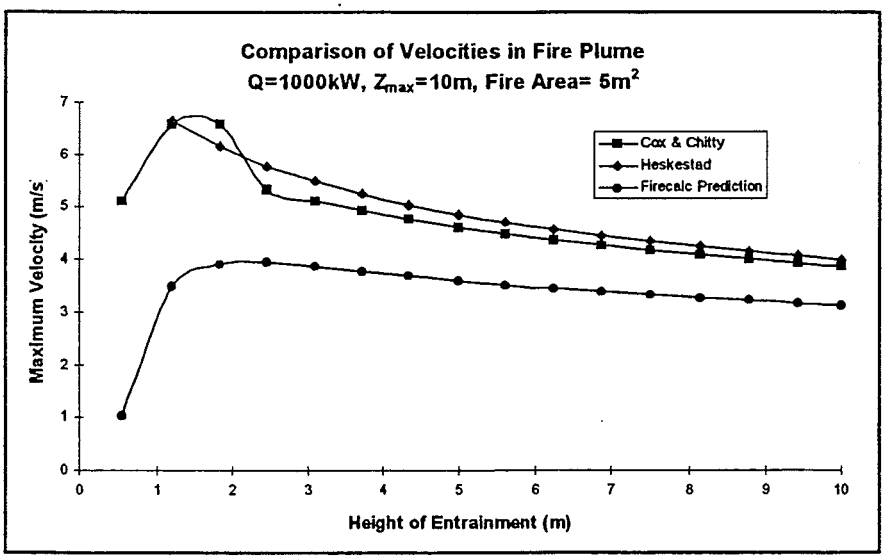

Figure 2.5: Comparison of different methods for determining the maximum velocity in the fire plume.

Figure 2.5 shows a significant difference between the velocities in the fire plume predicted with the correlations proposed by Heskestad and Cox and Chitty, and the velocities predicted by 'Firecalc'. Again, a relationship for the reduction in velocity at increasing elevation for all three models is observed and the findings are complimented with the sample runs in Appendix A.

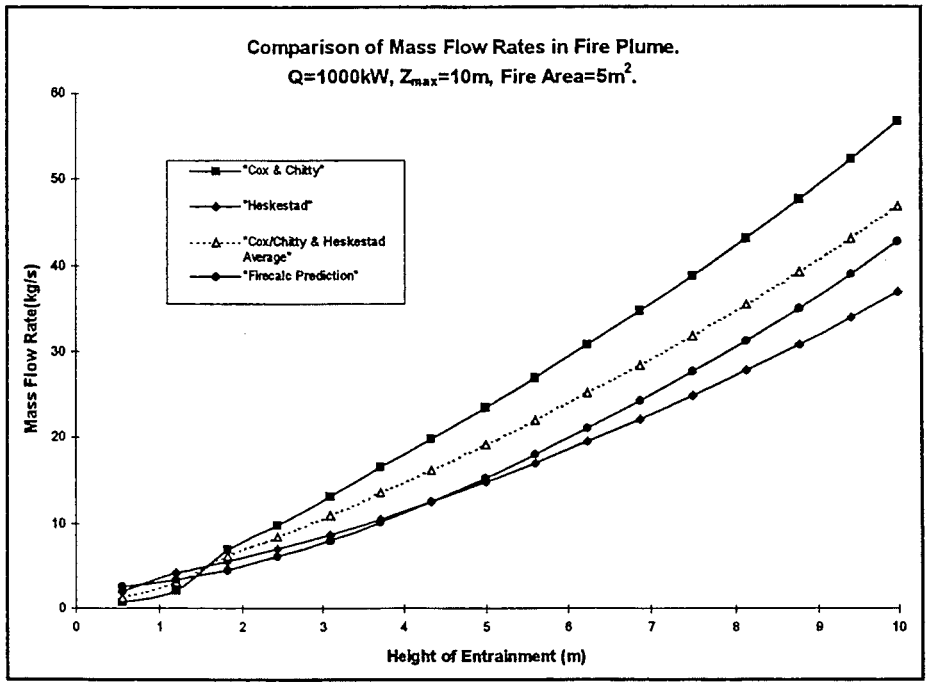

Figure 2.6: Comparison of different methods for determining the mass flow rates in the fire plume.

As can be seen in Figure 2.6, both correlations are in reasonable agreement with the entrainment rate predicted by the 'Firecalc' algorithms. A general observation from the sample runs in Appendix A, is that the Cox and Chitty correlation predicts higher entrainment rates than 'Firecalc' which in turn predicts higher entrainment rates than the correlations proposed by Heskestad.

These figures show that model predictions for the temperature, velocity and entrainment in a fire plume differ according to which correlations are chosen.

Chapter 3

Non Steady State Compartment Fires

3.1 Introduction

Chapter 2 detailed methods to determine the centreline temperature and velocity, and the mass flow rate of entrainment in the fire plume for steady state conditions. For time dependant fires, all of these correlations may still be used, but with the constant heat release rate, $\dot{Q}$, replaced with a time dependant heat release rate, $\dot{Q}(t)$. In making this replacement, a quasi-steady flow has been assumed.

Most fires follow a pattern of distinct phases, although the magnitudes and time scales of these phases may vary quite considerably for different fire conditions. After ignition, the first phase of a fire is the growth period. This is where the fire begins to develop and spread to adjacent fuel. As the fire continues to develop, the temperature within the firecell will rise and all exposed surfaces will be heated by radiation from the flames, the compartment surfaces and, possibly, a hot upper layer. If the temperature in the compartment exceeds approximately 600°C, spontaneous ignition of all exposed surfaces may occur. This is known as flashover. After flashover, the fire will burn in a fully developed phase. If this is left uncontrolled and vents are present, from broken windows or some other means, the fire will continue in this phase until the fuel is consumed and the fire enters the decay phase, Buchanan (1994).

In the early stages of a fire, the growth phase is very important when trying to evaluate the rate of smoke production, height of the smoke layer and conditions within a compartment. If sprinklers are present they will actuate when the fire is in the growth phase and act to reduce the heat release rate. This would significantly reduce any possibility of flashover occurring.

Figure 3.1 shows a typical schematic of the effects of sprinklers on the heat release rate. Chapter 5 looks at the reduction in heat release rate from sprinkler actuation in

more detail.

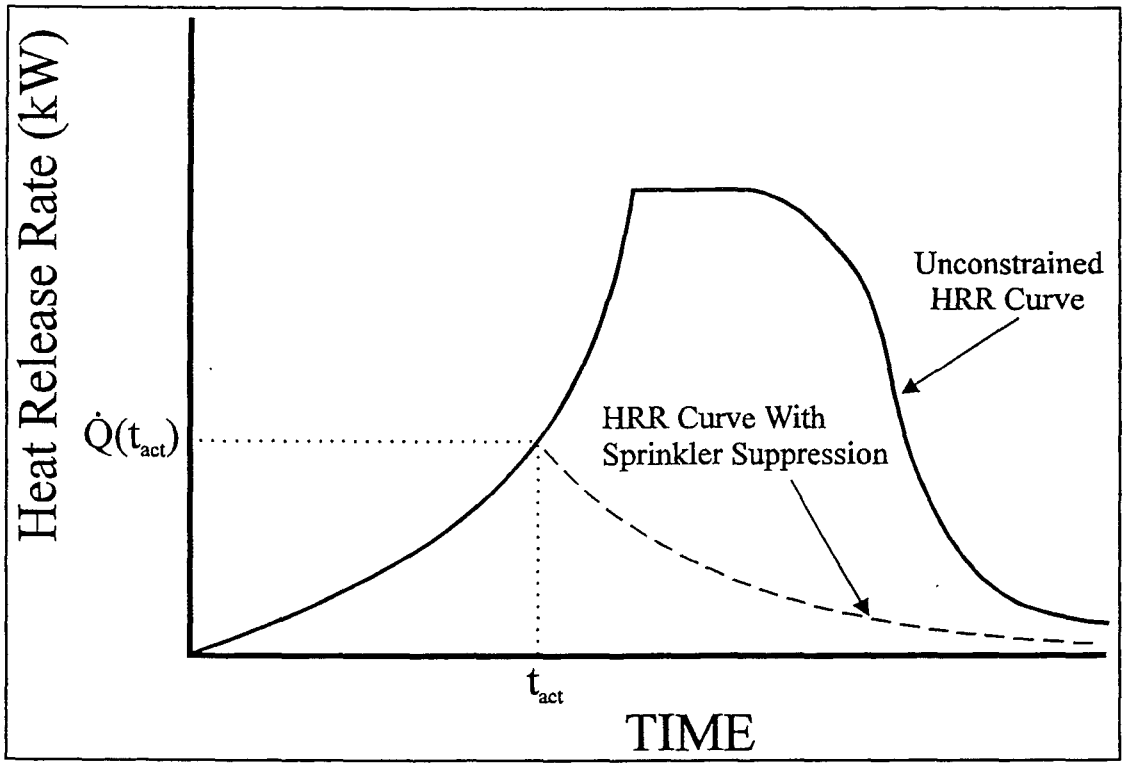

Figure 3.1: Schematic representation of the effects of sprinkler suppression on heat release rate.

A two layer zone model, incorporating Heskestad's correlations from Chapter 2, was developed to predict the temperature of the upper layer, the smoke production within a compartment and thus the height of the smoke layer for a growing fire. Mass flow rate out of vents has been included in the model.

This chapter outlines the development of the model and the correlations used for the predictions. A sub-program in Firecalc called 'HotLayer', computes parameters of a hot layer built up in the course of a single source fire, developing in a compartment which has an opening into unconfined space. The height of the smoke layer, average temperature and mass flow of hot gases from an opening are all computed with this package.

An arbitrary compartment with specified dimensions and wall lining materials was selected so that the predictions of the model developed in this chapter could be compared to those of 'HotLayer', for a growing fire.

3.2 Fire Growth

Most types of fuel may be assumed to have an increasing heat release rate according to a quadratic dependence on time. A factor α is introduced to account for varying fire growth rates.

The heat release rate of a fire may be assumed to grow with a t^2 relationship in the form of,

$$\dot{Q} = \alpha t^2 \tag{3.1}$$

Where α, the fire growth constant, is a function of the type of fire, such as slow, medium, fast and ultra fast. The choice of the growth rate is dependant on the type and arrangement of fuel. Table 3.1 gives the idealised growth rates for t^2 fires, Evans (1992a).

Fire Type	α
Slow	0.00293
Medium	0.01172
Fast	0.0469
Ultra Fast	0.1876

Table 3.1 : Fire types and corresponding α for $\dot{Q} = \alpha t^2$ fires.

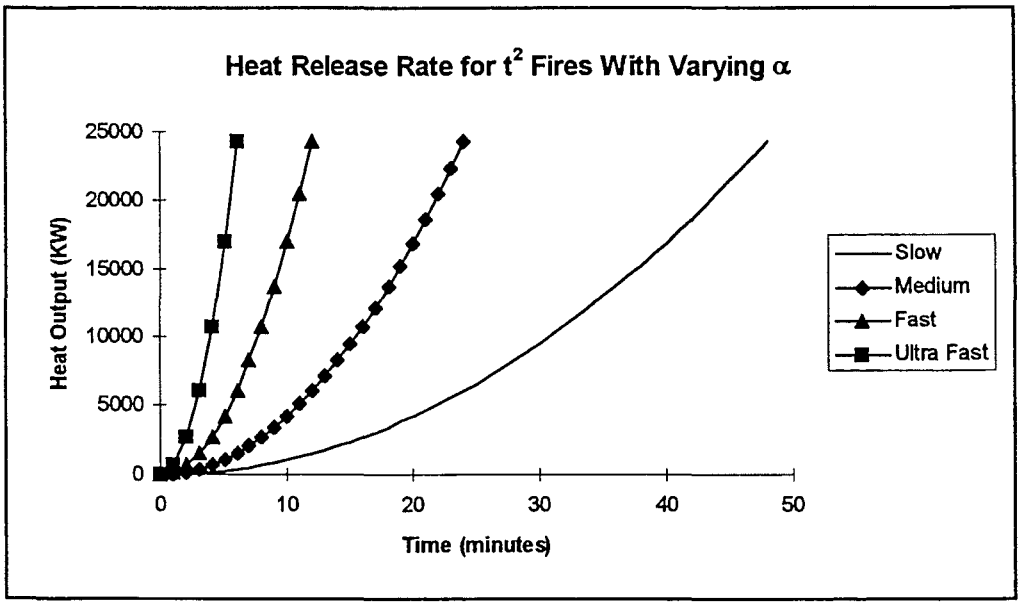

Figure 3.2: Heat output for various fire types.

Figure 3.2 shows how the heat release rate varies with different fire growth constants. The model was designed so that any desired fire growth constant could be selected and the corresponding heat release rate would automatically be calculated for any given time. The model assumes the convective heat release rate to be 70% of the total heat release, that is,

$$\begin{aligned} \dot{Q}_c &= 0.7\dot{Q} \\ &= 0.7\alpha t^2 \end{aligned} \tag{3.2}$$

The mean flame height and virtual origin are both functions of the fire diameter, D, and the heat release rate, Q, which will change with respect to time. As the fire grows the total heat release rate is estimated from equation (3.1), but the diameter of the fire is also required as a function of time.

3.3 Fire Diameter

Tewarson and Pion (1976) provided and alternative method for predicting the heat release rate as,

$$\begin{aligned} \dot{Q} &= \dot{m}''\Delta H_c A_f \\ &= \dot{m}''\Delta H_c\left(\frac{\pi D^2}{4}\right) \end{aligned} \tag{3.3}$$

Where $\dot{m}''$ is the mass loss rate per unit area of fuel, ΔH_c is the heat of combustion of the fuel and A_f is the area of the fire. The mass loss rate per unit area and heat of combustion for various combustibles are given in tables that may be found in Tewarson and Pion (1976) and Drysdale (1992).

Rearrangement of equation (3.3) gives,

$$D = \left(\frac{4\dot{Q}}{\dot{m}''\pi\ \Delta H_c}\right)^{1/2} \tag{3.4}$$

The heat release rate, $\dot{Q}$, determined from equation (3.1), may then be incorporated in equation (3.4) to give an instantaneous fire diameter. With the diameter and heat release rate now known, equations (2.1) and (2.32) from the previous chapter may be used to determine the mean flame height and virtual origin respectively.

3.4 Entrainment Into The Fire Plume

Equations (2.35) and (2.36) proposed by Heskestad (1983), were selected to predict the entrained mass flow rate into the fire plume. The maximum entrainment will occur at the interface between the upper and lower layer as these equations are invalid when the plume enters the smoke layer. Initially there will be no smoke in the compartment, at t=0, so the height, Z, required with equations (2.35) and (2.36) will simply be the height of the room. This height will reduce with the production of a smoke layer.

3.5 Upper Layer Temperature

Once the mass flow rate has been determined it needs to be converted to a volumetric flow rate so that the height of the smoke layer can be evaluated. The temperature of the upper gas layer may be approximated using the method of McCaffrey, Quintiere and Harkeleroid (1981), for pre-flashover compartment fires, which is,

$$\Delta T_g = 480\left(\frac{\dot{Q}}{\sqrt{g}\, c_p \rho_\infty T_\infty A_0 \sqrt{H_0}}\right)^{2/3}\left(\frac{h_k A_T}{\sqrt{g}\, c_p \rho_\infty A_0 \sqrt{H_0}}\right)^{-1/3} \qquad (3.5)$$

Where and h_k is the effective heat transfer coefficient of the wall lining materials, (kW/mK), and A_T is the total area of the compartment enclosing surfaces, (m^2). The effective heat transfer coefficient may be determined by,

$$h_k = \frac{k}{\delta} \qquad \text{for } t > t_p$$

$$h_k = \left(\frac{k\rho_c c}{t}\right)^{1/2} \qquad \text{for } t \le t_p \qquad (3.6)$$

Where t_p is the thermal penetration time, δ is the thickness of the compartment surface and k, ρ_c and c are thermal properties of the lining materials in the compartment.

Table 3.2 gives the thermal properties of some common materials, adapted from Drysdale (1992).

Material	k (W/mK)	ρ_c (kg/m^3)	c (J/kgK)
Gypsum Plaster	0.48	1440	840
Brick (common)	0.69	1600	840
Fibre Insulating Board	0.041	229	2090
Concrete	0.8-1.4	1900-2300	880
Steel (mild)	45.8	7850	460
Glass (plate)	0.76	2700	840

Table 3.2: Thermal properties of selected materials.

The thermal penetration time, t_p, is determined by,

$$t_p = \left(\frac{\rho_c c}{k}\right)\left(\frac{\delta}{2}\right)^2 \tag{3.7}$$

With t_p now known, the effective heat transfer coefficient may be determined from equation (3.6) at any given time, thus the temperature in the upper gas layer can be estimated with equation (3.5).

3.6 Smoke Layer Depth

As the upper layer consists mainly of air from the entrainment into the fire plume, the density of this layer may be approximated by,

$$\rho_{U.L} = \left(\frac{352.8}{T_g}\right) \tag{3.8}$$

Therefore the volumetric entrainment flow rate, (m^3/s), is,

$$\dot{V}_{ent} = \frac{\dot{m}_{ent}}{\rho_{U.L}} = \frac{\dot{m}_{ent}}{\left(\frac{352.8}{T_g}\right)} \tag{3.9}$$

With a known volumetric flow rate for the entrainment, the height of the smoke layer with increasing time can be determined.

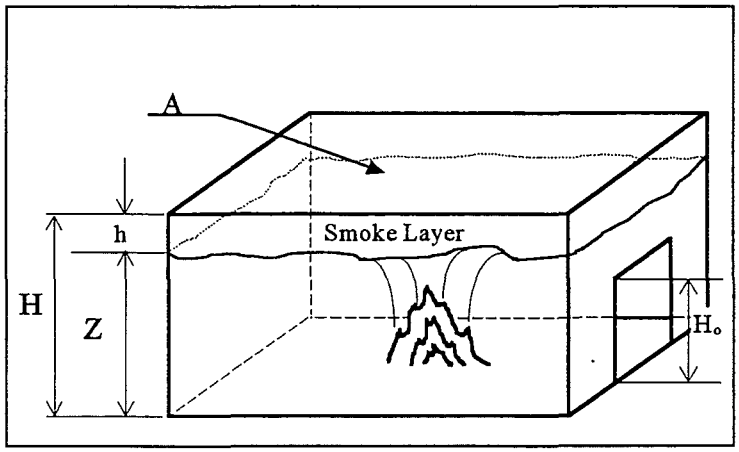

Figure 3.3: Schematic layout of compartment for determination of smoke layer height.

Figure 3.3 shows a compartment with a fire that is producing a smoke layer which will become hotter and thicker with increasing time. The following formulae for the calculation of the smoke layer height, refer to this figure.

As time progresses the volume of smoke will increase, such that at any time, the total smoke volume in the compartment is the sum of the preceding volumetric flow rates if one second intervals are taken, that is,

$$V_{smoke} = \sum_{t=0}^{t=n} \dot{V}_n \tag{3.10}$$

Where n is the time in seconds, with one second intervals.
One second intervals were chosen for the model as the volumetric flow rate is given per second and is not a linear function. If larger intervals were chosen, interpolation

would be required.

As the volumetric flow rate and smoke volume is calculated, if the volume of the room is known, then it is possible to determine the thickness of the smoke layer with respect to time by,

$$V_{smoke} = A_{room} h$$
$$\text{so} \qquad h = \frac{V_{smoke}}{A_{room}} \tag{3.11}$$

The maximum height at which air is entrained into the plume for the next time increment in the model, thus the maximum entrainment of air will then be given by,

$$Z_{(n+1)} = H - h_{(n)}$$
$$= H - \frac{V_{smoke,\,(n)}}{A_{room}} \tag{3.12}$$

This is an iterative process, such that at t = 0s and t = 1s the height, Z, that the mass flow rate of entrained air equations use, (2.35) and (2.36), is the height of the compartment.

As time increases a layer of smoke will be produced, the depth of which is determined from equation (3.11). The maximum height of the smoke plume is then calculated from equation (3.12), and this is the height that the next time increment will use to determine the entrainment rate, the volume of smoke to be added to the existing smoke and the depth of the layer.

Equation (3.12) assumes all of the smoke produced remains within the compartment, but when the layer falls to a level that is lower than the height of any openings, $Z<H_o$, see figure 3.3, then smoke flow out of a compartment needs to be considered.

3.7 Mass Flow Out Of A Compartment

A model, based on a steady state assumption, was proposed by Rockett (1976) to determine the flow rate of the products of combustion leaving through an opening in a compartment as shown in Figure 3.4, where H_o is the height of the opening, Z_N is the height of the 'neutral plane' above the floor and Z_D is the height of the thermal discontinuity above the floor.

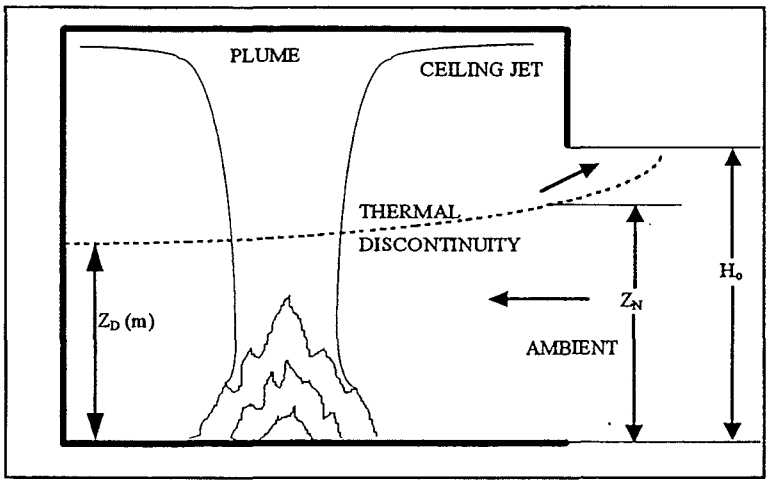

Figure 3.4: Fire Plume and Mass Flow Out Of A Compartment With A Vent.

In this model the gas in the enclosure is assumed to be stably stratified with a layer of fire heated gas above the cool ambient air below. These two layers are separated by a steep thermal gradient, the thermal discontinuity.

As Heskestad's entrainment correlations, equations (2.35) and (2.36), are invalid when the plume enters the smoke region, the maximum entrainment has been assumed to occur at the height of the thermal discontinuity, that is, at $Z=Z_D$.

The 'neutral plane' is the location where the pressure inside and outside the compartment are equal. The gases leave the compartment above the neutral plane and ambient air enters the compartment below it.

The heights of the thermal discontinuity and the neutral plane are not 'fixed' in this model but are set by the fire size. Rockett predicted the gas mass flow leaving an enclosure to be,

$$\dot{m}_{out} = \frac{2}{3}\rho_\infty A_o C\left[2gH_o\frac{T_\infty}{T_g}\left(1-\frac{T_\infty}{T_g}\right)\right]^{1/2}(1-N_F)^{3/2} \qquad (3.13)$$

Where C is the orifice constriction coefficient, usually taken as 0.7, A_o is the area of the opening and N_F is the fractional height of the neutral plane, Z_N/H_o.
If $N_F > 1$, ie $Z_N > H_o$, then $(1-N_F)^{3/2}$ is undefined, but as $Z_N > H_o$, it may be assumed that there is no flow out of the compartment.

The fractional height of the neutral plane for use with equation (3.13), is determined by solving the following equation:

$$\left[\frac{T_\infty}{T_g}\left(\frac{1-N_F}{N}\right)^3\right] = \left(1-\frac{D_F}{N_F}\right)\left(1+\frac{D_F}{2N_F}\right)^2\left(1+\frac{\dot{m}_{vf}}{\dot{m}_{in}}\right)^2 \qquad (3.14)$$

Where D_F is the fractional height of the thermal discontinuity, Z_D/H_O.
Normally $\dot{m}_{vf} \approx \dot{m}_{in}/15 << \dot{m}_{in}$, Rockett (1976), and the model developed for the prediction of the smoke production rate includes this assumption. The heights of the thermal discontinuity neutral plane are evaluated at every time interval, as the fire is growing.

The mass flow out of the compartment may then be determined using equations (3.13) and (3.14), so the depth of the smoke layer may now be accurately predicted taking into account the loss of smoke from the compartment.
The mass flow rate of smoke remaining in the compartment will then be the mass flow rate of entrainment into the plume less the mass flow out, so the volumetric flow rate remaining will be,

$$\dot{V}_{Remaining} = \frac{\dot{m}_{ent} - \dot{m}_{out}}{\rho_{UL}} \qquad (3.15)$$

As the model was written with one second time intervals, the volume of smoke at any time, t(n), in the compartment, accounting for mass flow out of vents, is therefore given by,

$$V_{smoke,(n)} = V_{smoke,(n-1)} + \dot{V}_{Remaining} \qquad (3.16)$$

This may then be used in equation (3.12) to give the elevation of the smoke layer, hence the elevation of the next time increment that the model will use to predict:

- the mass flow rate of entrainment,
- the mass flow rate out of the compartment, and ultimately,
- the depth of the smoke layer.

The model developed is based on a quasi-steady state assumption, thus the method proposed here by Rockett, for steady state conditions, is expected to hold.

3.8 Using The Model

Figure 3.5 shows the input screen that the model displays and it should be noted that this figure also shows the data that was used for the example in section 3.9. All of the information required by the model for analysis needs to be entered here. The following refers to the tables shown in this figure.

Table 1 shows the idealised growth rates for t^2 fires, Evans (1992a), that may be selected by the user for the analysis and the type of combustible to be investigated needs to be specified in Table 2. The compartment dimensions are set in Table 3 and the thermal properties of the lining materials within the compartment are defined in Table 4. The thermal properties of some common materials have been provided in

Table 3.2 of this report. Finally the ambient conditions within the compartment need to be specified in Table 5 of Figure 3.5.

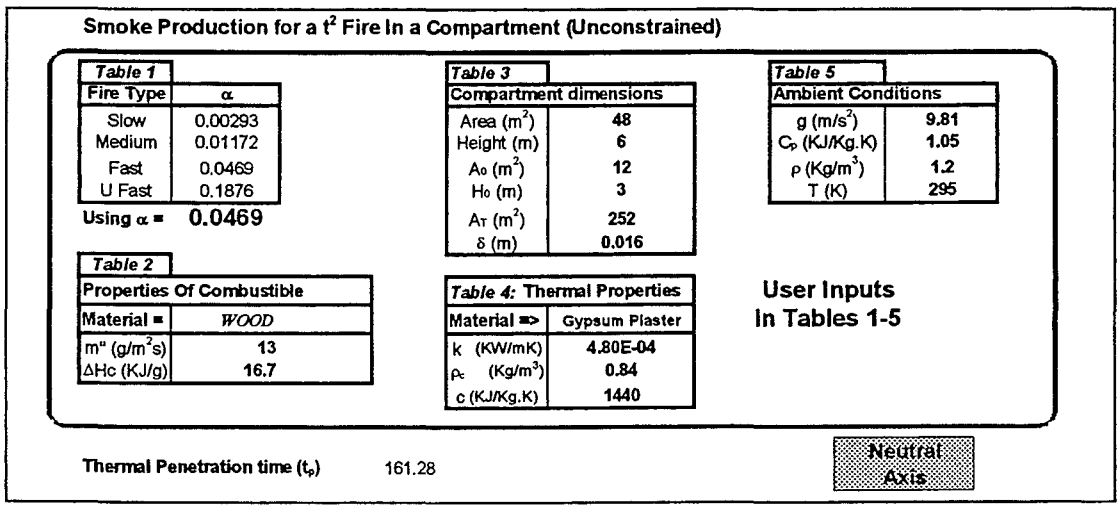

Figure 3.5: Input screen for model developed to predict smoke production for t^2 fires.

When all of the data has been input to Tables 1-5, the fractional height of the neutral plane, N_F, needs to be evaluated, and this is done by selecting the 'Neutral Axis' button. This button will start a sub-program that solves for the fractional height of the neutral plane from equation (3.14). This will then be used in equation (3.13) to determine the mass flow rate out of the compartment.

It is important to note, that if any changes are made in Tables 1-5 of the input screen, the 'Neutral Axis' button must be re-selected for the analysis.

3.9 Comparison Of Model With Firecalc

To compare the results of the model developed from the correlations detailed in this chapter with the predictions of 'HotLayer', a sub-program in Firecalc, an arbitrary fire scenario was selected. In this section, the sub-program 'HotLayer' will simply be referred to as Firecalc. The dimensions of the compartment chosen are shown in Figure 3.6.

Tables 1-5 in Figure 3.5 show the conditions and materials that were selected for this example. Firecalc requires the temperature of the flame to be specified and this was

assumed to be 982°C, from equation (2.30), as T_∞=22 °C. The same heat release rate for the model, from equation (3.1), was used in Firecalc for consistency.

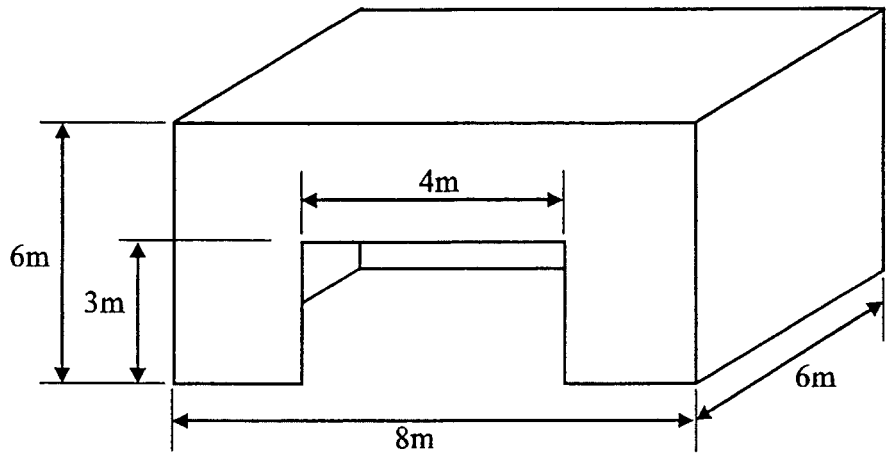

Figure 3.6: Schematic of compartment for model / Firecalc comparison.

Detector actuation will be discussed in Chapter 4 and it will be shown that a fast response sprinkler at a radial distance of 1m for the compartment of Figure 3.6, will actuate at t=177s, see Appendix C. The comparison between the model and Firecalc was performed for pre-sprinkler actuation, so the maximum time for comparison is 177s.

The model and Firecalc predictions for the upper layer gas temperature, mass flow rate out of the compartment and height of the smoke layer are shown in figures 3.7-3.9 respectively. A full summary of the results predicted by the model and some sample calculations are provided in Appendix B, for t=161 and t=162s.

Figure 3.7 shows good agreement between the model and Firecalc predictions for the upper layer gas temperature. A sharp rise in the temperature is observed, however, with the model prediction.

The model predicts the upper layer gas temperature with equation (3.5). This equation is a function of the effective heat transfer coefficient of the compartments lining materials which, in turn, is determined according to the thermal penetration time, equation (3.6). The thermal penetration time for the compartment, with the

conditions specified in Figure 3.5, is 161.28s. This accounts for the relatively large temperature increase between 161 and 162s. Figure 3.7 shows the sharp increase in temperature to begin at 153s, but this is due to the selection of data points from the Firecalc output, see Appendix B.12, as, from above, the actual sharp temperature increase occurs between 161 and 162s.

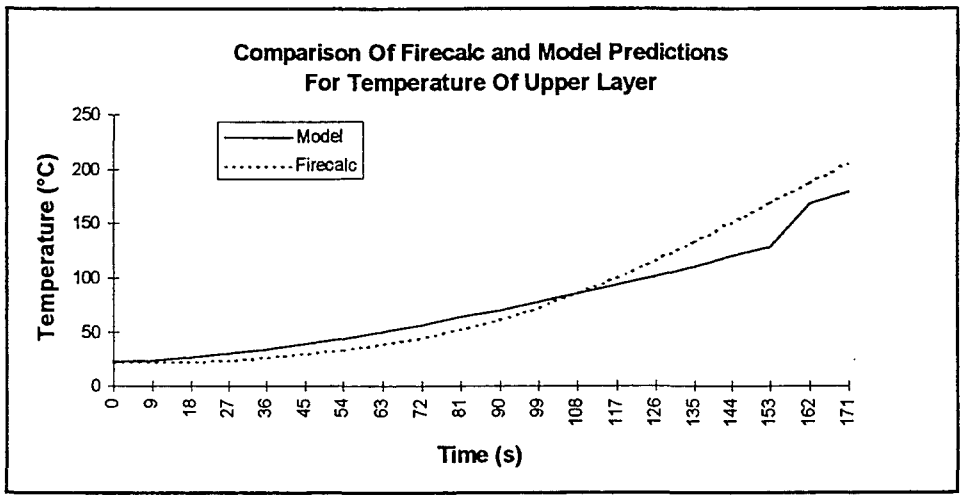

Figure 3.7: Firecalc and model prediction of upper layer gas temperature in the compartment for a fast fire.

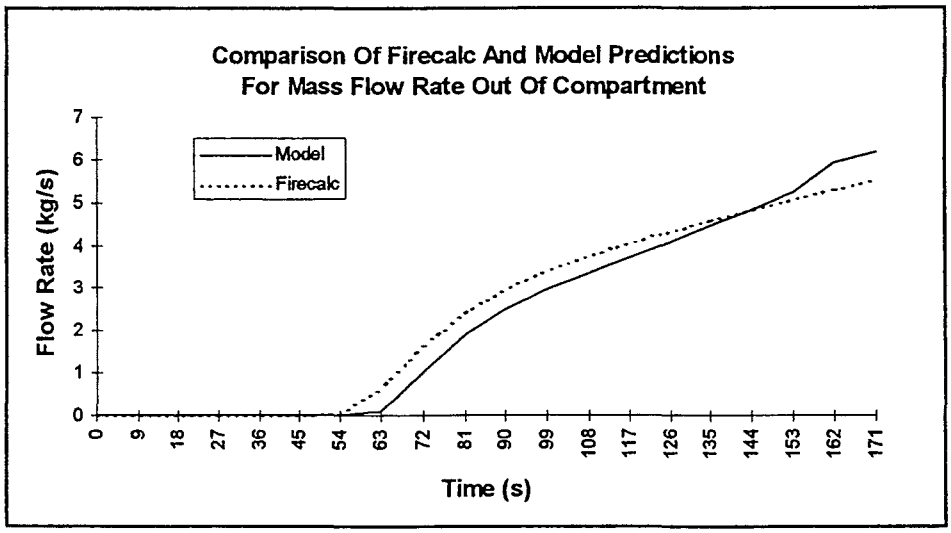

Figure 3.8: Firecalc and model prediction of mass flow out of the compartment for a fast fire.

Figure 3.8 shows good agreement between the model and Firecalc predictions for the mass flow rate out of the compartment. A sharp increase in the flow rate however, is observed at the same time that the sharp temperature increase occurs. The mass flow

rate out of the compartment, determined from equation (3.13) is a function of the upper layer temperature and the fractional height of the neutral plane, equation (3.14), which is itself a function of the upper layer temperature. Therefore this sudden increase in mass flow rate out is also attributable to the thermal penetration time.

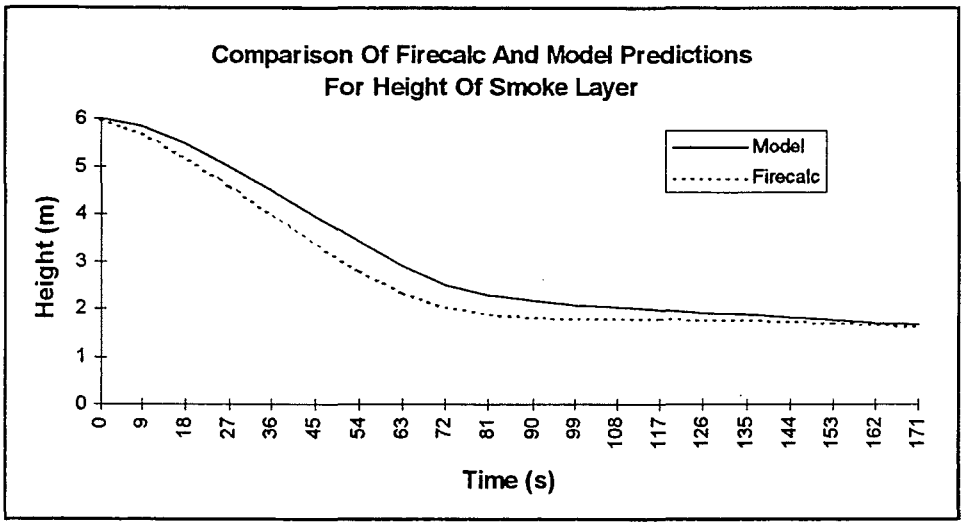

Figure 3.9: Firecalc and model prediction of the height of the smoke layer in the compartment for a fast fire.

As can be seen Figure 3.9 shows very close agreement between the model and Firecalc predictions for the height of the smoke layer in the compartment as a function of time.

Chapter 4
Detector Actuation

4.1 Introduction

Automatic sprinklers are increasingly used in commercial and residential occupancies to provide active fire protection. Models have been developed that predict the actuation times for sprinklers located under unobstructed ceilings, such as FPEtool and Firecalc, but these are conservative for residential sized rooms where a smoke layer may be produced.

Modelling detector actuation is very important for fire engineering design, as it may be the first notification occupants receive to begin evacuation from a building. With sprinklers it is very important to accurately model the response time, as this represents the time that automatic suppression will be applied to the fire. If the model predicts actuation times that are earlier than would occur in reality, then designing for life safety and property protection would be severely compromised, as the size of the actual fire may be significantly larger than that designed for.

In the event of a fire, hot gases from the products of combustion rise vertically in a plume above the fire source. This buoyant plume will continue to rise until it meets an obstacle, such as the ceiling. The obstacle then prevents the gas flow from rising any further so it turns and moves horizontally. Within this horizontal flow is a very shallow layer of relatively fast moving gases which is driven by the buoyancy of the combustion products. This shallow layer is referred to as the 'ceiling jet'.

The thickness of the ceiling jet flow is usually 5 to 12% of the height from the fire source to the ceiling. The maximum velocity and temperature in this ceiling jet is usually located within 1% of the height from the fire source to the ceiling, Evans (1992a). Figure 4.1 below gives an idealised visualisation of the ceiling jet flow underneath an unconfined ceiling where H is the height of the ceiling above the fuel

surface and R_D is the radial distance of a detector from the plume centreline.

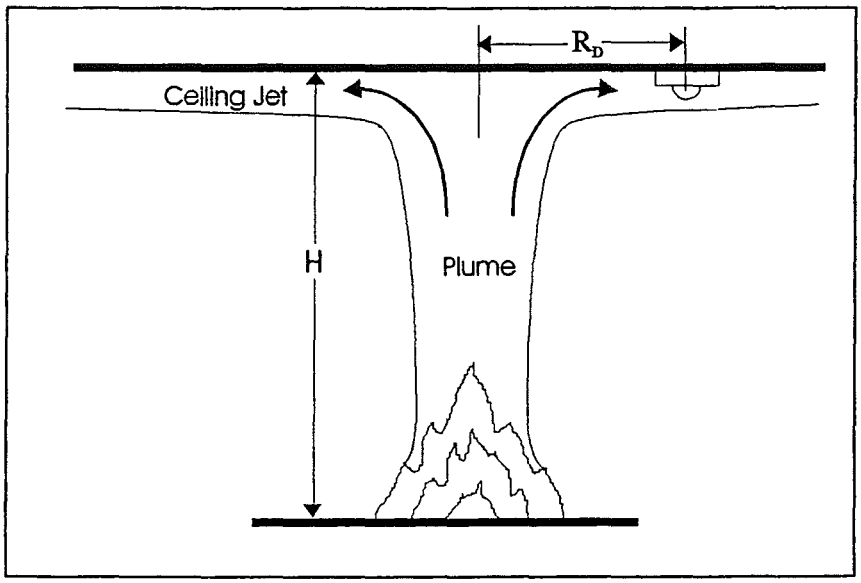

Figure 4.1: Ceiling Jet Flow Beneath An Unconfined Ceiling.

For an unconfined ceiling the plume will entrain cool air all the way to the ceiling where the jet will form. When a hot upper layer is produced however, the plume will entrain cool air to the depth of the smoke layer and then entrain warmer air as it passes through the layer. This will give a decrease in the cooling rate of the plume and hence the ceiling jet in a confined space will be at a higher temperature than that for an unconfined space.

As detector actuation is related to the temperature and velocity of the ceiling jet, the development of a smoke layer would lead to an earlier actuation time than for an unconfined ceiling.

This chapter investigates the validity of FPEtool and Firecalc which are commonly used in New Zealand to simulate detector actuation times. These models are based on a quasi-steady state assumption, which means that any change to the fire source will immediately be recognised at the detector location. The time taken for the fire signature to travel from the source to the detector is consequently neglected. The limitations of FPEtool and Firecalc are discussed and the detector actuation times predicted with these models are compared to an alternative model that has been derived for use with t^2 fires.

4.2 FPEtool/Firecalc Detector Response

FPEtool and Firecalc are two models that are commonly used for detecting the response time of sprinklers in New Zealand. Both of these models use the same method for this calculation, developed by Evans and Stroup (1985).

The sub programs 'Sprinkler/Detector Response' in FPEtool and Firecalc determine the thermal response of a detector or sprinkler that is placed at or near an unconfined ceiling whose area is large enough to neglect the effects of smoke layer development. In order to predict the time of thermal detector activation, time-dependant events from the fire must be linked to events resulting in the heating of the detector from ambient to its activation temperature. The heat source is accounted for by a user specified, time varying fire, in this case a t^2 fire.

The response time index of the detector, RTI, considers the detectors ability to absorb heat and the environments ability to provide heat. The time lag associated with heating the detector is accounted for with the RTI parameter.

The RTI parameter is determined from the *Plunge-Test* where the sprinkler head is suddenly lowered into a flow of hot gas, Heskestad and Smith (1976). The temperature and velocity of the gas are known and are constant during the test. The RTI is then determined by,

$$RTI = \frac{-t_{act}\sqrt{U}}{\ln\left(1 - \frac{T_{act} - T_{\infty}}{T_g - T_{\infty}}\right)} \qquad (4.1)$$

where t_{act} and T_{act} are the actuation time and temperature respectively.
To determine the sprinkler actuation time in a compartment, the environments temperature and velocity at the location of the sprinkler head needs to be calculated. Alpert (1972), developed correlations to determine the maximum gas temperature and velocity at a given position in a ceiling jet flow from a steady state fire. These

correlations were based on test results from the burning of wood and plastic pallets, cardboard boxes, plastic materials in cardboard boxes and liquid fuels under heights that ranged from 4.6 to 15.5m, Evans (1992a).

As Alpert's correlations are for a steady state fire, the heat release rate for use with Firecalc and FPEtool are represented as a series of straight lines, of which the end points are specified by user input. This quasi-steady assumption limits the accuracy of the model, especially when there are rapid changes in the heat release rate.

The correlations used for sprinkler/detector response in FPEtool and Firecalc are provided below,

$$T_{jet_t} - T_\infty = \frac{16.9\dot{Q}^{2/3}}{H^{5/3}} \qquad \text{for } \frac{R_D}{H} \le 0.18 \tag{4.2}$$

$$T_{jet_t} - T_\infty = \frac{5.38(\dot{Q}/R_D)^{2/3}}{H^{5/3}} \qquad \text{for } \frac{R_D}{H} > 0.18 \tag{4.3}$$

$$U_{jet_t} = 0.96\left(\frac{\dot{Q}}{H}\right)^{1/3} \qquad \text{for } \frac{R_D}{H} \le 0.15 \tag{4.4}$$

$$U_{jet_t} = 0.195\frac{\dot{Q}^{1/3}H^{1/2}}{R_D^{5/6}} \qquad \text{for } \frac{R_D}{H} > 0.15 \tag{4.5}$$

These equations, developed by Alpert give the maximum ceiling jet temperatures and velocities at a user specified location. With a known activation temperature for a given detector, the time to activation is then determined by, (Deal 1994),

$$T_{D,t+\Delta t} = \left[(T_{jet_{t+\Delta t}} - T_{D,t})(1 - e^{-1/\tau}) + (T_{jet_{t+\Delta t}} - T_{jet_t})^{\tau}(e^{-1/\tau} + \frac{1}{\tau} - 1)\right] + T_{D,t} \tag{4.6}$$

where

$$\tau = \frac{RTI}{\sqrt{U_{jet_t}}} \tag{4.7}$$

As can be seen, equation (4.6) is incremental and to determine the detector temperature at the required time, the detector temperature, ceiling jet temperature and ceiling jet velocity at the previous time step needs to be known. When $T_{D,\ t+\Delta t}$ equals or exceeds the value in $T_{D,\ activation}$, then detector response is predicted.

4.3 Limitations Of FPEtool/Firecalc Predictions

As previously mentioned FPEtool and Firecalc predict the response of thermal detectors in areas large enough to neglect the effects of smoke layer development. With reasonably small compartments a significant smoke layer may build up prior to detector response, hence these programs will predict a longer time to actuation than that which would actually occur.

In the event of a fire a plume rises to the ceiling which is cooled by the ambient air that it entrains. For an unconfined ceiling the plume will entrain ambient air all the way, but if the plume enters a hot upper layer below the ceiling then the rate of cooling in this region will be significantly reduced. This would lead to higher ceiling jet temperatures flowing past the detector, hence the actual activation time would be earlier than the predicted time.

The correlations proposed by Alpert are for the maximum ceiling jet temperatures and velocities, which would occur in a ceiling jet thickness of 5 to 12% ceiling-to-fire-source-height. If the detector is not located in this range, the results of 'FPEtool' and 'Firecalc' are invalid.

As the model assumes a quasi-steady approximation, this will mean that any changes in the fire source would be recognised as immediately affecting the gas flows at all distances from the fire. In reality a change in the fire source would not be registered

at the detecting element until some time after that change. This is referred to as the transportation lag time. The accuracy of the model therefore becomes very limited when there are rapid changes in the heat release rate and/or the distance of the detector from the source is large.

4.4 Accounting For Transport Lag

With the transport lag time ignored, in a growing fire the predicted temperature and velocity will always be greater than, or equal to, the actual values. The detector would therefore be predicted to actuate prematurely.

To avoid the quasi-steady state assumption in FPEtool and Firecalc, Heskestad (1972) proposed a generalisation of the steady state functional forms to include time. An extensive series of tests conducted by Heskestad and Delichatsios (1977, 1978) at the Factory Mutual Research Corporation led to the following dimensionless correlations for maximum ceiling jet temperatures and velocities for t^2 fires.

$$\Delta T_2^* = \begin{cases} 0, & t^* \le t_f^* \\ \left(\dfrac{t_2^* - t_f^*}{0.188 + 0.313 R_D / H} \right)^{4/3} & t^* > t_f^* \end{cases} \qquad (4.8)$$

$$U_2^* = 0.59 \left(\frac{R_D}{H} \right)^{-0.63} \sqrt{\Delta T_2^*} \qquad (4.9)$$

$$t_2^* = t / (A_{H,D}^{-1/5} \alpha^{-1/5} H^{4/5}) \qquad (4.10)$$

$$U_2^* = U / (A_{H,D}^{1/5} \alpha^{1/5} H^{1/5}) \qquad (4.11)$$

$$\Delta T_2^* = (T - T_\infty) / \left[A_{H,D}^{2/5} (T_\infty / g) \alpha^{2/5} H^{-3/5} \right] \qquad (4.12)$$

$$A_{H,D} = g / (c_p T_\infty \rho_\infty) \tag{4.13}$$

$$t_f^* = 0.954(1 + R_D / H) \tag{4.14}$$

$$\Delta T = T - T_\infty \tag{4.15}$$

Where the dimensionless variables are indicated with the superscript asterisk.
The dimensionless time t_2^* is reduced by the time t_f^* and it is this reduction that accounts for the transport lag time for the gases at the fire source to reach the location of interest along the ceiling at the specified R_D/H.

A method for predicting detector activation time was been developed by Beyler (1984) using the dimensionless correlations above. The temperature of a detector at a specified location may be determined by:

$$\begin{aligned} T_{D,t} &= T_\infty + \left(\frac{\Delta T}{\Delta T_2^*}\right)\Delta T_2^* \left[1 - \frac{(1 - e^{-Y})}{Y}\right] \\ &= T_\infty + \Delta T \left[1 - \frac{(1 - e^{-Y})}{Y}\right] \end{aligned} \tag{4.16}$$

Where

$$Y = .75\left(\frac{U}{U_2^*}\right)^{1/2}\left(\frac{U_2^*}{\Delta T_2^*}\right)^{1/2}\left(\frac{\Delta T_2^*}{RTI}\right)\left(\frac{t}{t_2^*}\right)(0.188 + 0.313 R_D / H) \tag{4.17}$$

A detector will be predicted to actuate when the temperature calculated from equation (4.16) exceeds $T_{D,\,activation}$.

This model does not account for the production of a smoke layer which would result in an earlier actuation time, as previously discussed, hence it can be considered conservative with respect to fire engineering design.

4.5 Comparison of Models

An arbitrary case was chosen to compare the results of FPEtool, Firecalc and the t^2 model which accounts for transport lag. A fast fire was assumed and the height of the room was chosen to be 5m. Various detector types with specified Response Time Indexes and detector actuation temperatures were investigated which were obtained from Buchanan (1994). The results are summarised in Table 4.1 and a full listing of the results for the example of Chapter 3-Section 9, with sample calculations is provided in Appendix C.

				Detection Time (s)			
Detector Type	**RTI $(m.s)^{1/2}$**	**T_{act} (°C)**	**Radial Dist. R_D (m)**	**Firecalc**	**FPEtool**	**Model Using FPEtool**	**Accounting For Transport Lag**
Heat Detector	20	57	2	102.9	104.3	104	125
Fast Response Sprinkler	30	93	1	122	123	122	156
Standard Sprinkler	190	93	1	178.8	180.2	180	267

Table 4.1: Comparison of detector actuation times for various detectors with H=5m.

Equations (4.6) and (4.7) were used to determine the detector actuation times for the 'Firecalc', 'FPEtool' and 'model using FPEtool' columns. The 'model using FPEtool' column was included to validate these equations, as equation (4.6) was misprinted by Deal (1994). The slight discrepancies in the results arise from the difference in the fire growth constant, α, used in each model. Table 4.2 summarises the growth constants for the models.

Fire Type	Firecalc α	FPEtool α	Model using FPEtool α
Medium	0.0111	0.0117	0.0117
Fast	0.0444	0.0466	0.0469
Ultrafast	0.1778	0.1874	0.1876

Table 4.2: Fire growth constants for various computer models with $Q=\alpha t^2$.

The activation times predicted by Firecalc and FPEtool from Table 4.1 are seen to be significantly less than those of Beyler's (1984) model which accounts for transport lag. As detection times are longer when transport lag is included, the fire would grow to a larger size than FPEtool and Firecalc would predict. The estimation of the standard sprinkler actuation is 87s earlier with FPEtool and Firecalc for the dimensions specified, which with a fast fire, $Q = 0.0469(87)^2$, represents 355kW.

Designing for protection against a larger fire size would be a conservative measure on behalf of the fire engineer. For this reason, the method proposed by Beyler (1984) for predicting detector actuation times for t^2 fires should be used.

Chapter 5

Effect of Sprinklers In Compartment Fires

5.1 Introduction

Automatic sprinklers provide a very efficient means of controlling fires within a building. They operate when the fire is relatively small and only in the vicinity of the fire, with the exclusion of deluge systems where many sprinklers will activate at the same time.
Sprinklers often confine the initial stage of fire growth and heat generation to a single compartment. Sprinkler spray may control or extinguish a fire by:

- Displacing air from the compartment with the production of steam,
- Cooling the fuel and room which will reduce the heat feedback, radiation, to the combustible elements,
- Direct contact of the water with the fuel, preventing the generation of combustible vapour, Pyrolizates, by cooling the fuel,
- Prewetting the combustible material to prevent further fire spread,

The effects of sprinklers on compartment fires has very mixed opinions. Some researchers believe that smoke control in sprinklered buildings will not be required as the sprinklers will limit the fire growth, minimise fire size and limit smoke production to negligible levels. Others believe that sprinklers will have a beneficial effect on smoke control systems as pressure differences and airflow rates are reduced which is needed to achieve effective smoke control.

Another opinion is that sprinklers actually worsen smoke conditions in a building by increasing the amount of smoke produced and causing it to descend to floor level reducing visibility, (Mawhinney 1993).

Many of the current quantitative prediction methods for fire hazard analysis are extremely limited in their ability to include fire suppression. The effects of an isolated sprinkler spray with the interaction of the fire gases and the fuel elements is an extremely complex physical, thermal and chemical problem, (Evans 1992b), including,

- The interaction of the sprinkler spray with the smoke layer is very important, as the cooling effect of the spray on this layer will reduce its buoyancy significantly. This induces the layer to fall to a lower level.

- As water droplets descend through a hot smoke layer to the fire source, they experience an air drag which is a function of their surface area. When the temperature of the droplet reaches boiling point it will evaporate, decreasing its diameter, thus reducing the drag effect.

- The reduction of the buoyancy of this layer and the air drag will pull a stratified smoke layer to a lower level. The combining effects will disturb the stability of the smoke layer as vigorous mixing with the cooler air below may occur. This phenomenon is described as smoke logging and at some time post sprinkler actuation, the compartment could be considered as a single zone.

The effects of drag, evaporative cooling and possible smoke logging, renders the method for determining the upper layer gas temperature, discussed in Chapter 3, Invalid.

This chapter investigates the effects of sprinklers in compartment fires on the,

- Heat Release Rate,
- Drag Effect on an upper layer,
- Evaporative cooling of an upper layer,
- Vent flow.

5.2 Smoke Control Definition

The term "smoke control" may have various meanings for different people, such as life safety for the engineer, property protection for the building owner, operational convenience for the building operator or fire suppression for the fire department, Dillon (1991).

Smoke control for life safety consists of barriers and air movements that are designed to create acceptable conditions for evacuation or relocation of building occupants to refuge areas. The barriers and air movements for property protection are designed to prevent smoke migration to areas where goods or equipment may be susceptible to smoke damage, such as electronic equipment. For operational convenience the barriers and air movements may be designed to allow for a return to normal operations within a building relatively quickly.

Smoke control for fire suppression assistance would consist of barriers and air movements that would help fire fighters locate the fire and provide them with areas that are safe to fight the fire from.
The primary objective of all engineering designs for "smoke control" is that of life safety with the other terms being of secondary importance.

5.3 Historical Development

The first simple theories of the interactions between sprinkler sprays and a hot smoke layer were developed by Bullen (1974). The effects of the drag force induced by the sprinkler spray on the smoke layer were examined to determine whether a stratified upper layer would fall to a lower level. The cooling effect of the spray as it passed through the hot smoke layer were not considered with this analysis.

The cooling of room fires was examined by Kung (1977). In his experiments, hexane pool fires were selected to simulate fire sources to avoid the complexity encountered in fires with solid fuels, such as prewetting of combustibles to prevent fire spread and direct extinction by contact of water droplets with the burning surface. Kung developed a method for determining the heat absorption rate of a sprinkler spray.

Morgan (1979) first investigated the effects of the heat transfer from a buoyant smoke layer to a sprinkler spray. A theory was developed to calculate the heat transfer to a single water drop as it moved through a hot smoke layer and thus the heat removed from the layer by the spray.

Chow (1989) developed a crude model for estimating the evaporative heat loss due to a sprinkler water spray in a smoke layer. Work in this area had previously concentrated on air drag and the convective heat transfer between water droplets and a hot smoke layer. Little attention had been paid to the evaporation of sprinkler water drops.

Chow and Fong (1991) created a field model using the cooling effects and air drag of water droplets to study the cooling of the fire induced hot air flow by sprinkler water sprays. The purpose of this model was to investigate how sprinkler water sprays interact with a stratified hot upper layer in a three dimensional sense. No experimental data was available to validate this model at this time.

Vettori and Madrzykowski (1992) experimented with various fuel packages to develop a method for determining the reduction in heat release rate after sprinkler actuation. The results obtained were for a specific sprinkler spray density, (0.07 mm/s). Evans (1994) used the data obtained with their experiments and also data from experiments by Walton (1988) to develop a method for the reduction in heat release rate of post-sprinkler actuated fires with any sprinkler spray density.

Mawhinney (1993) conducted a series of experiments to investigate the interactions of sprinklers with shielded fires and the corresponding effects on a zoned smoke control system. Tests were conducted in two phases. In the first phase, large wood crib fires were conducted in a one story test room equipped with sprinklers. These tests provided information about the interaction of sprinklers and partially suppressed fires, and the results were used for the second phase of testing. The second phase consisted of testing shielded wood crib fires on the seventh floor of a ten story experimental tower. The effects of the sprinklers on the heat release rate, the heat flux to surroundings, the room temperature, the buoyancy pressure, the gas concentrations and the smoke spread were all investigated.

Chow and Cheung (1994) used data obtained in the large scale tests of Swedish experiments conducted by Ingason and Olsson (1992) to validate their results for the field model analysis on the effects of sprinkler sprays with a stratified hot layer. The water droplets were assumed to be non evaporating and the predicted results included the gas flow, temperature, smoke concentration and the shape of the water spray. The average smoke layer temperature and smoke layer interface height are also calculated.

Cooper (1994) developed a model to simulate the interaction of a sprinkler spray and a two layer fire environment. The model simulates the effects of the sprinkler spray as it entrains, drives downward, humidifies and cools gas in the upper and lower layers. Six possible flow conditions were investigated in this model.

5.4 Reduction In Heat Release Rate

A method for predicting the reduction in the heat release rate, post sprinkler actuation, was originally developed by Vettori, R.L and Madrzykowski, D (1992).
A series of large scale experiments were performed to determine the heat release rate, HRR, of eight different fuel packages with and without sprinklers operating.

A schematic of the typical test configuration for each fuel package is shown in Figure 5.1.

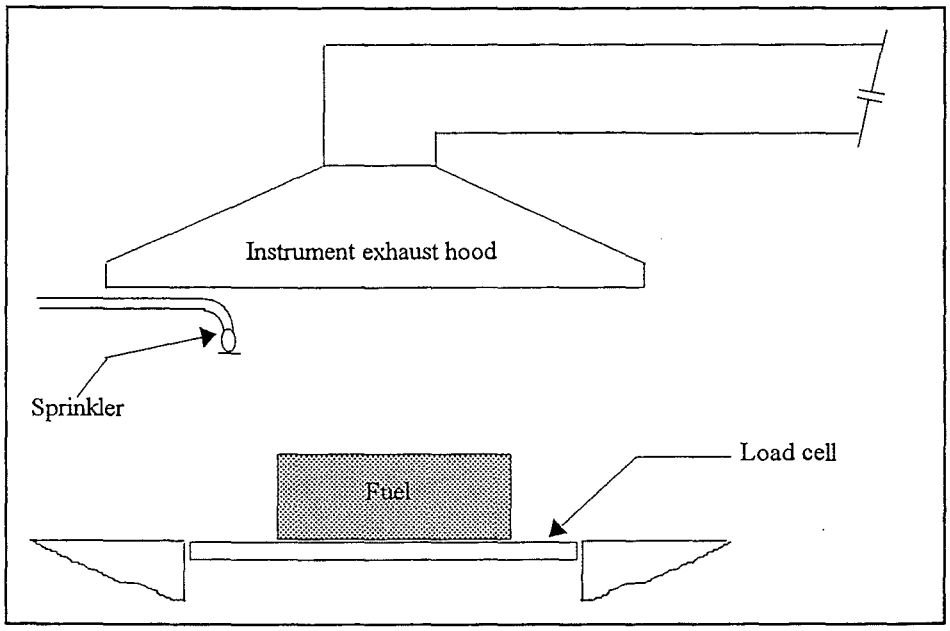

Figure 5.1:Test schematic configuration for experiments to determine sprinkler fire suppression performed by Vettori and Madrzykowski.

Figure 5.1 indicates that as the sprinkler is located underneath the exhaust hood, a smoke layer will not form, thus the results did not include the effects of sprinkler interaction with a hot upper layer.

The fire suppression method they provided is based on the assumption that suppression of all fuels have the same degree of resistance to fire suppression as a wood crib. From the experimental data for the range of office furnishings that were tested, this was shown to be a conservative assumption.

The data obtained, suggested that the heat release rate after sprinkler actuation decayed in an exponential manner bounded by the curve,

$$Q(t - t_{act}) = Q(t_{act})\exp\left[\frac{-(t - t_{act})}{435}\right] \qquad (5.1)$$

The limitation of the model developed by Vettori and Madrzykowski was that no variations in sprinkler spray density were accounted for and the suppression capabilities of all sprinklers were predicted to be the same.

Experiments were performed by (Walton 1988), in which different sprinkler water spray densities were tested on wood crib fires. As with the study performed by Vettori and Madrzykowski the measurements were again seen to be bounded by an exponential decay in the form of exp[-(t-tact)/τ], where τ is a time constant for the post-sprinkler actuation heat release rate reduction. Walton used a least squares fit to the experimental data to give a formula for the variation in the time constant, representing the heat release rate reduction of a wood crib fire during suppression with sprinkler sprays within ±50% as,

$$\tau = 3(\dot{w}'')^{-1.85} \tag{5.2}$$

where $\dot{w}''$ is the sprinkler spray density (mm/s).

This equation shows that the time constant decreases with increasing spray density.
The incorporation of this time constant formula into equation (5.1), developed by Vettori and Madrzykowski, provides the following to conservatively estimate the reduction in the heat release rate after sprinkler actuation.

$$Q(t - t_{act}) = Q(t_{act})\exp\left[\frac{-(t - t_{act})}{3(\dot{w}'')^{-1.85}}\right] \tag{5.3}$$

As can be seen, this equation is an improvement in the predictive capabilities, as the effects of varying sprinkler spray density are accounted for.
With increasing spray density and hence decreasing time constant, the reduction in heat release rate will be more rapid, thus suppression will be quicker, as one would expect.

5.5 Hazard Categories In New Zealand

Three classes of hazard are defined in NZS 4541:1987, these being Extra Light Hazard, (ELH), Ordinary Hazard, (OH), and Extra High Hazard, (EHH). The hazard classification of a building, or an area within a building, is very important and needs to be selected carefully, as it is the basis of design for any sprinkler system, (Buchanan 1994).

Extra light hazard occupancies are non-industrial occupancies where the amount and combustibility of the contents is low. Ordinary hazard is commercial and industrial occupancies involving the handling, processing and storage of mainly ordinary combustible materials unlikely to develop intensely burning fires in the initial stages. This particular class is divided into four sub-groups, light ordinary hazard, (OH1), medium ordinary hazard, (OH2), high ordinary hazard, (OH3) and Special high ordinary hazard, (OH3s).

Extra high hazard occupancies are commercial and industrial occupancies having fire loads where the materials handled or processed are mainly of an extra hazardous nature likely to develop rapid and intensely burning fire, or involving high piling of goods beyond specified limits in NZS 4541:1987.

Table 5.1 details the design requirements for the extra light and ordinary hazard classes, as specified by parts 7 and 8 of NZS 4541:1987.

Hazard	Min. Design Density of Discharge (mm/min)	Max. Area of Operation (m^2)	Flow of Water (Litres/min)
ELH	2.7	84	270
OH1	5	72	375-540
OH2	5	144	725-1000
OH3	5	216	1100-1350
OH3s	5	360	1800-2100

Table 5.1: Design criteria for extra light and ordinary hazard fire sprinkler systems.

Residential and commercial occupancies generally have an extra light or ordinary hazard classification. With the minimum design density of discharge from Table 5.1, the heat release rate for a sprinklered t^2 fire, using equation (5.3) for the reduction, is shown in Figure 5.2.

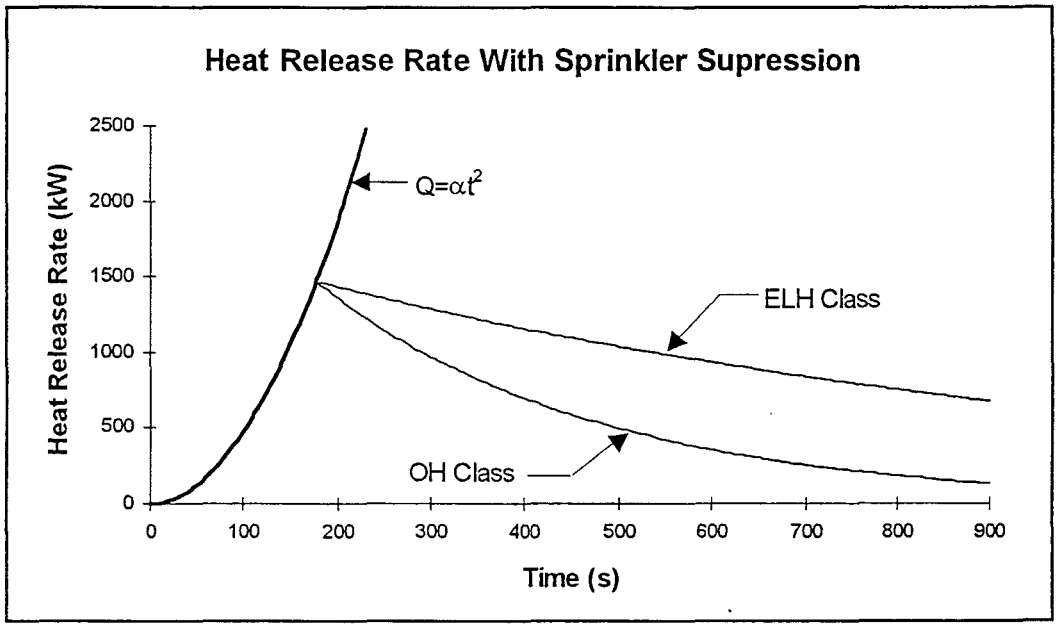

Figure 5.2: Heat release rate with sprinkler suppression for extra light and ordinary hazard classes.

The sprinkler activation time in Figure 5.2 is 177 seconds and was determined from the method detailed in Chapter 4-Section 4 For a 6m height, RTI=30, T_{act}=93°C and R_D=1m.

The method described above for the prediction of the heat release rate after sprinkler actuation is relatively crude as it does not take into account the effects of the interaction of the spray with the hot upper layer. This interaction would cause droplets to evaporate and decrease in diameter. If the diameter of the droplets decrease significantly, they may not be able penetrate the upper layer and reach the burning object.

5.6 Cooling Power And Expansion Of Water

The amount of energy required by water to change phase from liquid to gas is referred to as the latent heat of vaporisation, L_v. When water is heated to 100°C at atmospheric pressure it will transform to steam. This transformation will also cause the water to expand in volume.

The specific molar enthalpy of water in the liquid phase at 100°C, h_f, is 419.1 (kJ/kg) and the specific molar enthalpy of the gaseous phase at 100°C, h_g, is 2675.8 (kJ/kg), Rogers and Mayhew (1991). The latent heat of vaporisation to convert 1 kg of water at 100°C to steam at atmospheric pressure is then,

$$h_f - h_g = 2675.8 - 419.1$$
$$= 2256.7 \text{ (kJ/kg)}$$
$$= 2.26 \text{ (MJ/kg)}.$$

This indicates that if 1 litre of water is applied to a fire in a second, 2.26 MW of energy will be required to heat all of the water to steam. Figure 5.3 shows the cooling power of water with respect to temperature.

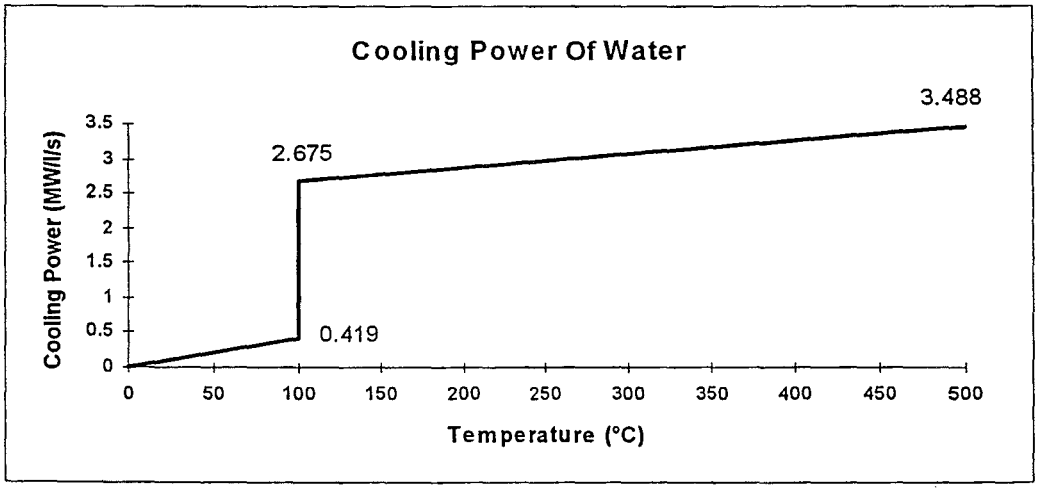

Figure 5.3: Cooling power of water.

To determine how much water expands as it is transformed to steam, the specific volume of water needs to be considered. If one litre of water at 20°C and atmospheric pressure is converted to steam the expansion is calculated as follows,

The specific volume of water at 100°C in the gaseous phase, v_g, is 1.673 (m^3/kg) and the specific volume in the liquid phase, v_f, at 20°C is 0.0010018 (m^3/kg), Rogers and Mayhew (1991), so,

$$\text{Expansion} = \frac{1.673}{0.0010018}$$
$$= 1669.9$$
$$= 1700$$

The expansion ratio increases with temperature and is shown in Figure 5.4.

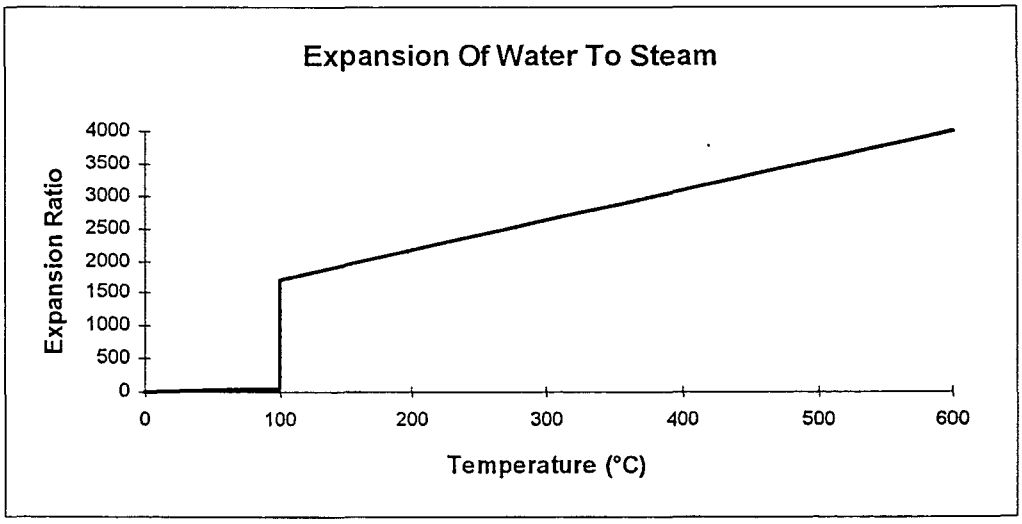

Figure 5.4: Expansion of steam, reprinted from Barnett 1994.

5.7 Steam Produced From Reduction in Heat Release Rate

With a known reduction in the heat release rate from equation (5.3) after sprinkler actuation, Figures 5.3 and 5.4 may then be used to determine how much steam is produced.

If the reduction in heat release rate in 1 second is divided by the latent heat of vaporisation, Lv, then the amount of water being converted to steam to account for the reduction will then be given in litres/second. As 1 litre is 0.001 m^3 and the expansion ratio of water to steam is 1700 the volume of steam produced is therefore,

$$1.7 \times \left(\frac{HRR_{\text{Reduction (for 1 second)}}}{L_v} \right) \quad (m^3 / s) \tag{5.4}$$

This equation gives the amount of steam produced in 1 second, so the total steam produced in a compartment would be iterative and the calculations for volume of steam produced at previous time increments would then be added to equation (5.4).

5.7.1 Example

If the reduction in heat release rate is 20kW in 1 second, then the volume of steam produced to account for this reduction is,

$$\begin{aligned} \text{Steam} &= \left(\frac{20}{2.26 \times 10^3} \right) && \left(\frac{kW}{(kW/1/s)} \right) \\ &= 8.85 \times 10^{-3} && (1/s) \\ &= \left(8.85 \times 10^{-3}\right)(0.001)(1700) && (m^3/s) \\ &= 0.015 && (m^3/s) \end{aligned}$$

The volume of steam produced to cause a 20 kW reduction in the heat release rate, shown above, seems extremely low and unrealistic.

5.8 Interaction Of Sprinkler Spray With A Smoke Layer

If a sprinkler is actuated when the depth of the smoke layer is negligible, such as for large

unconfined ceilings in shopping malls say, the effects of the interaction of this layer with the sprinkler spray need not to be considered. If a smoke layer is present however, the interaction effects become important and need to be considered.

A typical schematic of sprinkler spray moving through a stratified smoke layer is shown in Figure 5.5.

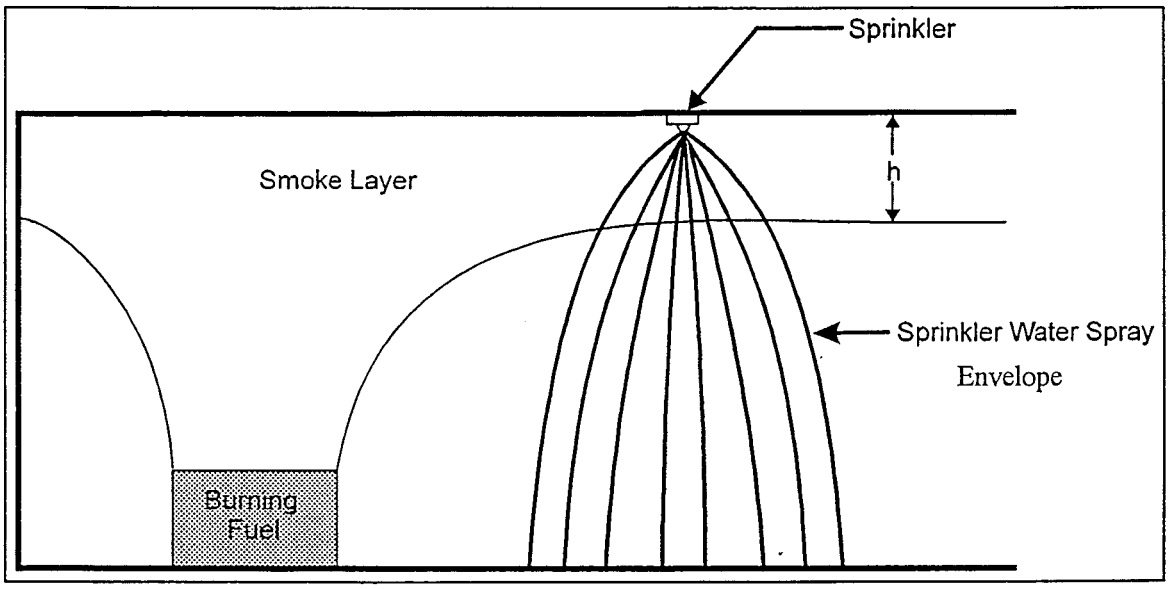

Figure 5.5: Schematic of sprinkler spray flowing through a smoke layer.

As water droplets from a sprinkler spray move through a hot smoke layer, the temperature of this layer will decrease. The layer will therefore experience a reduction in buoyancy which will cause it to fall to a lower level. The water droplets will also experience an air drag effect, which is dependant on the droplet diameter, and this will effectively pull the stratified smoke layer downward.

The evaporation of water droplets interacting with a smoke layer is an important consideration. As the droplets move through the layer they will be heated and when they reach boiling point they will begin to evaporate. This will reduce the diameter of the droplets and hence the air drag effect will reduce.

Cooper (1994) described three possible categories of interaction between sprinkler spray and smoke shown diagrammatically in Figures 5.6, 5.7 and 5.8.

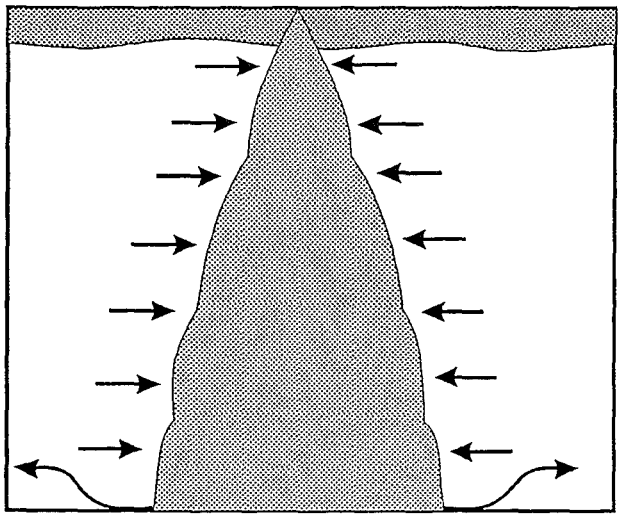

Figure 5.6: Sprinkler in lower layer, at or below the interface.

Figure 5.6 shows that when the sprinkler is in the lower layer, at or below the surface, as one might find in a shopping mall with large unconfined ceilings, there is little interaction between sprinkler spray and the buoyant smoke layer.

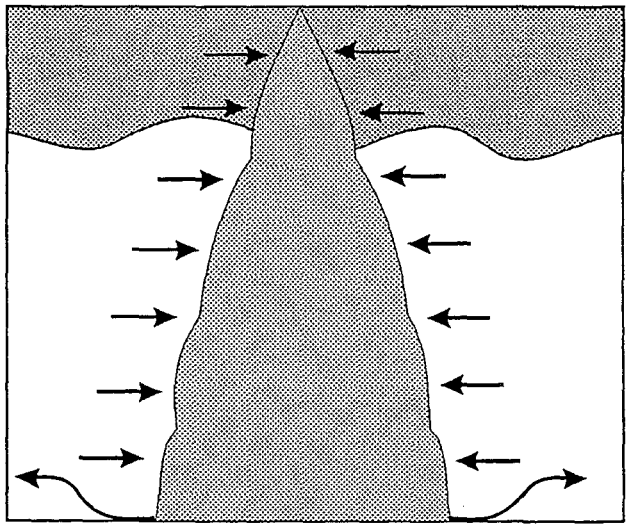

Figure 5.7: Sprinkler in upper layer, all entrainment deposited in lower layer.

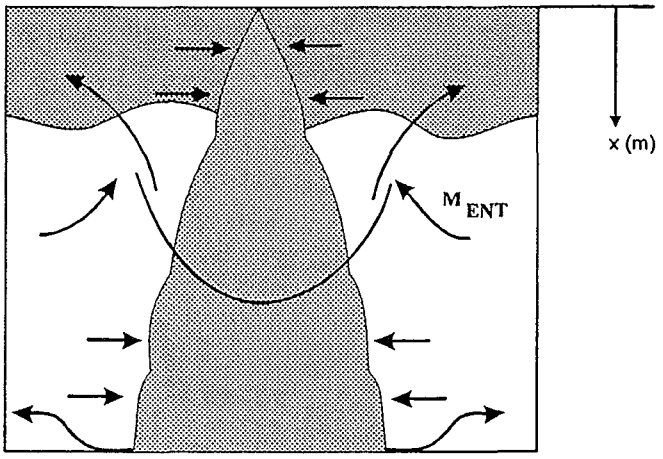

Figure 5.8: Sprinkler in upper layer, entrainment of lower layer gases deposited in upper layer.

In Figures 5.7 and 5.8, the sprinkler head is located in the upper layer and the spray interacts with this. When the sprinkler actuates, the spray entrains gases from the high temperature upper layer, drives downward, (with the drag on the droplets decreasing), and cools and humidifies the gases in this upper layer due to droplet evaporation. A jet of downward moving gases is thus formed and this jet is assumed to be a fixed spray cone envelope.

In the lower layer, upward buoyant forces would reduce the velocity of the jet. If the upward buoyant forces are not strong enough to drive the jet back to the upper layer then it will be deposited in the lower layer, as in Figure 5.7. If the upward buoyant forces are sufficient to drive the jet back to the upper layer then a very large flow of lower layer gases may be deposited here, as in Figure 5.8. The stability of the smoke layer will be compromised and this could lead to vigorous mixing with the cooler air below. This can be described as 'smoke logging'.

If $\dot{M}$ is the mass flow rate of jet gases through a section of the spray cone then the scenario shown in Figure 5.7 is where $d\dot{M} / dx > 0$ immediately below the upper and lower layer interface and the scenario shown in Figure 5.8 occurs where $d\dot{M} / dx \leq 0$ immediately below the interface.

5.9 Drag Effect Of Sprinklers On Smoke Layer

The downward droplet velocity from a sprinkler spray gives a momentum transfer due to drag force interactions between the droplets and the upper layer gases. This leads to a downward flow of the upper layer gases within the sprinkler spray envelope. The lower temperature within the spray envelope would result in a relatively low pressure here, in comparison to the pressure in the upper layer at large distances from the spray. The higher pressure in the upper layer will act to drive an entrainment of hot gases towards the centre of the lower pressure spray envelope. As the spray moves further from the sprinkler head, conservation of vertical momentum along the centreline of the spray area will require an acceleration of the upper layer gases at the expense of deceleration of the water droplets. This would therefore result in a downward jet of upper layer gases within the sprinkler spray, Cooper (1994).

The effect of drag forces experienced by water droplets moving through a smoke layer were first investigated by Bullen (1974). The results obtained with this analysis are summarised below.

A single drop of water, assumed to be spherical in shape, experiences a resistive drag force when it falls through air. Massey (1974), showed that if turbulent drag is assumed, the drag force is given by,

$$D_D(x) = -k_D V_D^2 \qquad (5.5)$$

Where $k_D = 0.5\, C_D\, \rho_a\, A_D$ is a constant. C_D is a function of the Reynolds Number based on the diameter of the water droplet, $\left(\frac{\rho_a D_w V_D}{\mu_a}\right)$, which has been accounted for in this analysis. With turbulent flow, changes in velocity have a negligible effect on C_D.

Chow and Cheung (1994), determined the drag coefficients with varying Reynolds numbers to be,

$$C_D = \begin{cases} 24Re^{1/2} & Re < 1 \\ 0.6 & 1 \leq Re \leq 1\times10^3 \\ 0.47 & 1\times10^3 \leq Re \leq 3\times10^5 \\ 0.2 & 3\times10^5 \leq Re \end{cases}$$

The free body diagram for a single drop of water is shown below in Figure 5.9.

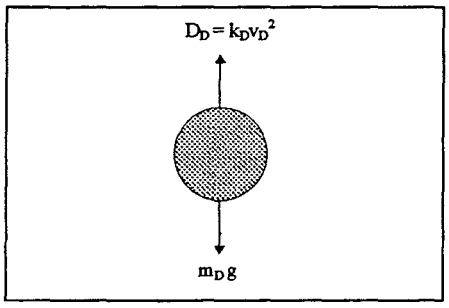

Figure 5.9: Free body diagram of water droplet falling under gravity.

From this it can be seen that the equation of motion for a single drop falling due to gravity is therefore, Bullen (1974),

$$m_D g - k_D V_D^{\,2} = m_D \frac{dV_D}{dt} = m_D V_D \frac{dV_D}{dx} \tag{5.6}$$

where the mass of a single drop is,

$$m_D = \frac{\rho_w \pi D_w^{\,3}}{6} \tag{5.7}$$

When a sprinkler is actuated, water under pressure is discharged from the orifice and strikes the deflection plate, to give the spray envelope. The initial vertical momentum of this water will therefore be zero upon striking the plate, thus the initial vertical velocity

component of the drop is also assumed to be zero. With this assumption, the solution to the equation of motion for a drop falling under gravity is,

$$V_D^{\,2} = \frac{m_D g}{k_D}\left[1 - \exp\left(\frac{-2k_D x}{m_D}\right)\right] \tag{5.8}$$

If all of the momentum from the drops is assumed to be parallel to the direction of the motion the total downward thrust exerted on the upper layer will then be the sum of all the drag forces on all of the drops.

The number of drops in the upper layer within the spray envelope is,

$$N_D = \dot{f}_w \frac{dx}{m_D V_D} \tag{5.9}$$

The total drag exerted on a drop as it falls through the layer is,

$$\int_0^h D_D(x).dx$$

where h is the depth of the smoke layer. The total drag, D_D, exerted on all the drops, from Bullen, is therefore,

$$D_D = \frac{\dot{f}_w k_D}{m_D}\int_0^h V_D dx, \text{ for constant } \dot{f}_w,\ k_D,\ m_D.$$

Which, when equation (5.8) is substituted, becomes,

$$D_D = \dot{f}_w\left(\frac{k_D g}{m_D}\right)^{1/2}\int_0^h 1 - \exp\left(\frac{-2k_D x}{m_D}\right)^{1/2} \tag{5.10}$$

The solution of this gives the total drag force exerted by all of the water droplets on the upper layer and was found to be,

$$D_D = \dot{f}_w \left(\frac{m_D g}{k_D}\right)^{1/2} \left\{ \tfrac{1}{2} \ln \left[\frac{1+\left(1-\exp\left(\frac{-2k_D h}{m_D}\right)\right)^{1/2}}{1-\left(1-\exp\left(\frac{-2k_D h}{m_D}\right)\right)^{1/2}} \right] - \left[1-\exp\left(\frac{-2k_D h}{m_D}\right)\right]^{1/2} \right\} \qquad (5.11)$$

The hot gases produced from the fire will create an upward buoyant force. If the downward drag force, detailed above, is greater than the upward buoyant force then the upper layer will descend to a lower level.

Bullen assumed the spray envelope to have a parabolic shape in the form of $y^2=C_{SE}x$, where C_{SE} is a constant.

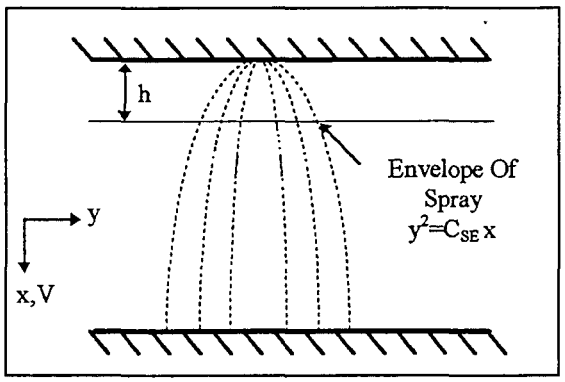

Figure 5.10: Sprinkler spray envelope, Bullen (1974)

Considering the volume of gas through which the spray envelope passes in the upper layer and assuming a constant temperature, the buoyancy force is,

$$B_F = (\rho_\infty - \rho_{UL}).\text{Volume}$$

Where the volume to the depth of the smoke layer is $\pi C_{SE} h^2/2$. Bullen (1974) determined from experimental observations and manufacturers data that the wetted area at 3m below the sprinkler was a circle of approximately 3m, that is $C_{SE} = 3$, giving a volume of,

$$\text{Volume} = \frac{3\pi h^2}{2} \tag{5.12}$$

thus the buoyancy force is,

$$\begin{aligned} B_F &= \tfrac{3}{2}(\rho_\infty - \rho_{UL}) g \pi h^2 \\ &= \tfrac{3}{2} \pi g \frac{\rho_\infty}{T} \sigma \, h^2 \end{aligned} \tag{5.13}$$

If the spray envelope is assumed to be approximated by a cone, an alternative method for predicting the volume of a sprinkler spray may also be used. Figure 5.11 shows how the spray displays a conical shape to the depth of the smoke layer, h.

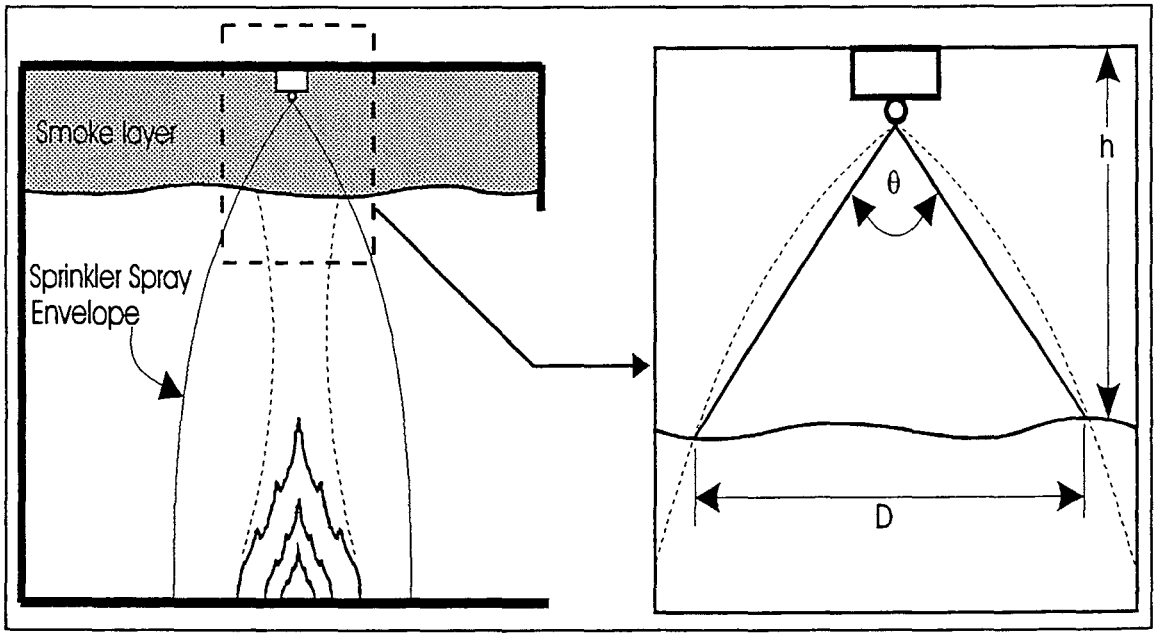

Figure 5.11:Cone approximation of sprinkler spray.

Some sprinkler spray devices have a characteristic cone angle, θ, that is specified by the manufacturer, Cooper (1994). If this is known, then the volume of gas through which the sprinkler spray discharges is then simply the volume on a cone,

$$V_{Cone} = \frac{1}{3}\pi r^2$$

With respect to the height of the smoke layer, and Figure 5.9, the radius of the cone is,

$$r = \frac{D}{2} = h \tan\left(\frac{\theta}{2}\right)$$

So the volume of the cone at the depth of the smoke layer will therefore be,

$$\text{Volume} = \frac{1}{3}\pi\left(h^2 \tan^2\left(\frac{\theta}{2}\right)\right) \qquad (5.14)$$

This alternative volume may then be used in equation (5.13) to determine the buoyancy force.

If the drag force is greater than the buoyancy force, $D_D > B_F$, meaning the ratio of drag to buoyancy is greater than 1, $D_D/B_F > 1$, then the upper layer will be pulled down. From equations (5.11) and (5.13) the following relationship for the drag to buoyancy is found.

$$\frac{D_D}{B_F} = \frac{2\dot{f}_w T}{3\rho_\infty \pi g^{1/2}}\left(\frac{m_D}{k_D}\right)^{1/2}\left\{\tfrac{1}{2}\ln\left[\frac{1+\left(1-\exp\left(\frac{-2k_D h}{m_D}\right)\right)^{1/2}}{1-\left(1-\exp\left(\frac{-2k_D h}{m_D}\right)\right)^{1/2}}\right]-\left[1-\exp\left(\frac{-2k_D h}{m_D}\right)\right]^{1/2}\right\} > 1 \qquad (5.15)$$

If the depth of a smoke layer is reasonably thick, as one might find in a small enclosed compartment, when sprinklers activate, the layer will would be sufficiently buoyant to remain stable for a small period of time. As the layer is then cooled by the spray, causing

a reduction in buoyancy, the downward flow would occur at some time after actuation. This would be advantageous to occupants escaping from a fire situation.

Where a smoke layer is present, but is relatively thin, smoke logging would be likely to occur. Smoke logging may cause serious problems for occupant evacuation. To help prevent this, and aid evacuation, the temperature rating of sprinklers away from high hazard areas, such as escape routes, could be raised above that of the sprinklers in areas where fire is more likely to occur. This would result in the actuation of fewer sprinklers and later actuation times, allowing greater smoke layer development, decreasing the possibility of the downward flow of the upper layer, Bullen (1974).

5.10 Limitations Of Drag Force Analysis

Due to the complex nature of this problem, some of the assumptions made in the above analysis for the drag and buoyancy forces, only approximates what occurs in reality. Sprinkler spray droplets have been assumed to be spherical in shape and the upper layer temperature is assumed to be constant throughout which would almost certainly not be the case in a real situation.

The assumption that the drag force acts over the entire area that the sprinkler spray envelope covers, does not accurately predict the momentum transfer between individual drops and the surrounding air. The cooling effect of the sprinkler spray on the buoyant smoke layer has not been accounted for in this analysis.

The theory proposed for this analysis gives reasonable agreement with experimental data, so with these simple assumptions, the theory gives a viable indication of the likelihood of the downward flow of smoke from a sprinkler.

5.11 Sprinkler Spray Cooling

Experimental and theoretical works have shown that the evaporative heat loss is negligible in comparison with convective heat loss, Kung (1977) and Beyler (1978). The amount of heat that is extracted by a sprinkler spray may be determined by considering the convective term only. To evaluate the convective heat loss of the upper layer the Nusselt number, N_u, needs to be determined.

Whitaker (1972) showed that for a hot gas stream flowing towards a water sphere of diameter D_w, and thus a water droplet falling through a hot layer, the Nusselt number is given by,

$$Nu = 2 + \left(0.4(Re_d)^{1/2} + 0.06(Re_d)^{2/3}\right)Pr^{2.4}\left[\frac{\mu_1}{\mu_w}\right]^{1/4} \qquad (5.16)$$

Where μ_1 is the viscosity of the free stream of air (kg/ms), μ_w is the viscosity of water (kg/ms), Re_d is the Reynolds number of the water droplets and Pr is the Prandtl number. The Prandtl number is relatively constant and may be assumed to be 0.7.

The heat transfer coefficient of each water droplet, h_w, is then determined by,

$$h_w = Nu\left(\frac{k_a}{D_w}\right) \qquad (5.17)$$

Where k_a is the thermal conductivity of air. The mean diameter of a water droplet from a sprinkler, D_{wm}, was shown by Prahl and Wendt (1988) to be a function of the nozzle diameter, D_N, and the Weber number.

$$\frac{D_{wm}}{D_N} = 3.21 W_e^{-1/3} \tag{5.18}$$

where the Weber number is,

$$W_e = \frac{\rho_w V_r^2 D_N}{\sigma_w}$$

V_r is the nozzle discharge velocity and σ_w is the surface tension of water.
The nozzle discharge velocity is then easily determined for a given flow rate of water and known sprinkler orifice diameter by,

$$\begin{aligned} V_r &= \frac{\dot{f}_w}{\text{Orifice Area}} \\ &= \frac{\dot{f}_w}{\pi\left(\frac{D_N^2}{4}\right)} \end{aligned} \tag{5.19}$$

where $\dot{f}_w$ is the flow rate of water (m^3/s).

Cooper (1994) proposed an alternative method for determining the mean diameter of a single water droplet in the form of,

$$D_{wm} = r_p\left(\frac{D_N}{V_r}\right)^{2/3} \tag{5.20}$$

where r_p is a characteristic drop size parameter of the sprinkler spray device that may be specified by the manufacturer. If this parameter is not given then re-arrangement of equations (5.18) and (5.19) gives,

$$r_p = D_{wm}\left(\frac{V_r}{D_N}\right)^{2/3}$$

$$= 3.21 W_e^{-1/3} D_N \left(\frac{\dot{f}_w}{\pi\left(\frac{D_N^2}{4}\right)} \right)^{2/3} \frac{1}{D_N}$$

$$= 3.21 W_e^{-1/3} D_N \left(\frac{4\dot{f}_w}{\pi D_N}\right)^{2/3}$$

$$= 3.21 W_e^{-1/3} D_N^{1/3} \left(\frac{4\dot{f}_w}{\pi}\right)^{2/3} \qquad (5.21)$$

where the flow rate and diameter of the sprinkler would be known.

This may be used in an alternative method to equation (5.9) for determining the number of droplets in a sprinkler spray. This alternative method will be discussed later in this chapter. As the diameter of the water drop is now determinable, the heat transfer coefficient for each droplet may be calculated by solving equations (5.16) and (5.17).

Energy is absorbed by a water droplet as it passes through a hot upper layer and this energy will be returned to the layer in the form of water vapour. The heat flux to each drop is a function of its diameter, which will decrease with evaporation. Chow and Fong (1991) showed that by ignoring this reduction, a simplified expression for the convective cooling, q_d, between a water droplet and the gases in a hot upper layer is given by,

$$q_d = h_w A_{droplet}(T_d - T_s) \qquad (5.22)$$

where T_d is the droplet temperature and T_s is the temperature in the spray cone envelope.

Heskestad (1990) provided the following approximation to $T_d(T_s)$ in the range of $373K \leq T_s \leq 1273K$, which was reprinted by Cooper (1994).

$$T_d = 266\left[1 + 3.23 \times 10^{-4} T_s\, K^{-1}\right] \tag{5.23}$$

Cooper did not define 'K', in his nomenclature so it is unclear whether this stands for Kelvin or is some constant. Time constraints for this paper prevented clarification of this equation from the source, Heskestad (1990).

With the convective cooling calculated from equation (5.22), the rate of water evaporation from a single drop will therefore be given by,

$$\dot{m}_d = \frac{q_d}{L_v}$$

where Lv is the latent heat of vaporisation of water, (2.26MJ/kg).
The total amount of heat absorbed by the sprinkler spray due to convection is the sum of all the convective heat transfer, q_d, for each water droplet travelling through the hot upper layer.

The initial droplet velocity may determined by,

$$V_{Di} = C_m\left(\frac{\dot{f}_w}{\pi\left(\frac{D_N^{\,2}}{4}\right)}\right)$$

$$= \left(\frac{D_N}{D_{cw}}\right)^2\left(\frac{\dot{f}_w}{\pi\left(\frac{D_N^{\,2}}{4}\right)}\right)$$

$$= \frac{4\dot{f}_w}{\pi D_{cw}^{\ 2}} \tag{5.24}$$

where C_m is the momentum coefficient and is the ratio of the initial momentum of spray to momentum of water flow out of a nozzle and D_{cw} is the spray cone diameter at the elevation where the breakup of the sprinkler water stream into drops, by impingement on the striker plate is assumed to be completed, Cooper (1994).

If the spray is assumed to be well represented by a cone like volume of influence, as shown in Figure 5.11, with a characteristic cone angle θ, then Cooper proposed the following method, which, as mentioned earlier, may be used as an alternative to equation (5.9) for determining the number of drops per unit volume,

$$N_D = \frac{\left(\frac{3}{2}\right) V_r^{\ 2}}{\pi r_p^{\ 3} D_N^{\ 2} \tan^2\left(\frac{\theta}{2}\right)\left(\frac{V_D}{V_{Di}}\right)\left(\frac{x_s}{D_{cw}}\right)^2} \tag{5.25}$$

where x_s is the vertical distance from the sprinkler head.
With the number of drops per unit volume now known, the total amount of heat absorbed by the sprinkler spray due to convection may be determined.

Sprinkler spray cooling in compartment fires reduces the buoyancy of the upper layer. This reduction in buoyancy will cause the upper layer to fall to a lower level. The evaporation of the water droplets as they move through the hot gases will result in a reduction in their diameter. The drag effect will therefore reduce as it is a function of this droplet diameter.

Due to the evaporative cooling effects of sprinkler spray on compartment temperatures, the method proposed by McCaffrey, Quintiere and Harkeleroid, printed in Walton and

Thomas (1992), for calculating the upper layer gas temperature, ceases to be valid post-sprinkler actuation.

An energy balance would need to be evaluated to accurately determine the temperature within the compartment at any time after sprinklers actuate.

5.12 Flow Out Of Compartment

The combined effects of evaporative cooling and drag due to sprinkler spray disturb the stability of the upper layer. If there is vigorous mixing between the upper and lower layers then smoke logging may occur, where the compartment could be considered as one zone. This zone would contain all the products of combustion and the steam from the sprinklers.

The model proposed by Rockett (1976) to determine the flow rate of gases out of a vent, assumed the compartment to have two distinct regions, one of which is a stably stratified upper layer. When sprinklers actuate the upper layer will no longer be stable and after a period of time the compartment will effectively be one zone. If the temperature of the floor and layer are not significantly different, then the model will still be valid.

The model assumes an average density of air in the hot layer, but if there is a large amount of water present in the layer, in the form of steam, then the density of this needs to be considered. An average density of the hot layer including all of the species within it will need to be determined.

Chapter 6
Conclusions

6.1 Summary

The two layer quasi-steady zone model produced for the prediction of smoke layer development compares well with the output of 'Firecalc'. The accuracy of zone models is limited however by the user inputs and the algorithms used in the analysis. The algorithms used in the model developed with this report are based on experimental data from various researchers, and as no two fires will display exactly the same characteristics this limits the accuracy of the model. Care should be taken when data is entered into zone models and the fire engineer should check the results to see that they are in fact reasonable.

The method detailed for determining detector actuation for growing fires, which accounts for transport lag, is recommended. Transport lag becomes quite significant when the distance from the detector to the fire source is relatively large and/or there are significant changes in the heat release rate. When transport lag is included, predicted detection times are longer, thus a larger fire size would be designed for by the fire engineer. The method detailed for detector actuation does not include the effects of the development of a hot upper layer. This would result in earlier actuation predictions, hence the model is conservative.

The interaction of a sprinkler spray with compartment fires is an extremely complicated problem. The spray may interact with a buoyant upper layer. The combining effects of drag and evaporative cooling may disturb the stability of a smoke layer and cause vigorous mixing with the cooler air below. This is known as smoke logging and at some time after sprinkler actuation, the compartment could be considered as a single zone.

The method detailed for the reduction in heat release rate post-sprinkler actuation,

does not account for the development of a hot smoke layer. If a relatively thick smoke layer is present, the water droplets may evaporate. This would result in less water coming into direct contact with the fire, hence the reduction in heat release rate may not be quite as significant. The expansion of the water to steam however, may displace oxygen from a compartment and this may offset less water contacting the fuel surface.

To date, the zone model developed is only valid for pre-sprinkler actuation. The method outlined for determining the upper layer temperature becomes invalid when sprinklers actuate. To accurately predict the temperature in a compartment post-sprinkler actuation, an energy balance would need to be performed.

The method for predicting vent flows proposed by Rockett (1976) will remain valid if the compartment is considered as a single zone and the temperature of the floor and layer are not significantly different. The model assumes an average density of air in the hot layer, but if a large amount of water is present, as steam, then the density of this needs to be considered. An average density of the hot layer including all of the species within it would need to be determined.

6.2 Future Work

This report provides a basis for the investigation on the effects of sprinklers on fire severity and smoke production. Some methods for determining the interaction of a sprinkler spray on a fire induced hot upper layer have been outlined. These may be incorporated into a model to predict the effects of sprinklers on compartment fires.

Further research on the reduction in heat release rate post-sprinkler actuation needs to be performed that includes the development of a hot upper layer in a compartment. Experiments should be performed to validate the predictions of a zone model for the effects of a sprinkler spray on a compartment fire. The model should be assessed with respect to a full compartment fire model simulation. Full scale testing to investigate

the drag and cooling effects of sprinkler spray on a hot upper layer needs to be performed.

Due to the complexity of the problem, zone models would provide very limited predictions. For increased accuracy on the effects of sprinkler sprays with compartment fires, three dimensional field modelling techniques should be used.

References

Alpert, R.L. 1972, "Calculation of Response Time of Ceiling Mounted Fire Detectors", *Fire Technology,* Vol. 8, pp181-195.

Barnett, C. 1994, "Fire Control And Water Supplies", *Fire Engineering Design Guide,* pg160.

Buchanan, A.H. 1994, Fire Engineering Design Guide, Centre For Advanced Engineering, University of Canterbury, Christchurch, NZ.

Bullen, M.L. 1974, "The Effect Of A Sprinkler On The Stability Of A Smoke Layer Beneath A Ceiling", Fire Research Note 1016, Fire Research Station, Borehamwood.

Beyler, C.L. 1978, "The Interaction of Fire and Sprinklers", NBS-GCR-78-121, National Bureau of Standards, Washington, DC.

Beyler, C.L. 1984, "A Design Method for Flaming Fire Protection", *Fire Technology,* Vol.20, No.4, pp5-15.

Beyler, C.L. 1986, "Fire Plumes and Ceiling Jets"; *Fire Safety Journal,* Vol. 11, pp 53-75.

Cetegen, B.M., Zukoski, E.E. and Kubota, T. 1982, "Entrainment and Flame Geometry of Fire Plumes", Report NBS-GCR-82-402, Centre for Fire Research, National Bureau of Standards, Gaithersburg, MD.

Chow, W.K. (1989), "On The Evaporation Effect Of A Sprinkler Water Spray", *Fire Technology,* Vol. 25, No. 4, pp364-373.

Chow, W.K. and Cheung, Y.L. 1994, "Simulation Of Sprinkler-Hot Layer Interaction Using A Field Model", *Fire And Materials,* Vol. 18, p359-379.

Chow, W.K. and Fong, N.K. 1991, "Numerical Simulation On Cooling Of The Fire Induced Air Flow By Sprinkler Water Sprays", *Fire Safety Journal,* Vol. 17, p263-290.

Cooper, L.Y. 1994, "The Interaction Of An Isolated Sprinkler Spray And A Two Layer Compartment Fire Environment", *Journal Of Heat And Mass Transfer,* Vol. 38, No. 4, p679-690.

Cox, G. And Chitty, R. 1980, "A Study of The Deterministic Properties of Unbounded Fire Plumes", *Combustion and Flame,* Vol. 39, pp191-209.

Cox, G. And Chitty, R. 1985, Some Source Dependant Effects of Unbounded Fires", *Combustion and Flame,* Vol. 60, pp219-232.

Deal, S. 1994, "Technical Reference Guide for FPEtool Version 3.2", Building and Fire Research Laboratory, National Institute of Standards and Technology, Gaithersburg.

Dillon, M.E 1991, "The Other Risk In Smoke Control Design", *Ashrae Journal,* Volume 33.

Drysdale, D. 1992, "An Introduction to Fire Dynamics", A Wiley-Interscience Publication.

Evans, D.D. and Stroup, D.W, 1985, "Methods to Calculate the Response Time of Heat and Smoke Detectors Installed Below Large Unobstructed Ceilings" *Fire Technology,* Vol.22, No. 1, pp54-65.

Evans, D.D. 1992a, "Ceiling Jet Flows", The SFPE Handbook of Fire Protection Engineering, Section1/Chapter9 , pp138-145.

Evans, D.D. 1992b, "Sprinkler Fire Suppression Algorithm For Hazard", *NISTIR 5245,* Building and Fire Research Laboratory, Gaithersburg.

Gross, D., Loftus, J.J, and Robertson, A.F, 1967. "Method for Measuring Smoke From Burning Materials", Symposium on Fire Test Methods-Restraint and Smoke, ASTM STP 422, American Society for Testing and Materials, pp166-294.

Heskestad, G.H. 1972, "Similarity Correlations for the Initial Convective Flow Generated by Fire", ASME Paper 72-WA/HT-17, American Society of Mechanical Engineers.

Heskestad, G.H. and Smith, H. 1976, "Investigation of a new Sprinkler Sensitivity Approval Test: The Plunge Test", FMRC Technical Report 22485, Factory Mutual Research Corporation, Norwood, MA.

Heskestad, G.H. and Delichatsios, M. 1977, "NBS-GCR-77-86 and NBS-GCR-77-95, National Bureau of Standards, Gaithersburg.

Heskestad, G.H. and Delichatsios, M. 1978, "The Initial Convective Flow in Fire", 17th International Symposium on Combustion, The Combustion Institute, pp1113-1123.

Heskestad, G.H. 1983, "Luminous Heights of Turbulent Diffusion Flames", *Fire Safety Journal,* Vol. 5, pp103.

Heskestad, G.H. 1990, "Sprinkler/Hot Layer Interaction", Technical Report FMRC J. I. OT1N2.RU, Factory Mutual Research Corporation, Norwood, MA.

Ingason, H. And Olsson, S. 1992, "Interaction Between Sprinklers And Fire Vents-Full Scale Experiments", *Fire Technology SP Report 1992:11,* Swedish National Testing And Research Institute, Sweden.

Kung, H.C. 1977, "Cooling Of Room Fires By Sprinkler Spray", *Journal Of Heat Transfer,* Vol 99, p353-359.

Madrzykowski, D. and Vettori, R.L, 1992, "A Sprinkler Fire Suppression Algorithm for the GSA Engineering Fire Assessment System", *NISTIR 4833,* National Technical Information Service, Springfield, VA.

Massey, B.S. 1968, "*Mechanics Of Fluids*", Van Nostrand, New York.

McCaffrey, B.J., 1979, "Purely Buoyant Diffusion Flames: Some Experimental Results", Report NBSIR 79-1910, Centre for Fire Research, National Bureau of Standards, Gaithersburg, MD.

McCaffrey, B.J., Quintiere, J., Harkeleroid, M. 1981, "Estimating Room Fire Temperatures and the Likelihood of Flashover Using Fire Test Data Correlations", *Fire Technology,* Vol. 17, No. 2, pp98-119.

Morgan, H.P. 1979, "Heat Transfer From A Buoyant Smoke Layer Beneath A Ceiling To A Sprinkler Spray", *Fire And Materials,* Vol 3, No. 1, p27-38.

Mawhinney, J.R. 1993, "Effects of Automatic Sprinkler Protection On A Smoke Control System", *Journal of Applied Fire Science,* Vol 3, No 1, pp 43-48.

NZS4541:1987, New Zealand Standard, "Automatic Fire Sprinkler Systems, Standards Association of New Zealand, pp19-26, 89-98.

Prahl, J.M. and Wendt, B. 1988, "Discharge Distribution Performance for an Axisymmetric Model of a Fire Sprinkler Head", *Fire Safety Journal,* Vol. 14, pp101-111.

Rockett, J.A. 1976, 'Fire Induced Gas Flow in an Enclosure", *Combined Science and Technology*, Vol 12, pp165-175.

Rogers, G.F.C. and Mayhew, Y.R 1991, "Thermodynamic And Transport Properties of Fluids", Fourth Edition.

Shestopal, V.O. and Grubits, S.J. 1993, "Computer Program for an Uninhibited Smoke Plume and Associated Computer Software", *Fire Technology,* Third Quarter, pp246-267.

Tewarson , A. and Pion, R.F. (1976), 'Flammability of Plastics. I. Burning Intensity", *Combustion and Flame,* Vol. 26, pp85-103.

Walton, W.D. 1988, "Suppression of Wood Crib Fires With Sprinkler Sprays: Test Results", *NISTIR 88-3696,* National Technical Information Service, Springfield, VA.

Whitaker, S. 1972, 'Forced Convection Heat-Transfer Correlations for Flow in Pipes, Past Flat Plates, Single Cylinders, Single Spheres, and Flow Packed Bids and Tube Bundles", *AIChemical Journal*, Vol. 18 pp361.

Zukoski, E.E., Kubota, T., and Cetegen, B. 1981, 'Entrainment in Fire Plumes", *Fire Safety Journal,* Vol. 3, pp107-121.

Appendix A

Sample Calculations For Steady State Conditions.

Model output shown at end of calculations.

User Inputs

$\dot{Q} = 1000$ kW

Plume Height, $Z_{max} = 10$ m

Area of Fire = 5 m²

Flame Temp = 986°C

Room Temp = 26°C

now, $A = \frac{\pi D^2}{4}$

so fire diameter is, $D = \left(\frac{5 \times 4}{\pi}\right)^{1/2}$

$= 2.5231$

Mean Flame Height

Heskestad, from Equation 2.1,

$$L = -1.02D + 0.235\dot{Q}^{2/5}$$
$$= -1.02(2.5231) + 0.235(1000)^{2/5}$$
$$= 1.1509$$

Virtual Origin

Heskestad from equation 2.32,

$$Z_0 = -1.02D + 0.083\dot{Q}^{2/5}$$
$$= -1.2581$$

Cox and Chitty From equation 2.33,

$$\frac{Z_0}{D} = -0.158\dot{Q}^{2/5} + 15.6\left(0.0607\frac{\dot{Q}^{2/5}}{D}\right)^5$$

$$Z_0 = -0.99248 + 0.125717$$
$$= -2.1869$$

$$\frac{\dot{Q}^{2/5}}{D} = \frac{1000^{2/5}}{2.523}$$
$$= 6.2815$$

Sample Calculations for Z=0.56m.

$$\frac{Z}{\dot{Q}^{2/5}} = \frac{0.56}{1000^{2/5}}$$
$$= 0.0353$$

Calculations using Cox and Chitty's correlations with Z_0=-2.1869m.

From Table 2.1, as $0.02 < 0.0353 < 0.06$, and $\frac{\dot{Q}^{2/5}}{D} < 10.2$, ***Continuous Flame Region***.

From equation 2.30 where $\frac{\dot{Q}^{2/5}}{D} < 10.2$, $\Delta T = 960°C$.

So Flame Temp = 960 + 26
= 986°C

From equation 2.31,

$$U_m = 6.83Z^{1/2}$$
$$= 6.83(0.56)^{1/2}$$
$$= 5.1111$$

Heskestad's correlations for temperature and velocity within the fire plume are only valid above the mean flame height so as Z<L, they are displayed as "N/A" in the model.

Mass Flow

From equation 2.39, where $0.03 < \frac{Z}{\dot{Q}^{2/5}} < 0.08$, Cox and Chitty's correlation predict the mass flow rate of entrainment to be,

$$\dot{m}_{ent} = 0.284\dot{Q}\tan^{-1}\left[3.34\left(\frac{Z}{\dot{Q}^{2/5}}\right)\right]^{1/2}.\left[\left(\frac{Z}{\dot{Q}^{2/5}}\right)^{5/2} + 0.32\left(\frac{Z}{\dot{Q}^{2/5}}\right)^{3/2} + 0.0256\left(\frac{Z}{\dot{Q}^{2/5}}\right)^{1/2}\right]$$

$$= 0.284(1000)\tan^{-1}\left[3.34(0.0353)\right]^{1/2}.\left[0.0353^{5/2} + 0.32(0.0353)^{3/2} + 0.0256(0.0353)^{1/2}\right]$$

$$= 284\tan^{-1}(0.3434)(0.00717)$$

$$= 0.6735$$

Noting that constant B1 displayed in the model is simply,

$$\left[\left(\frac{Z}{\dot{Q}^{2/5}}\right)^{5/2} + 0.32\left(\frac{Z}{\dot{Q}^{2/5}}\right)^{3/2} + 0.0256\left(\frac{Z}{\dot{Q}^{2/5}}\right)^{1/2}\right]$$

Heskestad's correlation, equation 2.36, predicts the entrainment to be,

$$\dot{m}_{ent} = 0.0056\dot{Q}_c\frac{Z}{L}$$

$$= 0.0056(0.7\times 1000)\left(\frac{0.56}{1.1509}\right)$$

$$= 1.9074$$

Sample Calculations for Z=1.82m.

$$\frac{Z}{\dot{Q}^{2/5}} = \frac{1.82}{1000^{2/5}}$$

$$= 0.1148$$

Calculations using Cox and Chitty's correlations with Z_0=-2.1869m.

From Table 2.1, as $0.06 < 0.1148 < 0.12$, and $\frac{\dot{Q}^{2/5}}{D} < 10.2$, ***Intermittent Flame Region.***

From equation 2.26 where $\frac{\dot{Q}^{2/5}}{D} < 10.2$,

$$\Delta T_m = 20.5\dot{Q}^{2/3}(Z - Z_0)^{-5/3}$$

$$= 20.5(1000)^{2/3}(1.82 + 2.1870)^{-5/3}$$

$$= 202.7939$$

$$T_m = 202.7939 + 26$$
$$= 228.7939°C$$

Equation 2.27 gives,

$$U_m = 1.65\dot{Q}^{1/5}$$
$$= 1.65(1000)^{1/5}$$
$$= 6.5688$$

Mass Flow

From equation 2.38, where $0.08 < \frac{Z}{Q^{2/5}} < 0.2$,

$$\dot{m}_{ent} = 0.272\dot{Q}\tan^{-1}\left[0.266\left(\frac{Z}{\dot{Q}^{2/5}}\right)^{-1}\right]^{1/2}.\left[\left(\frac{Z}{\dot{Q}^{2/5}}\right)^{5/2} + 0.32\left(\frac{Z}{\dot{Q}^{2/5}}\right)^{3/2} + 0.0256\left(\frac{Z}{\dot{Q}^{2/5}}\right)^{1/2}\right]$$
$$= 0.272(1000)\tan^{-1}\left[0.266(0.1148)\right]^{1/2}.\left[0.1148^{5/2} + 0.32(0.1148)^{3/2} + 0.0256(0.1148)^{1/2}\right]$$
$$= 272\tan^{-1}(1.5222)(0.0256)$$
$$= 6.8905$$

N.B.: differences due to rounding error.

Sample Calculations for Z=5m.

$$\frac{Z}{Q^{2/5}} = \frac{5}{1000^{2/5}}$$
$$= 0.3155$$

Calculations using Cox and Chitty's correlations with Z_0=-2.1869m.

From Table 2.1, as $0.3155 > 0.12$, and $\frac{\dot{Q}^{2/5}}{D} < 10.2$, ***Plume Region.***

From equation 2.22 where $\frac{\dot{Q}^{2/5}}{D} < 10.2$,

$$\Delta T_m = 20.5\dot{Q}^{2/3}(Z - Z_0)^{-5/3}$$
$$= 20.5(1000)^{2/3}(5 + 2.1870)^{-5/3}$$
$$= 76.5904$$

$$T_m = 76.5904 + 26$$
$$= 102.5904°C$$

From equation 2.23,

$$U_m = 0.89\dot{Q}^{1/3}(Z - Z_0)^{-1/3}$$
$$= 0.89(1000)^{1/3}(7.1870)^{-1/3}$$
$$= 4.6118$$

Mass Flow

From equation 2.37, where $\frac{Z}{\dot{Q}^{2/5}} > 0.2$,

$$\dot{m}_{ent} = 0.289\dot{Q}\tan^{-1}\left[0.0805\left(\frac{Z}{\dot{Q}^{2/5}}\right)^{-5/3}\right]^{1/2}.\left[\left(\frac{Z}{\dot{Q}^{2/5}}\right)^{5/2} + 0.32\left(\frac{Z}{\dot{Q}^{2/5}}\right)^{3/2} + 0.0256\left(\frac{Z}{\dot{Q}^{2/5}}\right)^{1/2}\right]$$
$$= 0.289(1000)\tan^{-1}\left[0.0805(0.3155)\right]^{1/2}.\left[0.3155^{5/2} + 0.32(0.3155)^{3/2} + 0.0256(0.3155)^{1/2}\right]$$
$$= 289\tan^{-1}(0.7419907)(0.1270)$$
$$= 23.4294$$

Calculations using Heskestad's correlations, with Z_0=-1.2581m.

Now Z > L so correlations for centreline temperature and velocity are valid.

$$Q_C = 0.7Q_T$$
$$= 700 \text{ kW}$$

From equation 2.14,

$$\Delta T_m = 9.1\left[\frac{T\infty}{gc_p^2\rho_\infty^2}\right]^{1/3}\dot{Q}_c^{2/3}(Z - Z_0)^{-5/3}$$

$$= 9.1\left[\frac{299}{9.81 \times 1.05^2 \times 1.2^2}\right]^{1/3}(0.7 \times 1000)^{2/3}(5 + 1.2581)^{-5/3}$$
$$= 90.3905$$

$$T_m = 90.3905 + 26$$
$$= 116.3905°C$$

From equation 2.15,

$$U_m = 3.4\left[\frac{g}{c_p \rho_\infty T_\infty}\right]^{1/3} \dot{Q}_c^{1/3}(Z - Z_0)^{-1/3}$$

$$= 3.4\left[\frac{9.81}{1.05 \times 1.2 \times 299}\right]^{1/3} (700)^{1/3}(5 + 1.2581)^{-1/3}$$

$$= 4.8556$$

From equation 2.35, as $Z > L$,

$$\dot{m}_{ent} = 0.071\dot{Q}_c^{1/3}(Z - Z_0)^{5/3}.[1 + 0.027\dot{Q}_c^{2/3}(Z - Z_0)^{-5/3}]$$

$$= 0.071(700)^{1/3}(6.2581)^{5/3}.[1 + 0.027(700)^{2/3}(6.2581)^{-5/3}]$$

$$= 14.7395 \text{ kg / s}$$

Mass Entrainment For Steady State Fire Using Heskestad and Cox & Chitty Correlations To Compare With FireCalc

User Inputs	
HRR (kW)	1000
Plume Height (m)	10
Area of Fire (m^2)	5
Flame Temp (°C)	986
Room Temp (°C)	26
Fire Diameter (m)	2.52313

Ambient Conditions	
g (m/s^2)	9.81
C_p (KJ/Kg.K)	1.05
ρ (Kg/m^3)	1.2
T (K)	299

Heskestad	
L =	1.150904
Z_0 =	-1.258134

Cox & Chitty	
L =	#N/A
Z_0 =	-2.18694977
$Q^{2/5}/D$	6.28145045

			Cox And Chitty					Heskestad					AVERAGE	FIRECALC PREDICTION		
Z (m)	$Z/Q^{2/5}$	Region	ΔT_m	Max Temp (°C)	Max Velocity (m/s)	Const B1	Mass Flow (kg/s)	IS Z > L	ΔT_m	Max Temp (°C)	Max Velocity (m/s)	M_{ent} (kg/s)	M_{ent} (kg/s)	Max Temp (°C)	Max Vel. (m/s)	M_{ent} (kg/s)
0.56	0.035334	Cont	960	986	5.11110399	0.007172	0.6740073	no	N/A	N/A	N/A	1.90737	1.2906889	983.9	1.03	2.48
1.2	0.075715	Int.	268.373276	294.3732757	6.56876831	0.015288	2.0231164	yes	429.06	455.05988	6.630081203	4.164398	3.093757	701.4	3.47	3.32
1.82	0.114834	Int.	202.708169	228.7081692	6.56876831	0.025596	6.888987	yes	294.927	320.92706	6.151176509	5.448069	6.1685282	501.5	3.91	4.51
2.46	0.155216	Plume	158.418986	184.4189864	5.33335731	0.039146	9.7794906	yes	215.271	241.27095	5.7758027	6.967464	8.3734772	366.6	3.95	6.06
3.09	0.194966	Plume	128.168783	154.1687829	5.11205699	0.055636	13.055967	yes	165.84	191.83987	5.482177014	8.644248	10.850108	279.3	3.87	7.92
3.71	0.234085	Plume	106.506181	132.5061812	4.92622447	0.075139	16.515824	yes	132.802	158.80211	5.243922442	10.46089	13.488355	222	3.77	10.02
4.35	0.274466	Plume	89.7005861	115.7005861	4.75990506	0.098891	19.855443	yes	108.517	134.51668	5.036334483	12.50166	16.178553	180.8	3.68	12.48
5	0.315479	Plume	76.5913124	102.5913124	4.61184961	0.126983	23.427493	yes	90.3897	116.38972	4.855557183	14.73967	19.08358	151.6	3.59	15.18
5.61	0.353967	Plume	66.8671223	92.86712232	4.4882988	0.157164	26.942022	yes	77.4098	103.40979	4.707327766	16.98618	21.964101	131.2	3.51	17.95
6.25	0.394348	Plume	58.6288562	84.6288562	4.37181241	0.192977	30.795687	yes	66.7278	92.727846	4.569584228	19.49055	25.143119	114.9	3.44	21.05
6.88	0.434099	Plume	51.997825	77.99782497	4.26811655	0.232547	34.753045	yes	58.3426	84.342594	4.44848789	22.09896	28.426	102.7	3.37	24.25
7.51	0.473849	Plume	46.4902574	72.49025741	4.1736077	0.276561	38.870717	yes	51.5247	77.524664	4.339286233	24.8456	31.85816	92.8	3.31	27.68
8.15	0.51423	Plume	41.7926443	67.79264432	4.08563161	0.325983	43.21562	yes	45.8164	71.816436	4.238571624	27.77391	35.494764	84.8	3.26	31.31
8.78	0.553981	Plume	37.8684419	63.86844194	4.00585036	0.37942	47.649795	yes	41.125	67.124959	4.147977207	30.78924	39.219515	78.2	3.21	35.09
9.42	0.594362	Plume	34.4527336	60.45273358	3.93082737	0.438717	52.311844	yes	37.0995	63.099511	4.063393691	33.98439	43.148118	72.8	3.16	39.03
10	0.630957	Plume	31.7635347	57.76353471	3.8674526	0.496942	56.672159	yes	33.969	59.969027	3.992380136	36.99263	46.832392	68.6	3.12	42.8

Sample calculations provided for shaded cells

Mass Entrainment For Steady State Fire Using Heskestad and Cox & Chitty Correlations To Compare With FireCalc

User Inputs	
HRR (kW)	1100
Plume Height (m)	27.7
Area of Fire (m^2)	1.71
Flame Temp (°C)	1006
Room Temp (°C)	26
Fire Diameter (m)	1.47555

Ambient Conditions	
g (m/s^2)	9.81
C_p (KJ/Kg.K)	1.05
ρ (Kg/m^3)	1.2
T (K)	299

Heskestad	
L =	2.364175
Z_0 =	-0.138478

Cox & Chitty	
L =	1.41766949
Z_0 =	0
$Q^{2/5}/D$	11.1584523

			Cox And Chitty					Heskestad						FIRECALC PREDICTION		
Z (m)	$Z/Q^{2/5}$	Region	ΔT_m	Max Temp (°C)	Max Velocit (m/s)	Const B1	Mass Flow (kg/s)	IS Z > L	ΔT_m	Max Temp (°C)	Max Velocity (m/s)	M_{ent} (kg/s)	AVERAGE M_{ent} (kg/s)	Max Tem (°C)	Max Vel. (m/s)	M_{ent} (kg/s)
0.97	0.058913	Cont.	980	1006	6.72676988	0.011632	1.5171545	no	N/A	N/A	N/A	1.769175	1.6431648	996.3	3.19	2.8
2.75	0.167023	Int.	467.002261	493.0022607	7.50672084	0.043706	11.778429	yes	349.414	375.41416	6.48577537	5.288536	8.5334823	394.8	4.18	6.44
4.64	0.275739	Plume	204.597318	230.597318	6.7329083	0.099702	21.959958	yes	156.416	182.41604	5.52268227	9.992624	15.976291	200.1	3.84	12.68
6.38	0.387493	Plume	116.044678	142.0446777	6.01101425	0.18659	33.142508	yes	89.9937	115.99366	4.94465717	16.27849	24.710501	126	3.58	21.22
8.09	0.491351	Plume	78.1169878	104.1169878	5.55356437	0.297389	44.807329	yes	61.0365	87.036516	4.57521754	23.3011	34.054214	93.6	3.4	30.68
9.92	0.602497	Plume	55.6083793	81.60837926	5.18860679	0.451287	58.597034	yes	43.6752	69.675223	4.27898564	31.97674	45.286884	74.3	3.25	42.22
11.75	0.713643	Plume	41.9369247	67.93692472	4.90390477	0.644775	73.688645	yes	33.0556	59.055608	4.04708972	41.77553	57.732087	62.6	3.12	55.12
13.45	0.816893	Plume	33.4802905	59.48029047	4.68792393	0.862535	88.83468	yes	26.4548	52.454784	3.87074576	51.83078	70.332731	55.3	3.02	68.11
15.45	0.938364	Plume	26.5733037	52.57330373	4.47622412	1.168634	107.99664	yes	21.0434	47.043407	3.69757518	64.77965	86.388143	49.4	2.92	84.67
17.12	1.039793	Plume	22.3951215	48.39512154	4.32567012	1.467863	125.07581	yes	17.7603	43.760346	3.5742431	76.48153	100.77867	45.8	2.84	99.38
18.99	1.153368	Plume	18.8416132	44.84161317	4.17874942	1.852494	145.33208	yes	14.962	40.961951	3.45375436	90.5101	117.92109	42.8	2.77	116.66
20.72	1.25844	Plume	16.2933395	42.29333946	4.05905311	2.257036	165.10924	yes	12.9514	38.951435	3.35550105	104.3313	134.72027	40.6	2.72	133.39
22.62	1.373838	Plume	14.0768459	40.07684591	3.94206502	2.757571	187.94993	yes	11.2	37.199971	3.25939638	120.4159	154.18292	38.7	2.66	152.46
24.33	1.477696	Plume	12.466834	38.46683398	3.84745853	3.260311	209.48631	yes	9.92607	35.92607	3.18162702	135.6805	172.58341	37.4	2.62	170.06
26.17	1.589449	Plume	11.0404511	37.04045114	3.75508763	3.858567	233.67403	yes	8.79622	34.796219	3.10565357	152.9187	193.29637	36.2	2.58	189.44
27.7	1.682375	Plume	10.0429217	36.04292168	3.68463716	4.402681	254.57174	yes	8.00534	34.00534	3.04768274	167.8803	211.22604	35.3	2.55	205.89

Comparison Of Maximum Temperature In Fire Plume
Q=1100kW, Zmax=27.7m, Fire Area=1.71m^2.

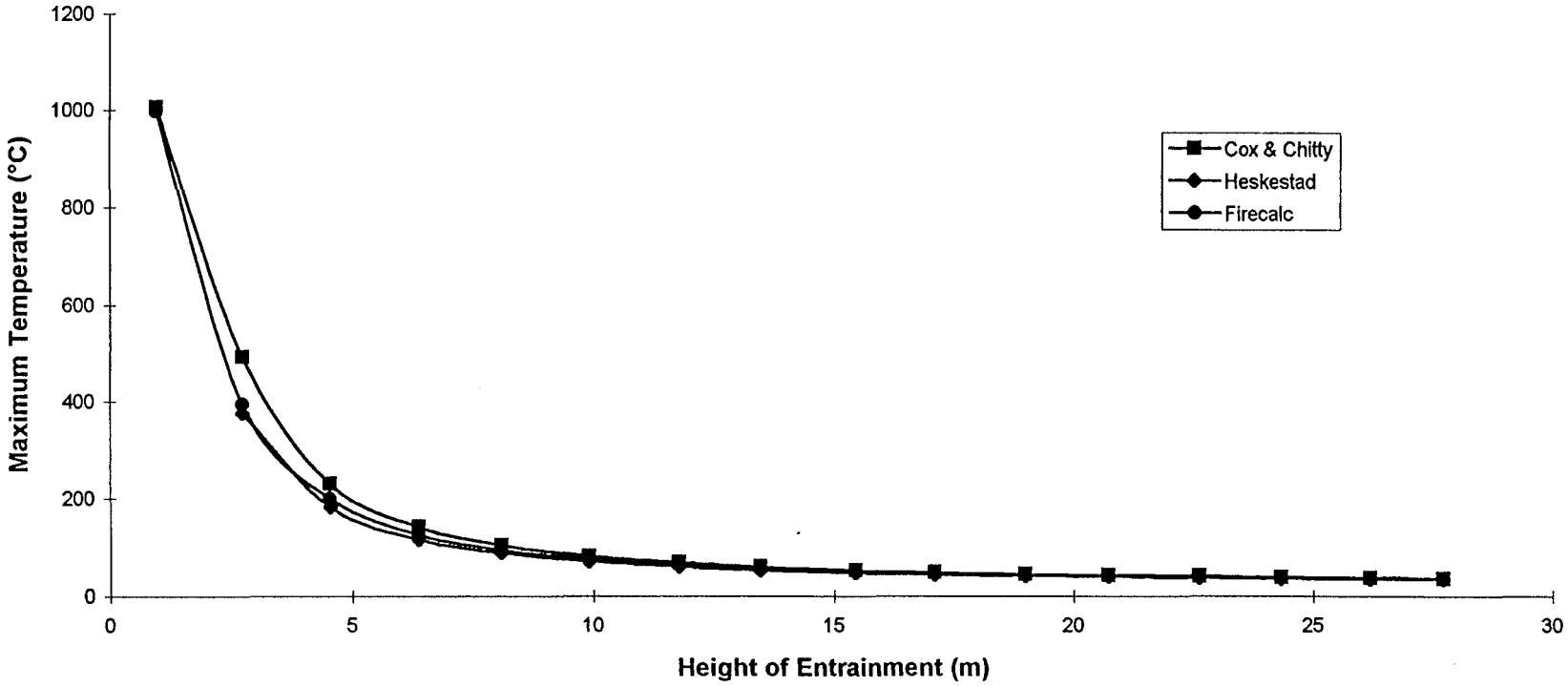

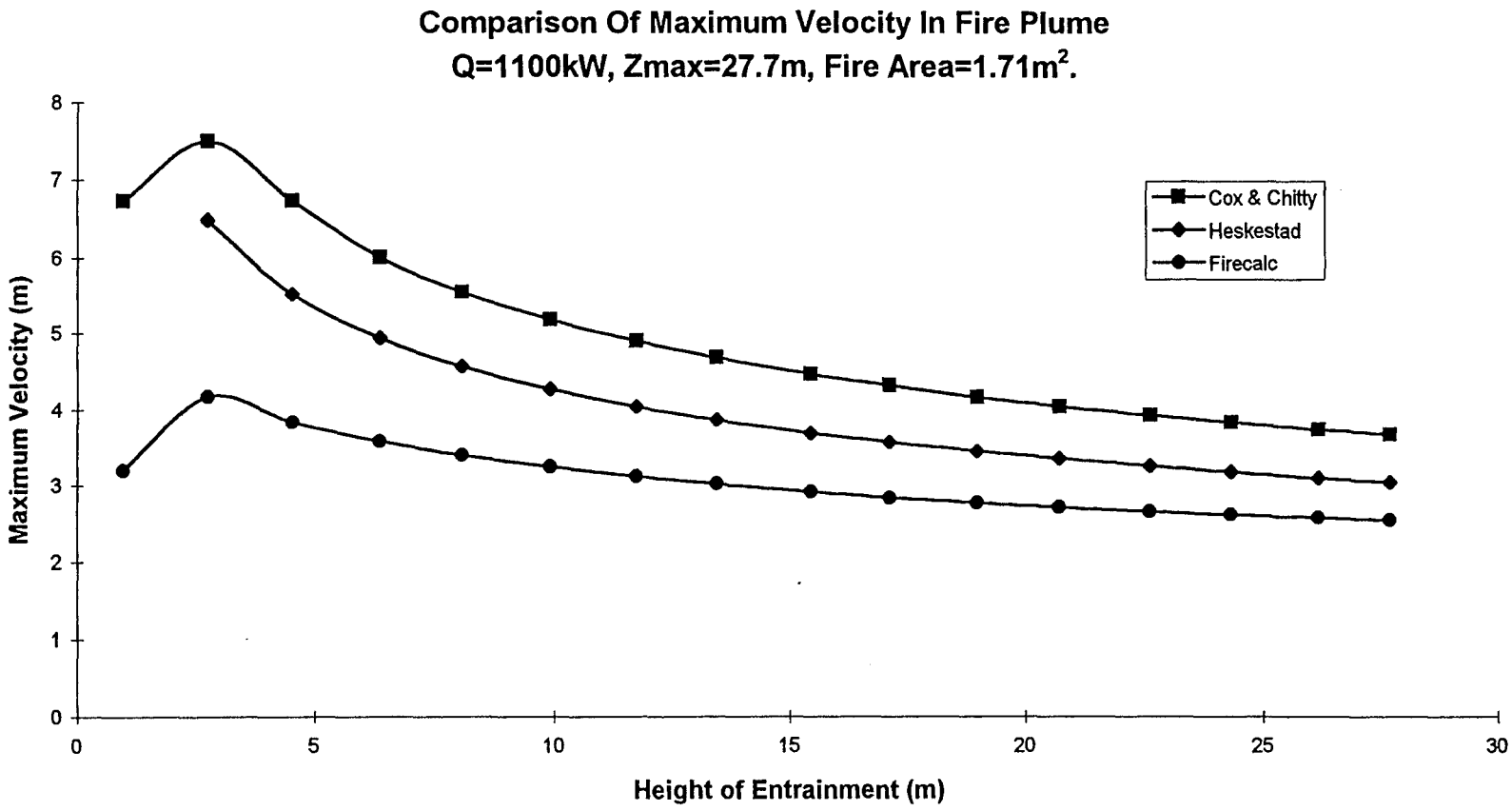
Comparison Of Maximum Velocity In Fire Plume
Q=1100kW, Zmax=27.7m, Fire Area=1.71m2.
Maximum Velocity (m)
Height of Entrainment (m)
Cox & Chitty
Heskestad
Firecalc
0
1
2
3
4
5
6
7
8
0
5
10
15
20
25
30

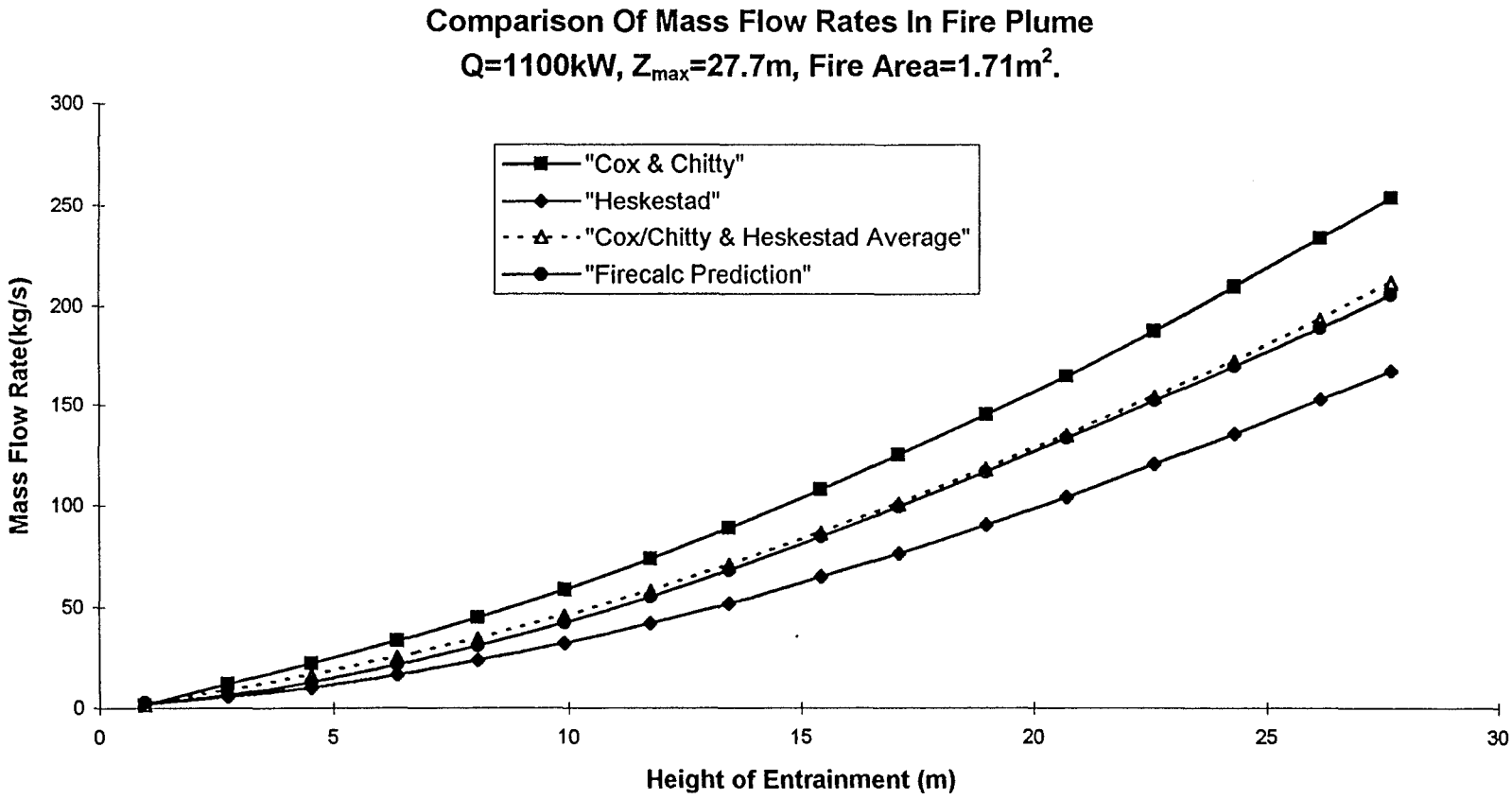
Comparison Of Mass Flow Rates In Fire Plume
Q=1100kW, Z_max=27.7m, Fire Area=1.71m².
"Cox & Chitty"
"Heskestad"
"Cox/Chitty & Heskestad Average"
"Firecalc Prediction"
Mass Flow Rate(kg/s)
Height of Entrainment (m)
0
50
100
150
200
250
300
0
5
10
15
20
25
30

Mass Entrainment For Steady State Fire Using Heskestad and Cox & Chitty Correlations To Compare With FireCalc

User Inputs	
HRR (kW)	2500
Plume Height (m)	27.7
Area of Fire (m^2)	1.71
Flame Temp (°C)	1006
Room Temp (°C)	26
Fire Diameter (m)	1.47555

Ambient Conditions	
g (m/s^2)	9.81
C_p (KJ/Kg.K)	1.05
ρ (Kg/m^3)	1.2
T (K)	299

Heskestad	
L =	3.868276
Z_ϕ =	0.392758

Cox & Chitty	
L =	4.57305052
Z_ϕ =	0
$Q^{2/5}/D$	15.4961171

			Cox And Chitty					Heskestad						FIRECALC PREDICTION		
Z (m)	$Z/Q^{2/5}$	Region	ΔT_m	Max Temp (°C)	Max Velocit (m/s)	Const B1	Mass Flow (kg/s)	IS Z > L	ΔT_m	Max Temp (°C)	Max Velocity (m/s)	M_{ent} (kg/s)	AVERAGE M_{ent} (kg/s)	Max Tem (°C)	Max Vel. (m/s)	M_{ent} (kg/s)
1.77	0.07741	Cont.	980	1006	9.086724	0.015682	5.2375553	no	N/A	N/A	N/A	4.484168	4.8608616	1000.2	7.2	6.398
3.53	0.154383	Int.	505.237876	531.2378761	8.84626062	0.038834	24.288637	no	N/A	N/A	N/A	8.943002	16.615819	534.1	6.06	11.15
5.3	0.231793	Plume	273.252907	299.2529069	8.40707913	0.073903	40.82899	yes	249.704	275.7035	7.14641435	15.47933	28.154162	297.4	5.1	19.43
7	0.306141	Plume	171.867796	197.8677956	7.66251042	0.120225	56.496126	yes	152.097	178.0968	6.4718327	23.26017	39.878149	192.7	4.61	30.3
8.69	0.380053	Plume	119.855586	145.8555859	7.12957813	0.179802	73.530267	yes	104.055	130.05529	5.99868562	32.45035	52.990308	140.3	4.34	43.01
10.5	0.459212	Plume	87.4397838	113.4397838	6.69381942	0.259828	93.339995	yes	74.8915	100.89152	5.61681087	43.78057	68.560282	108.8	4.15	58.22
12.3	0.537934	Plume	67.1711403	93.17114031	6.34992683	0.357267	114.60294	yes	56.9904	82.990414	5.3181873	56.47862	85.540779	89	3.99	75.35
13.9	0.607909	Plume	54.785619	80.78561901	6.09628822	0.459769	134.77775	yes	46.1894	72.189434	5.09931447	68.90115	101.83945	76.8	3.87	92.48
15.8	0.691005	Plume	44.2516459	70.25164589	5.84141502	0.602011	160.2535	yes	37.0919	63.091888	4.88044086	84.97775	122.61562	66.9	3.75	113.8
17.4	0.76098	Plume	37.6798495	63.67984951	5.65658098	0.739924	182.95493	yes	31.4604	57.46038	4.72232702	99.58853	141.27173	60.7	3.66	133.1
19.1	0.835329	Plume	32.2578656	58.25786559	5.48351837	0.905444	208.29662	yes	26.8413	52.841339	4.57471561	116.1491	162.22285	55.6	3.57	155.4
21.1	0.922798	Plume	27.3246001	53.32460009	5.30448151	1.126284	239.68527	yes	22.6612	48.661223	4.4224195	136.9553	188.32027	51.1	3.48	181.8
22.9	1.00152	Plume	23.8395893	49.83958931	5.16169015	1.350153	269.35845	yes	19.722	45.721956	4.30123591	156.8665	213.11245	48	3.41	206.9
24.4	1.067121	Plume	21.4474104	47.44741043	5.05367314	1.555543	295.09518	yes	17.7113	43.711282	4.20972054	174.2939	234.69453	45.7	3.36	229.6
26.1	1.14147	Plume	19.1700713	45.17007129	4.94147864	1.809675	325.35213	yes	15.8026	41.802579	4.11480123	194.9406	260.14638	43.7	3.3	254.6
27.7	1.211445	Plume	17.3603426	43.3603426	4.84444283	2.070183	354.86815	yes	14.2897	40.289731	4.03281293	215.2238	285.04596	42.1	3.25	279.8

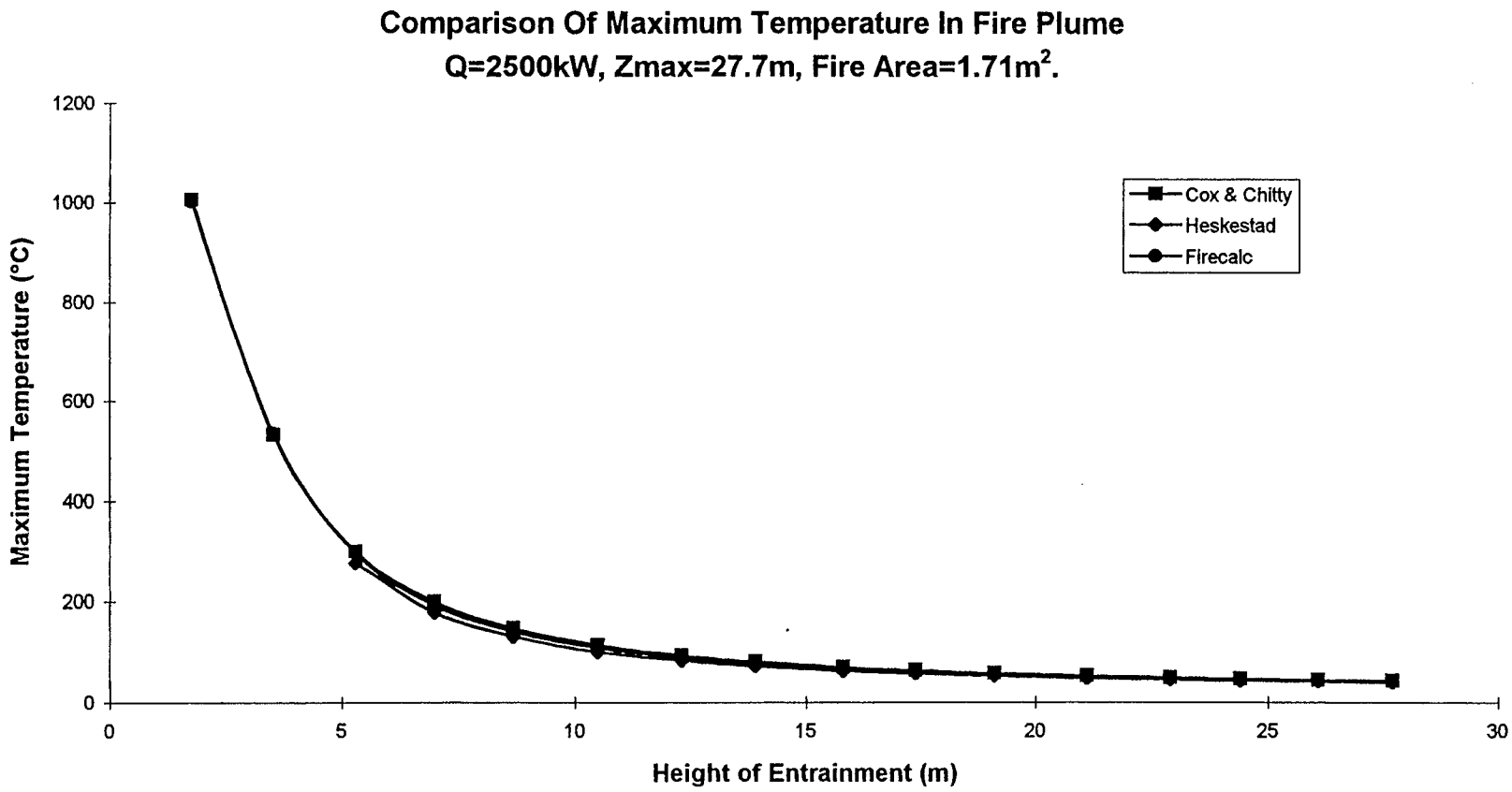
Comparison Of Maximum Temperature In Fire Plume
Q=2500kW, Zmax=27.7m, Fire Area=1.71m2.
Maximum Temperature (°C)
1200
1000
800
600
400
200
0
0
5
10
15
20
25
30
Height of Entrainment (m)
Cox & Chitty
Heskestad
Firecalc

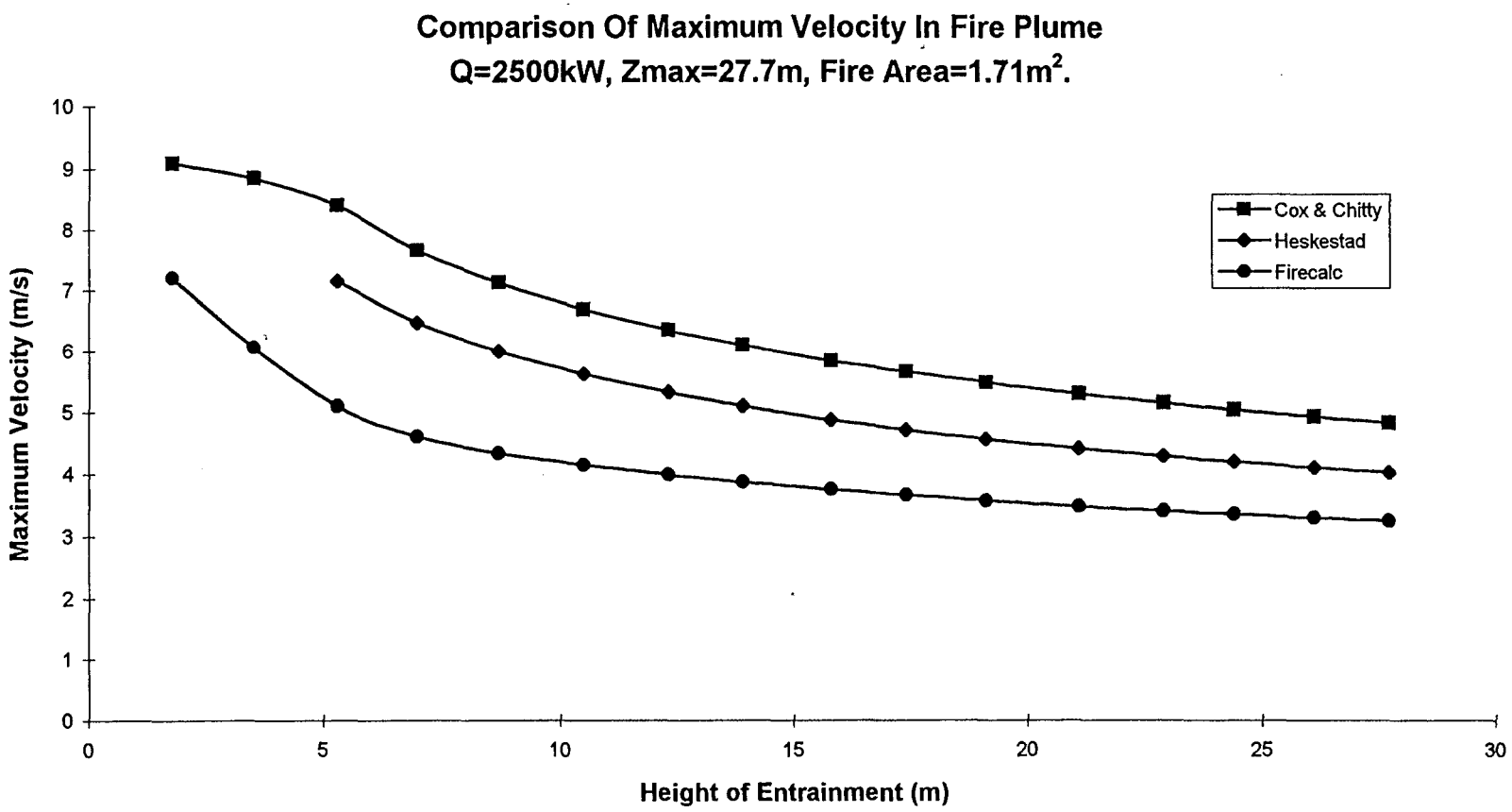
Comparison Of Maximum Velocity In Fire Plume
Q=2500kW, Zmax=27.7m, Fire Area=1.71m2.
Maximum Velocity (m/s)
Height of Entrainment (m)
Cox & Chitty
Heskestad
Firecalc
0
1
2
3
4
5
6
7
8
9
10
0
5
10
15
20
25
30

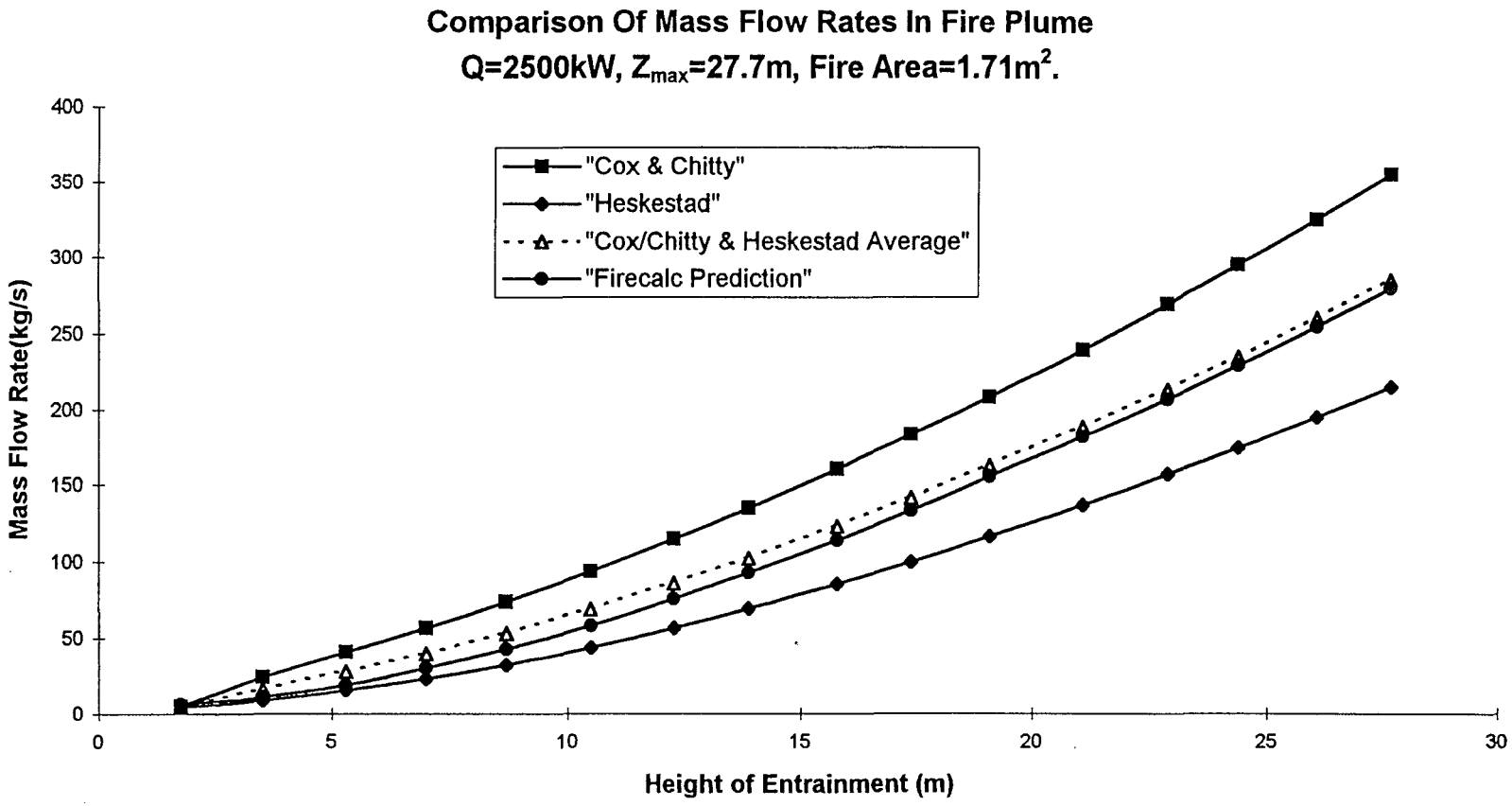
Comparison Of Mass Flow Rates In Fire Plume
Q=2500kW, Z_max=27.7m, Fire Area=1.71m^2.
"Cox & Chitty"
"Heskestad"
"Cox/Chitty & Heskestad Average"
"Firecalc Prediction"
Mass Flow Rate(kg/s)
Height of Entrainment (m)
0
50
100
150
200
250
300
350
400
0
5
10
15
20
25
30

Appendix B

Sample Calculations For Non Steady State Model.

Model Output shown at end of calculations.

Schematic of Trial Compartment

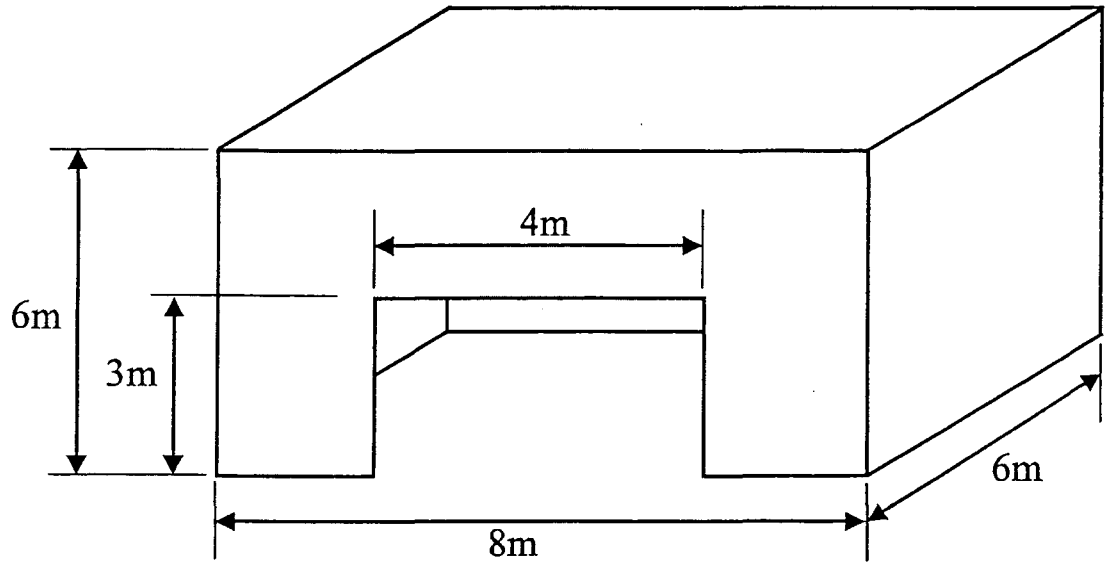

$A_0=12m^2$

$H_0=3m^2$

$A_T = [(6 x6) x 2]+[4(8 x 6)] - 12$

$= 252m^2$

Thermal penetration time t_p

From equation 3.7,

$$t_P = \left(\frac{\rho_c c}{k}\right)\left(\frac{\delta}{2}\right)^2$$

$$= \left(\frac{0.84 \text{ x } 1440}{4.8 \text{ x } 10^{-4}}\right)\left(\frac{0.016}{2}\right)^2$$

$$= 161.28$$

Calculations for t=161 seconds

Note: Differences between values for sample calculations and Model calculations are due to rounding.

For fast fire $\alpha = 0.0469$

Heat release rate

From equation 3.1,

$$\dot{Q} = \alpha t^2$$
$$= 0.0469\ (161)^2$$
$$= 1215.695\ \text{kW}$$

From equation 3.2,

$$\dot{Q}_c = 0.7\dot{Q}$$
$$= 850.986\ \text{kW}$$

Diameter of the fire

From equation 3.4

$$D = \left(\frac{4\dot{Q}}{\dot{m}''\pi\ \Delta H_c}\right)^{1/2}$$

$$= \left(\frac{4(1215.695)}{13\pi(16.7)}\right)^{1/2}$$
$$= 2.6702\ \text{m}$$

Mean flame height

Heskestad, from equation 2.1,

$$L = -1.02D + 0.235\dot{Q}^{2/5}$$
$$= -1.02(2.6702) + 0.235(1215.695)^{2/5}$$
$$= 1.3035\text{m}$$

Virtual origin

Heskestad from equation 2.32,

$$Z_0 = -1.02D + 0.083\dot{Q}^{2/5}$$
$$= -1.02(2.6702) + 0.083(1215.695)^{2/5}$$
$$= -1.3012$$

Effective heat transfer coefficient

From equation 3.6,

$$h_k = \left(\frac{k\rho_c c}{t}\right)^{1/2} \quad \text{for } t \le t_p$$

$$= \left(\frac{4.8\times10^{-4}(0.84)(1440)}{161}\right)^{1/2}$$

$$= 0.0601 \ \text{kW/mK}$$

Temperature of upper gas layer

From equation 3.5,

$$\Delta T_g = 480\left(\frac{\dot{Q}}{\sqrt{g}\, c_p \rho_\infty T_\infty A_0 \sqrt{H_0}}\right)^{2/3}\left(\frac{h_k A_T}{\sqrt{g}\, c_p \rho_\infty A_0 \sqrt{H_0}}\right)^{-1/3}$$

$$= 480\left(\frac{1215.695}{\sqrt{9.81}\times1.05\times1.2\times295\times12\sqrt{3}}\right)^{2/3}\left(\frac{0.0601\times252}{\sqrt{9.81}\times1.05\times1.2\times12\sqrt{3}}\right)^{-1/3} + 295$$

$$= 480(0.13616)(1.7561) + 295$$

$$= 409.77 \ \text{K}$$

Entrainment

Z = 1.7038 from calculation at t =161s

From equation 2.35, as Z > L

$$\dot{m}_{ent} = 0.071\dot{Q}_c^{1/3}(Z - Z_0)^{5/3}.[1 + 0.027\dot{Q}_c^{2/3}(Z - Z_0)^{-5/3}]$$

$$= 0.071(850.986)^{1/3}(1.7038 + 1.3012)^{5/3}.[1 + 0.027(850.986)^{2/3}(1.7038 + 1.3012)^{-5/3}]$$

$$= 4.2102(1.3875)$$

$$= 5.8416 \text{ kg/}s$$

Density of upper layer

From equation 3.8,

$$\rho_{UL} = \frac{352.8}{T_g}$$

$$= \frac{352.8}{409.77}$$

$$= 0.8610 \text{ kg/m}^3$$

Volumetric entrainment flowrate

From equation 3.9,

$$\dot{V}_{ent} = \frac{\dot{m}_{ent}}{\rho_{UL}}$$

$$= \frac{5.8416}{0.8610}$$

$$= 6.7847 \text{ m}^3/\text{s}$$

Fractional height to thermal discontinuity

Assuming $Z=Z_D$,

$$D_F = {}^{Z_D}\!/_{H_0}$$

$$= {}^{1.7038}\!/_{3}$$

$$= 0.5679$$

Mass flowrate out of compartment

Model prediction of fractional height of neutral plane, N_F, is 1.0022 this is proved below,

From equation 3.14,

$$\left[\frac{T_\infty}{T_g}\left(\frac{1-N_F}{N_F}\right)^3\right] = \left(1-\frac{D_F}{N_F}\right)\left(1+\frac{D_F}{2N_F}\right)^2\left(1+\frac{\dot{m}_{vf}}{\dot{m}_{in}}\right)^2$$

$$\text{now } \frac{\dot{m}_{vf}}{\dot{m}_{in}} = \frac{1}{15}$$

$$\left[\frac{295}{409.77}\left(\frac{1-0.6134}{0.6134}\right)^3\right] = \left(1-\frac{0.5679}{0.6134}\right)\left(1+\frac{0.5679}{2(0.6134)}\right)^2\left(\frac{16}{15}\right)^2$$

$0.18023 \approx 0.18062$ Difference of 0.00039

Mass flowrate out

From equation 3.13,

$$\dot{m}_{out} = \frac{2}{3}\rho_\infty A_o C\left[2gH_o\frac{T_\infty}{T_g}\left(1-\frac{T_\infty}{T_g}\right)\right]^{1/2}(1-N_F)^{3/2}$$

$$= \frac{2}{3}(1.2)(12)(0.7)\left[2(9.81)(3)\frac{295}{409.77}\left(1-\frac{295}{409.77}\right)\right]^{1/2}(1-0.6134)^{3/2}$$

$$= 6.72(3.9561)^{1/2}(0.24038)$$

$$= 5.5650 \text{ kg/}s$$

Volume flowrate remaining in compartment

From equation 3.15,

$$\dot{V}_{Remaining} = \frac{\dot{m}_{ent} - \dot{m}_{out}}{\rho_{U.L}}$$

$$= \frac{5.8416 - 5.5650}{0.8610}$$

$$= 0.3213 \ m^3/s$$

Smoke volume at 161 seconds

From equation 3.16,

$$V_{Smoke\ @\ 161s} = V_{Smoke\ @\ 160s} + \dot{V}_{Remaining}$$

$$= 206.2164 + 0.3213$$

$$= 206.5377 \ m^3$$

Elevation at 162 seconds

From equation 3.12,

$$Z_{t=162s} = H - h$$

$$= H - \frac{V_{smoke\ at\ 161s}}{A_{room}}$$

$$= 6 - \frac{206.5377}{48}$$

$$= 1.6971 \ m$$

Calculations for t = 162 seconds

For fast fire $\alpha = 0.0469$

Heat release rate

From equation 3.1,

$$\dot{Q} = \alpha t^2$$
$$= 0.0469\ (162)^2$$
$$= 1230.8436\ \text{kW}$$

From equation 3.2,

$$\dot{Q}_c = 0.7\dot{Q}$$
$$= 861.5905\ \text{kW}$$

Diameter of the fire

From equation 3.4,

$$D = \left(\frac{4\dot{Q}}{\dot{m}''\pi\ \Delta H_c} \right)^{1/2}$$

$$= \left(\frac{4(1230.8436)}{13\pi(16.7)} \right)^{1/2}$$
$$= 2.6867\ \text{m}$$

Mean flame height

Heskestad, from equation 2.1,

$$L = -1.02D + 0.235\dot{Q}^{2/5}$$
$$= -1.02(2.6867) + 0.235(1230.8436)^{2/5}$$
$$= 1.3067\text{m}$$

Virtual origin

Heskestad from equation 2.32,

$$\begin{aligned} Z_0 &= -1.02D + 0.083\dot{Q}^{2/5} \\ &= -1.02(2.6867) + 0.083(1230.8436)^{2/5} \\ &= -1.3110 \end{aligned}$$

Effective heat transfer coefficient

From equation 3.6,

$$\begin{aligned} h_k &= k/\delta \qquad \text{for } t > t_p \\ &= 4.8\times10^{-4}/0.016 \\ &= 0.03 \text{ kW/m}K \end{aligned}$$

Temperature of upper gas layer

From equation 3.5,

$$\Delta T_g = 480\left(\frac{\dot{Q}}{\sqrt{g}\, c_p \rho_\infty T_\infty A_0 \sqrt{H_0}}\right)^{2/3}\left(\frac{h_k A_T}{\sqrt{g}\, c_p \rho_\infty A_0 \sqrt{H_0}}\right)^{-1/3}$$

$$= 480\left(\frac{1230.8436}{\sqrt{9.81}\times1.05\times1.2\times295\times12\sqrt{3}}\right)^{2/3}\left(\frac{0.03\times252}{\sqrt{9.81}\times1.05\times1.2\times12\sqrt{3}}\right)^{-1/3} + 295$$

$$= 480(0.13728)(2.21382) + 295$$

$$= 440.8833 \text{ K}$$

Entrainment

Z = 1.6972 from calculation at t = 162s

From equation 2.35, as Z > L,

$$\dot{m}_{ent} = 0.071\dot{Q}_c^{1/3}(Z_D - Z_0)^{5/3}.[1 + 0.027\dot{Q}_c^{2/3}(Z_D - Z_0)^{-5/3}]$$

$$= 0.071(861.5905)^{1/3}(1.6972+1.3111)^{5/3}.[1+0.027(861.5905)^{2/3}(1.6972+1.3111)^{-5/3}]$$

$$= 4.7701(1.38997)$$

$$= 5.8870 \text{ kg/}s$$

Density of upper layer

From equation 3.8,

$$\rho_{UL} = \frac{352.8}{T_g}$$

$$= \frac{352.8}{440.8833}$$

$$= 0.8002 \text{ kg/m}^3$$

Volumetric entrainment flowrate

From equation 3.9,

$$\dot{V}_{ent} = \frac{\dot{m}_{ent}}{\rho_{UL}}$$

$$= \frac{5.8870}{0.8002}$$

$$= 7.3568 \text{ m}^3/\text{s}$$

Fractional height to thermal discontinuity

Assuming $Z=Z_D$,

$$D_F = {}^{Z_D}\!/_{H_0}$$

$$= {}^{1.6972}\!/_{3}$$

$$= 0.5657$$

Mass flowrate out of compartment

Model prediction of fractional height of neutral plane, N_F, is 0.6096 this is proved below,

From equation 3.14,

$$\left[\frac{T_\infty}{T_g}\left(\frac{1-N_F}{N_F}\right)^3\right] = \left(1-\frac{D_F}{N_F}\right)\left(1+\frac{D_F}{2N_F}\right)^2\left(1+\frac{\dot{m}_{vf}}{\dot{m}_{in}}\right)^2$$

$$\text{now } \frac{\dot{m}_{vf}}{\dot{m}_{in}} = \frac{1}{15}$$

$$\left[\frac{295}{440.8833}\left(\frac{1-0.6096}{0.6096}\right)^3\right] = \left(1-\frac{0.5657}{0.6096}\right)\left(1+\frac{0.5657}{2(0.6096)}\right)^2\left(\frac{16}{15}\right)^2$$

$$0.17575 \approx 0.17561 \qquad \text{Difference of } 0.00014$$

Mass flowrate out

From equation 3.13,

$$\dot{m}_{out} = \frac{2}{3}\rho_\infty A_o C\left[2gH_o\frac{T_\infty}{T_g}\left(1-\frac{T_\infty}{T_g}\right)\right]^{1/2}(1-N_F)^{3/2}$$

$$= \frac{2}{3}(1.2)(12)(0.7)\left[2(9.81)(3)\frac{295}{440.8833}\left(1-\frac{295}{440.8833}\right)\right]^{1/2}(1-0.6096)^{3/2}$$

$$= 6.72(13.0317)^{1/2}(0.2439)$$

$$= 5.9174 \text{ kg/s}$$

Volume flowrate remaining in compartment

From equation 3.15,

$$\dot{V}_{Remaining} = \frac{\dot{m}_{ent} - \dot{m}_{out}}{\rho_{U.L}}$$

$$= \frac{5.887 - 5.9174}{0.8002}$$

$$= -0.03805 \ m^3/s$$

Smoke volume at 162 seconds

From equation 3.16,

$$V_{Smoke\ @\ 162s} = V_{Smoke\ @\ 161s} + \dot{V}_{Remaining}$$

$$= 206.5364 + -0.03805$$

$$= 206.4984 \ m^3$$

Elevation at 163 seconds

From equation 3.12,

$$Z_{t=163s} = H - h$$

$$= H - \frac{V_{smoke\ at\ 162s}}{A_{room}}$$

$$= 6 - \frac{206.4984}{48}$$

$$= 1.6980 \ m$$

Data For Firecalc And Developed Model Comparison

	Height of Hot Layer		Hot Layer Temperature		Flow Of Smoke Through Opening	
Time t (s)	Model Height (m)	Firecalc Height (m)	Model Temp (°C)	Firecalc Temp (°C)	Model Mass Flo (kg/s)	Firecalc Mass Flow (kg/s)
0	6	6	21.85	22	0	0
9	5.84	5.68	23.37	22	0	0
18	5.47	5.19	26.14	22.7	0	0
27	5	4.58	29.73	24.1	0	0
36	4.48	3.96	33.99	26.2	0	0
45	3.94	3.36	38.81	29.3	0	0
54	3.41	2.81	44.15	33.1	0	0.024
63	2.9	2.34	49.95	38.2	0.093	0.631
72	2.5	2.04	56.18	44.4	1.055	1.635
81	2.27	1.89	62.82	52	1.925	2.417
90	2.15	1.82	69.83	61.4	2.524	2.981
99	2.07	1.79	77.21	72.5	2.97	3.412
108	2.02	1.78	84.92	85.4	3.35	3.76
117	1.97	1.77	92.97	99.9	3.712	4.056
126	1.92	1.76	101.33	115.9	4.075	4.324
135	1.87	1.74	110	133.1	4.445	4.572
144	1.81	1.73	118.96	151	4.825	4.811
153	1.76	1.7	128.2	169.2	5.214	5.048
162	1.7	1.67	167.74	187.3	5.917	5.279
171	1.67	1.63	178.64	205	6.15	5.525

Smoke Production for a t^2 Fire In a Compartment (Unconstrained)

Adjustable Variables In Bold Red

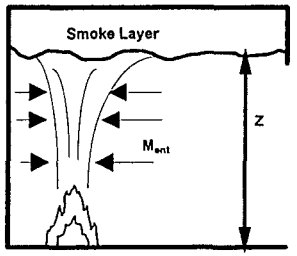

Table 1

Fire Type	α
Slow	0.00293
Medium	0.01172
Fast	0.0469
U Fast	0.1876

Using α = **0.0469**

Table 2

Properties Of Combustible	
Material =	*WOOD*
m" (g/m²s)	13
ΔHc (KJ/g)	16.7

Table 3

Compartment dimensions	
Area (m^2)	48
Height (m)	6
A_o (m^2)	12
H_o (m)	3
A_T (m^2)	252
δ (m)	0.016

Table 4: Thermal Properties

Material =>	Gypsum Plaster
k (KW/mK)	4.80E-04
ρ_c (Kg/m³)	0.84
c (KJ/Kg.K)	1440

Table 5

Ambient Conditions	
g (m/s²)	9.81
C_p (KJ/Kg.K)	1.05
ρ (Kg/m³)	1.2
T (K)	295

User Inputs In Tables 1-5

Thermal Penetration time (t_p) 161.28

Neutral Axis

t (s)	$Q = \alpha t^2$ (KW)	Qc (KW)	D (m)	L (m)	Z_o (m)	Z (m)	IS ($Z_o > L$) ?	M_{ent} (kg/s)	h_k (KW/mK)	T_g (°K)	$\rho_{U.L}$ (Kg/m³)	V_{ent} (m³/s)	D_F Z/H_o	N_F	Equation for N_F	Mass Flow Out (kg/s)	M_{ent} less M_{out} (kg/s)	$V_{remaining\ in\ compt.}$ (m³/s)	Smoke Volume (m³)
0	0.000	0.000	0.0000	0.0000	0.0000	6.0000	Yes	0.0000	#########	295.0000	1.1959	0.0000	2.0000	-	#VALUE!	0.0000	0.0000	0.0000	0.0000
1	0.047	0.033	0.0166	0.0522	0.0075	6.0000	Yes	0.4495	0.7620	295.0562	1.1957	0.3760	2.0000	1.9200	3.46E-04	0.0000	0.4495	0.3760	0.3760
2	0.188	0.131	0.0332	0.0865	0.0087	5.9922	Yes	0.7119	0.5388	295.1589	1.1953	0.5956	1.9974	1.9176	3.78E-09	0.0000	0.7119	0.5956	0.9718
3	0.422	0.295	0.0498	0.1157	0.0080	5.9798	Yes	0.9301	0.4399	295.2920	1.1947	0.7785	1.9933	1.9141	-6.18E-11	0.0000	0.9301	0.7785	1.7501
4	0.750	0.525	0.0663	0.1418	0.0063	5.9635	Yes	1.1225	0.3810	295.4496	1.1941	0.9400	1.9878	1.9095	-1.81E-10	0.0000	1.1225	0.9400	2.6901
5	1.173	0.821	0.0829	0.1659	0.0039	5.9440	Yes	1.2967	0.3408	295.6283	1.1934	1.0866	1.9813	1.9040	-3.87E-10	0.0000	1.2967	1.0866	3.7767
6	1.688	1.182	0.0995	0.1883	0.0008	5.9213	Yes	1.4568	0.3111	295.8259	1.1926	1.2215	1.9738	1.8976	-6.97E-10	0.0000	1.4568	1.2215	4.9982
7	2.298	1.609	0.1161	0.2094	-0.0026	5.8959	Yes	1.6050	0.2880	296.0408	1.1917	1.3468	1.9653	1.8904	-1.12E-09	0.0000	1.6050	1.3468	6.3450
8	3.002	2.101	0.1327	0.2294	-0.0065	5.8678	Yes	1.7432	0.2694	296.2716	1.1908	1.4639	1.9559	1.8824	-1.68E-09	0.0000	1.7432	1.4639	7.8089
9	3.799	2.659	0.1493	0.2486	-0.0107	5.8373	Yes	1.8723	0.2540	296.5173	1.1898	1.5736	1.9458	1.8738	-2.38E-09	0.0000	1.8723	1.5736	9.3825
10	4.690	3.283	0.1658	0.2669	-0.0152	5.8045	Yes	1.9932	0.2410	296.7771	1.1888	1.6767	1.9348	1.8645	-3.23E-09	0.0000	1.9932	1.6767	11.0592
11	5.675	3.972	0.1824	0.2845	-0.0199	5.7696	Yes	2.1066	0.2297	297.0502	1.1877	1.7737	1.9232	1.8545	-4.24E-09	0.0000	2.1066	1.7737	12.8329
12	6.754	4.728	0.1990	0.3015	-0.0248	5.7326	Yes	2.2129	0.2200	297.3361	1.1865	1.8650	1.9109	1.8440	-5.41E-09	0.0000	2.2129	1.8650	14.6979
13	7.926	5.548	0.2156	0.3180	-0.0299	5.6938	Yes	2.3127	0.2113	297.6341	1.1853	1.9510	1.8979	1.8329	-6.76E-09	0.0000	2.3127	1.9510	16.6490
14	9.192	6.435	0.2322	0.3339	-0.0353	5.6531	Yes	2.4061	0.2036	297.9438	1.1841	2.0320	1.8844	1.8213	-8.28E-09	0.0000	2.4061	2.0320	18.6809
15	10.553	7.387	0.2488	0.3494	-0.0407	5.6108	Yes	2.4936	0.1967	298.2647	1.1828	2.1081	1.8703	1.8091	-9.98E-09	0.0000	2.4936	2.1081	20.7891
16	12.006	8.404	0.2654	0.3644	-0.0464	5.5669	Yes	2.5754	0.1905	298.5966	1.1815	2.1797	1.8556	1.7965	-1.19E-08	0.0000	2.5754	2.1797	22.9688
17	13.554	9.488	0.2819	0.3791	-0.0521	5.5215	Yes	2.6517	0.1848	298.9390	1.1802	2.2469	1.8405	1.7834	-1.39E-08	0.0000	2.6517	2.2469	25.2157
18	15.196	10.637	0.2985	0.3933	-0.0580	5.4747	Yes	2.7228	0.1796	299.2916	1.1788	2.3099	1.8249	1.7699	-1.62E-08	0.0000	2.7228	2.3099	27.5256
19	16.931	11.852	0.3151	0.4073	-0.0640	5.4265	Yes	2.7889	0.1748	299.6542	1.1774	2.3688	1.8088	1.7560	-1.87E-08	0.0000	2.7889	2.3688	29.8944
20	18.760	13.132	0.3317	0.4209	-0.0702	5.3772	Yes	2.8502	0.1704	300.0264	1.1759	2.4238	1.7924	1.7417	-2.13E-08	0.0000	2.8502	2.4238	32.3182
21	20.683	14.478	0.3483	0.4342	-0.0764	5.3267	Yes	2.9067	0.1663	300.4081	1.1744	2.4751	1.7756	1.7271	-2.42E-08	0.0000	2.9067	2.4751	34.7933
22	22.700	15.890	0.3649	0.4472	-0.0828	5.2751	Yes	2.9588	0.1625	300.7989	1.1729	2.5227	1.7584	1.7120	7.04E-10	0.0000	2.9588	2.5227	37.3160

t (s)	$Q = \alpha t^2$ (KW)	Qc (KW)	D (m)	L (m)	Z_0 (m)	Z (m)	IS ($Z_0 > L$) ?	M_{ent} (kg/s)	h_k (KW/mK)	T_g (°K)	$\rho_{U,L}$ (Kg/m^3)	V_{ent} (m^3/s)	D_F Z/H_0	N_F	Equation for N_F	Mass Flow Out (kg/s)	M_{ent} less M_{out} (kg/s)	$V_{remaining\ in\ compt.}$ (m^3/s)	Smoke Volume (m^3)
23	24.810	17.367	0.3815	0.4599	-0.0892	5.2226	Yes	3.0066	0.1589	301.1987	1.1713	2.5668	1.7409	1.6967	8.13E-10	0.0000	3.0066	2.5668	39.8828
24	27.014	18.910	0.3980	0.4724	-0.0957	5.1691	Yes	3.0502	0.1555	301.6074	1.1697	2.6076	1.7230	1.6810	9.32E-10	0.0000	3.0502	2.6076	42.4904
25	29.313	20.519	0.4146	0.4847	-0.1024	5.1148	Yes	3.0898	0.1524	302.0246	1.1681	2.6451	1.7049	1.6651	1.06E-09	0.0000	3.0898	2.6451	45.1355
26	31.704	22.193	0.4312	0.4967	-0.1091	5.0597	Yes	3.1255	0.1494	302.4503	1.1665	2.6795	1.6886	1.6489	1.20E-09	0.0000	3.1255	2.6795	47.8150
27	34.190	23.933	0.4478	0.5085	-0.1158	5.0039	Yes	3.1576	0.1466	302.8842	1.1648	2.7108	1.6680	1.6324	1.36E-09	0.0000	3.1576	2.7108	50.5258
28	36.770	25.739	0.4644	0.5201	-0.1227	4.9474	Yes	3.1861	0.1440	303.3262	1.1631	2.7393	1.6491	1.6156	1.52E-09	0.0000	3.1861	2.7393	53.2651
29	39.443	27.610	0.4810	0.5314	-0.1296	4.8903	Yes	3.2112	0.1415	303.7763	1.1614	2.7649	1.6301	1.5987	1.71E-09	0.0000	3.2112	2.7649	56.0300
30	42.210	29.547	0.4975	0.5426	-0.1366	4.8327	Yes	3.2330	0.1391	304.2341	1.1596	2.7879	1.6109	1.5815	1.90E-09	0.0000	3.2330	2.7879	58.8179
31	45.071	31.550	0.5141	0.5536	-0.1437	4.7746	Yes	3.2516	0.1369	304.6996	1.1579	2.8083	1.5915	1.5641	2.11E-09	0.0000	3.2516	2.8083	61.6262
32	48.026	33.618	0.5307	0.5644	-0.1508	4.7161	Yes	3.2673	0.1347	305.1727	1.1561	2.8262	1.5720	1.5465	2.34E-09	0.0000	3.2673	2.8262	64.4525
33	51.074	35.752	0.5473	0.5751	-0.1580	4.6572	Yes	3.2801	0.1326	305.6533	1.1542	2.8418	1.5524	1.5288	2.58E-09	0.0000	3.2801	2.8418	67.2942
34	54.216	37.951	0.5639	0.5855	-0.1652	4.5980	Yes	3.2902	0.1307	306.1412	1.1524	2.8550	1.5327	1.5109	2.85E-09	0.0000	3.2902	2.8550	70.1493
35	57.453	40.217	0.5805	0.5959	-0.1725	4.5386	Yes	3.2976	0.1288	306.6363	1.1505	2.8661	1.5129	1.4928	3.13E-09	0.0000	3.2976	2.8661	73.0154
36	60.782	42.548	0.5971	0.6060	-0.1799	4.4788	Yes	3.3026	0.1270	307.1385	1.1487	2.8751	1.4929	1.4747	3.44E-09	0.0000	3.3026	2.8751	75.8905
37	64.206	44.944	0.6136	0.6160	-0.1873	4.4189	Yes	3.3052	0.1253	307.6478	1.1468	2.8822	1.4730	1.4563	3.77E-09	0.0000	3.3052	2.8822	78.7727
38	67.724	47.407	0.6302	0.6259	-0.1947	4.3589	Yes	3.3055	0.1236	308.1640	1.1448	2.8873	1.4530	1.4379	4.13E-09	0.0000	3.3055	2.8873	81.6600
39	71.335	49.934	0.6468	0.6358	-0.2022	4.2987	Yes	3.3038	0.1220	308.6870	1.1429	2.8907	1.4329	1.4193	4.52E-09	0.0000	3.3038	2.8907	84.5507
40	75.040	52.528	0.6634	0.6452	-0.2098	4.2385	Yes	3.3000	0.1205	309.2168	1.1409	2.8923	1.4128	1.4007	4.94E-09	0.0000	3.3000	2.8923	87.4430
41	78.839	55.187	0.6800	0.6547	-0.2174	4.1783	Yes	3.2942	0.1190	309.7533	1.1390	2.8923	1.3928	1.3820	5.40E-09	0.0000	3.2942	2.8923	90.3353
42	82.732	57.912	0.6966	0.6640	-0.2250	4.1180	Yes	3.2867	0.1176	310.2963	1.1370	2.8908	1.3727	1.3631	5.90E-09	0.0000	3.2867	2.8908	93.2260
43	86.718	60.703	0.7131	0.6732	-0.2327	4.0578	Yes	3.2775	0.1162	310.8458	1.1350	2.8878	1.3526	1.3443	6.45E-09	0.0000	3.2775	2.8878	96.1138
44	90.798	63.559	0.7297	0.6823	-0.2405	3.9976	Yes	3.2667	0.1149	311.4018	1.1329	2.8834	1.3325	1.3253	7.04E-09	0.0000	3.2667	2.8834	98.9972
45	94.973	66.481	0.7463	0.6912	-0.2482	3.9376	Yes	3.2544	0.1136	311.9641	1.1309	2.8777	1.3125	1.3063	7.70E-09	0.0000	3.2544	2.8777	101.8749
46	99.240	69.468	0.7629	0.7001	-0.2561	3.8776	Yes	3.2407	0.1123	312.5327	1.1288	2.8708	1.2925	1.2873	8.42E-09	0.0000	3.2407	2.8708	104.7457
47	103.602	72.521	0.7795	0.7088	-0.2639	3.8178	Yes	3.2257	0.1111	313.1075	1.1268	2.8627	1.2726	1.2682	9.22E-09	0.0000	3.2257	2.8627	107.6084
48	108.058	75.640	0.7961	0.7174	-0.2718	3.7582	Yes	3.2094	0.1100	313.6885	1.1247	2.8536	1.2527	1.2491	1.01E-08	0.0000	3.2094	2.8536	110.4620
49	112.607	78.825	0.8127	0.7260	-0.2797	3.6987	Yes	3.1920	0.1089	314.2755	1.1226	2.8435	1.2329	1.2300	1.11E-08	0.0000	3.1920	2.8435	113.3055
50	117.250	82.075	0.8292	0.7344	-0.2877	3.6395	Yes	3.1736	0.1078	314.8688	1.1205	2.8324	1.2132	1.2108	1.22E-08	0.0000	3.1736	2.8324	116.1379
51	121.987	85.391	0.8458	0.7427	-0.2957	3.5805	Yes	3.1541	0.1067	315.4676	1.1183	2.8204	1.1935	1.1917	1.34E-08	0.0000	3.1541	2.8204	118.9582
52	126.818	88.772	0.8624	0.7509	-0.3038	3.5217	Yes	3.1338	0.1057	316.0726	1.1162	2.8076	1.1739	1.1725	1.48E-08	0.0000	3.1338	2.8076	121.7658
53	131.742	92.219	0.8790	0.7590	-0.3118	3.4632	Yes	3.1126	0.1047	316.6833	1.1140	2.7940	1.1544	1.1534	1.63E-08	0.0000	3.1126	2.7940	124.5598
54	136.760	95.732	0.8956	0.7671	-0.3199	3.4050	Yes	3.0907	0.1037	317.2999	1.1119	2.7797	1.1350	1.1343	1.80E-08	0.0000	3.0907	2.7797	127.3395
55	141.873	99.311	0.9122	0.7750	-0.3281	3.3471	Yes	3.0681	0.1027	317.9222	1.1097	2.7648	1.1157	1.1153	2.00E-08	0.0000	3.0681	2.7648	130.1043
56	147.078	102.955	0.9288	0.7828	-0.3362	3.2895	Yes	3.0449	0.1018	318.5502	1.1075	2.7493	1.0965	1.0962	2.22E-08	0.0000	3.0449	2.7493	132.8536
57	152.378	106.665	0.9453	0.7906	-0.3444	3.2322	Yes	3.0211	0.1009	319.1838	1.1053	2.7332	1.0774	1.0773	2.47E-08	0.0000	3.0211	2.7332	135.5869
58	157.772	110.440	0.9619	0.7983	-0.3527	3.1753	Yes	2.9968	0.1001	319.8230	1.1031	2.7167	1.0584	1.0584	2.76E-08	0.0000	2.9968	2.7167	138.3036
59	163.259	114.281	0.9785	0.8058	-0.3609	3.1187	Yes	2.9721	0.0992	320.4677	1.1009	2.6997	1.0396	1.0395	3.08E-08	0.0000	2.9721	2.6997	141.0032
60	168.840	118.188	0.9951	0.8134	-0.3692	3.0624	Yes	2.9469	0.0984	321.1179	1.0987	2.6823	1.0208	1.0208	3.45E-08	0.0000	2.9469	2.6823	143.6855
61	174.515	122.160	1.0117	0.8208	-0.3776	3.0066	Yes	2.9214	0.0976	321.7738	1.0964	2.6645	1.0022	1.0022	3.87E-08	0.0000	2.9214	2.6645	146.3500
62	180.284	126.199	1.0283	0.8281	-0.3859	2.9510	Yes	2.8957	0.0968	322.4347	1.0942	2.6464	0.9837	0.9837	4.35E-08	0.0300	2.8657	2.6190	148.9691
63	186.146	130.302	1.0448	0.8354	-0.3943	2.8965	Yes	2.8704	0.0960	323.1011	1.0919	2.6288	0.9655	0.9655	4.67E-08	0.0931	2.7773	2.5435	151.5126
64	192.102	134.472	1.0614	0.8426	-0.4027	2.8435	Yes	2.8465	0.0952	323.7728	1.0897	2.6123	0.9478	0.9479	-3.09E-09	0.1745	2.6720	2.4521	153.9648
65	198.153	138.707	1.0780	0.8497	-0.4111	2.7924	Yes	2.8245	0.0945	324.4498	1.0874	2.5975	0.9308	0.9309	-3.00E-09	0.2688	2.5557	2.3503	156.3151
66	204.296	143.007	1.0946	0.8567	-0.4196	2.7434	Yes	2.8047	0.0938	325.1320	1.0851	2.5847	0.9145	0.9147	4.38E-08	0.3722	2.4325	2.2417	158.5568
67	210.534	147.374	1.1112	0.8637	-0.4281	2.6967	Yes	2.7873	0.0931	325.8194	1.0828	2.5741	0.8989	0.8994	4.02E-08	0.4817	2.3055	2.1292	160.6860
68	216.866	151.806	1.1278	0.8706	-0.4366	2.6524	Yes	2.7724	0.0924	326.5120	1.0805	2.5659	0.8841	0.8848	3.60E-08	0.5952	2.1773	2.0151	162.7011

t (s)	$Q = \alpha t^2$ (KW)	Qc (KW)	D (m)	L (m)	Z_o (m)	Z (m)	IS ($Z_D > L$) ?	M_{ent} (kg/s)	h_k (KW/mK)	T_g (°K)	ρ_{UL} (Kg/m^3)	V_{ent} (m^3/s)	D_F Z/H_o	N_F	Equation for N_F	Mass Flow Out (kg/s)	M_{ent} less M_{out} (kg/s)	$V_{remaining\ in\ compt}$ (m^3/s)	Smoke Volume (m^3)
69	223.291	156.304	1.1444	0.8774	-0.4451	2.6104	Yes	2.7603	0.0917	327.2096	1.0782	2.5601	0.8701	0.8711	3.14E-08	0.7106	2.0497	1.9010	164.6021
70	229.810	160.867	1.1609	0.8842	-0.4536	2.5708	Yes	2.7508	0.0911	327.9124	1.0759	2.5568	0.8589	0.8583	2.68E-08	0.8265	1.9244	1.7886	166.3907
71	236.423	165.496	1.1775	0.8908	-0.4622	2.5335	Yes	2.7440	0.0904	328.6202	1.0736	2.5560	0.8445	0.8463	2.24E-08	0.9416	1.8025	1.6789	168.0697
72	243.130	170.191	1.1941	0.8975	-0.4708	2.4985	Yes	2.7399	0.0898	329.3329	1.0713	2.5577	0.8328	0.8351	1.83E-08	1.0549	1.6850	1.5729	169.6426
73	249.930	174.951	1.2107	0.9040	-0.4795	2.4658	Yes	2.7384	0.0892	330.0507	1.0689	2.5619	0.8219	0.8247	1.47E-08	1.1658	1.5726	1.4712	171.1138
74	256.824	179.777	1.2273	0.9105	-0.4881	2.4351	Yes	2.7395	0.0886	330.7734	1.0666	2.5684	0.8117	0.8150	1.16E-08	1.2737	1.4658	1.3743	172.4880
75	263.813	184.669	1.2439	0.9169	-0.4968	2.4065	Yes	2.7429	0.0880	331.5009	1.0643	2.5773	0.8022	0.8061	8.98E-09	1.3781	1.3648	1.2824	173.7705
76	270.894	189.626	1.2604	0.9233	-0.5055	2.3798	Yes	2.7487	0.0874	332.2334	1.0619	2.5885	0.7933	0.7978	6.89E-09	1.4789	1.2699	1.1958	174.9663
77	278.070	194.649	1.2770	0.9296	-0.5142	2.3549	Yes	2.7568	0.0868	332.9707	1.0596	2.6018	0.7850	0.7901	5.23E-09	1.5758	1.1809	1.1146	176.0809
78	285.340	199.738	1.2936	0.9359	-0.5229	2.3316	Yes	2.7669	0.0863	333.7128	1.0572	2.6172	0.7772	0.7830	3.94E-09	1.6689	1.0980	1.0386	177.1195
79	292.703	204.892	1.3102	0.9420	-0.5317	2.3100	Yes	2.7791	0.0857	334.4596	1.0548	2.6346	0.7700	0.7764	2.94E-09	1.7581	1.0209	0.9679	178.0873
80	300.160	210.112	1.3268	0.9482	-0.5405	2.2898	Yes	2.7931	0.0852	335.2112	1.0525	2.6539	0.7633	0.7703	2.18E-09	1.8436	0.9495	0.9022	178.9896
81	307.711	215.398	1.3434	0.9542	-0.5493	2.2711	Yes	2.8090	0.0847	335.9675	1.0501	2.6750	0.7570	0.7647	1.62E-09	1.9254	0.8836	0.8414	179.8310
82	315.356	220.749	1.3600	0.9602	-0.5581	2.2535	Yes	2.8265	0.0841	336.7285	1.0477	2.6977	0.7512	0.7595	1.19E-09	2.0037	0.8228	0.7853	180.6163
83	323.094	226.166	1.3765	0.9662	-0.5669	2.2372	Yes	2.8456	0.0836	337.4942	1.0454	2.7221	0.7457	0.7546	8.82E-10	2.0786	0.7669	0.7337	181.3500
84	330.926	231.648	1.3931	0.9721	-0.5758	2.2219	Yes	2.8662	0.0831	338.2644	1.0430	2.7481	0.7406	0.7501	6.52E-10	2.1504	0.7157	0.6862	182.0362
85	338.853	237.197	1.4097	0.9780	-0.5846	2.2076	Yes	2.8881	0.0826	339.0393	1.0406	2.7754	0.7359	0.7460	4.83E-10	2.2192	0.6689	0.6428	182.6790
86	346.872	242.811	1.4263	0.9837	-0.5935	2.1942	Yes	2.9113	0.0822	339.8188	1.0382	2.8042	0.7314	0.7421	3.60E-10	2.2853	0.6261	0.6030	183.2820
87	354.988	248.490	1.4429	0.9895	-0.6025	2.1816	Yes	2.9358	0.0817	340.6027	1.0358	2.8343	0.7272	0.7384	-1.27E-08	2.3487	0.5871	0.5668	183.8488
88	363.194	254.236	1.4595	0.9952	-0.6114	2.1698	Yes	2.9613	0.0812	341.3913	1.0334	2.8656	0.7233	0.7350	-1.01E-08	2.4098	0.5516	0.5337	184.3825
89	371.495	260.046	1.4761	1.0008	-0.6203	2.1587	Yes	2.9879	0.0808	342.1843	1.0310	2.8980	0.7196	0.7318	-8.14E-09	2.4686	0.5194	0.5037	184.8862
90	379.890	265.923	1.4926	1.0064	-0.6293	2.1482	Yes	3.0155	0.0803	342.9817	1.0286	2.9316	0.7161	0.7288	-6.59E-09	2.5254	0.4902	0.4765	185.3628
91	388.379	271.865	1.5092	1.0119	-0.6383	2.1383	Yes	3.0440	0.0799	343.7836	1.0262	2.9662	0.7128	0.7260	-5.38E-09	2.5803	0.4637	0.4519	185.8146
92	396.962	277.873	1.5258	1.0174	-0.6473	2.1289	Yes	3.0733	0.0794	344.5900	1.0238	3.0018	0.7096	0.7233	-4.44E-09	2.6335	0.4399	0.4296	186.2443
93	405.638	283.947	1.5424	1.0229	-0.6563	2.1199	Yes	3.1035	0.0790	345.4007	1.0214	3.0384	0.7066	0.7208	-3.69E-09	2.6851	0.4184	0.4096	186.6538
94	414.408	290.086	1.5590	1.0283	-0.6654	2.1114	Yes	3.1343	0.0786	346.2158	1.0190	3.0758	0.7038	0.7184	-3.10E-09	2.7353	0.3990	0.3915	187.0454
95	423.273	296.291	1.5756	1.0336	-0.6744	2.1032	Yes	3.1659	0.0782	347.0352	1.0166	3.1141	0.7011	0.7161	-2.63E-09	2.7843	0.3816	0.3754	187.4208
96	432.230	302.561	1.5921	1.0389	-0.6835	2.0954	Yes	3.1981	0.0778	347.8590	1.0142	3.1533	0.6985	0.7139	-2.25E-09	2.8321	0.3660	0.3609	187.7818
97	441.282	308.897	1.6087	1.0442	-0.6926	2.0879	Yes	3.2308	0.0774	348.6871	1.0118	3.1932	0.6960	0.7118	-1.95E-09	2.8788	0.3520	0.3479	188.1295
98	450.428	315.299	1.6253	1.0494	-0.7017	2.0806	Yes	3.2642	0.0770	349.5194	1.0094	3.2338	0.6935	0.7098	-1.71E-09	2.9246	0.3396	0.3364	188.4659
99	459.667	321.767	1.6419	1.0545	-0.7108	2.0736	Yes	3.2980	0.0766	350.3560	1.0070	3.2752	0.6912	0.7078	-1.51E-09	2.9696	0.3284	0.3262	188.7921
100	469.000	328.300	1.6585	1.0596	-0.7199	2.0668	Yes	3.3324	0.0762	351.1969	1.0046	3.3172	0.6889	0.7060	-1.35E-09	3.0138	0.3185	0.3171	189.1092
101	478.427	334.899	1.6751	1.0647	-0.7291	2.0602	Yes	3.3671	0.0758	352.0419	1.0022	3.3599	0.6867	0.7041	-1.22E-09	3.0574	0.3097	0.3091	189.4183
102	487.948	341.563	1.6917	1.0697	-0.7382	2.0538	Yes	3.4023	0.0754	352.8912	0.9997	3.4032	0.6846	0.7023	-1.11E-09	3.1004	0.3020	0.3020	189.7203
103	497.562	348.293	1.7082	1.0747	-0.7474	2.0475	Yes	3.4379	0.0751	353.7446	0.9973	3.4471	0.6825	0.7006	-1.03E-09	3.1429	0.2951	0.2959	190.0162
104	507.270	355.089	1.7248	1.0797	-0.7566	2.0413	Yes	3.4739	0.0747	354.6022	0.9949	3.4917	0.6804	0.6989	-9.56E-10	3.1849	0.2890	0.2905	190.3066
105	517.073	361.951	1.7414	1.0846	-0.7658	2.0353	Yes	3.5102	0.0744	355.4639	0.9925	3.5367	0.6784	0.6973	-8.97E-10	3.2265	0.2837	0.2858	190.5925
106	526.968	368.878	1.7580	1.0894	-0.7751	2.0293	Yes	3.5469	0.0740	356.3297	0.9901	3.5824	0.6764	0.6956	-8.49E-10	3.2679	0.2790	0.2818	190.8743
107	536.958	375.871	1.7746	1.0942	-0.7843	2.0235	Yes	3.5838	0.0737	357.1996	0.9877	3.6285	0.6745	0.6940	-8.09E-10	3.3089	0.2749	0.2784	191.1526
108	547.042	382.929	1.7912	1.0990	-0.7935	2.0177	Yes	3.6211	0.0733	358.0736	0.9853	3.6752	0.6726	0.6925	-7.77E-10	3.3497	0.2714	0.2754	191.4281
109	557.219	390.053	1.8077	1.1038	-0.8028	2.0119	Yes	3.6586	0.0730	358.9517	0.9829	3.7224	0.6706	0.6909	-7.52E-10	3.3903	0.2683	0.2730	191.7011
110	567.490	397.243	1.8243	1.1085	-0.8121	2.0062	Yes	3.6964	0.0727	359.8338	0.9805	3.7701	0.6687	0.6894	-7.31E-10	3.4308	0.2657	0.2710	191.9721
111	577.855	404.498	1.8409	1.1131	-0.8214	2.0006	Yes	3.7345	0.0723	360.7199	0.9780	3.8183	0.6669	0.6878	-7.15E-10	3.4711	0.2634	0.2693	192.2414
112	588.314	411.820	1.8575	1.1177	-0.8307	1.9950	Yes	3.7728	0.0720	361.6100	0.9756	3.8670	0.6650	0.6863	-7.03E-10	3.5113	0.2615	0.2680	192.5094
113	598.866	419.206	1.8741	1.1223	-0.8400	1.9894	Yes	3.8113	0.0717	362.5040	0.9732	3.9161	0.6631	0.6848	-6.95E-10	3.5514	0.2599	0.2670	192.7764
114	609.512	426.659	1.8907	1.1269	-0.8494	1.9838	Yes	3.8500	0.0714	363.4021	0.9708	3.9657	0.6613	0.6833	-6.89E-10	3.5915	0.2585	0.2663	193.0427

t (s)	$Q = \alpha t^2$ (KW)	Qc (KW)	D (m)	L (m)	Z_0 (m)	Z (m)	IS ($Z_0 > L$) ?	M_{ent} (kg/s)	h_k (KW/mK)	T_g (°K)	$\rho_{U,L}$ (Kg/m^3)	V_{ent} (m^3/s)	D_F Z/H_0	N_F	Equation for N_F	Mass Flow Out (kg/s)	M_{ent} less M_{out} (kg/s)	$V_{remaining\ in\ compt.}$ (m^3/s)	Smoke Volume (m^3)
115	620.253	434.177	1.9073	1.1314	-0.8587	1.9783	Yes	3.8890	0.0711	364.3041	0.9684	4.0158	0.6594	0.6818	-6.86E-10	3.6316	0.2574	0.2658	193.3084
116	631.086	441.760	1.9238	1.1358	-0.8681	1.9727	Yes	3.9281	0.0707	365.2100	0.9660	4.0663	0.6576	0.6803	-6.86E-10	3.6716	0.2565	0.2655	193.5739
117	642.014	449.410	1.9404	1.1403	-0.8775	1.9672	Yes	3.9674	0.0704	366.1199	0.9636	4.1172	0.6557	0.6789	-6.87E-10	3.7117	0.2557	0.2654	193.8393
118	653.036	457.125	1.9570	1.1447	-0.8868	1.9617	Yes	4.0070	0.0701	367.0336	0.9612	4.1686	0.6539	0.6774	-6.91E-10	3.7518	0.2552	0.2655	194.1048
119	664.151	464.906	1.9736	1.1490	-0.8962	1.9562	Yes	4.0467	0.0699	367.9512	0.9588	4.2205	0.6521	0.6759	-6.96E-10	3.7919	0.2548	0.2657	194.3705
120	675.360	472.752	1.9902	1.1533	-0.9057	1.9506	Yes	4.0866	0.0696	368.8727	0.9564	4.2728	0.6502	0.6745	-7.02E-10	3.8321	0.2545	0.2661	194.6365
121	686.663	480.664	2.0068	1.1576	-0.9151	1.9451	Yes	4.1266	0.0693	369.7980	0.9540	4.3255	0.6484	0.6730	-7.10E-10	3.8723	0.2543	0.2666	194.9031
122	698.060	488.642	2.0234	1.1619	-0.9245	1.9395	Yes	4.1669	0.0690	370.7272	0.9516	4.3788	0.6465	0.6715	-7.20E-10	3.9126	0.2542	0.2671	195.1702
123	709.550	496.685	2.0399	1.1661	-0.9340	1.9340	Yes	4.2073	0.0687	371.6602	0.9493	4.4322	0.6447	0.6701	-7.30E-10	3.9530	0.2542	0.2678	195.4380
124	721.134	504.794	2.0565	1.1703	-0.9434	1.9284	Yes	4.2478	0.0684	372.5970	0.9469	4.4862	0.6428	0.6686	-7.42E-10	3.9935	0.2543	0.2686	195.7068
125	732.813	512.969	2.0731	1.1744	-0.9529	1.9228	Yes	4.2885	0.0682	373.5375	0.9445	4.5406	0.6409	0.6672	-7.54E-10	4.0340	0.2545	0.2695	195.9761
126	744.584	521.209	2.0897	1.1786	-0.9624	1.9172	Yes	4.3294	0.0679	374.4818	0.9421	4.5955	0.6391	0.6657	-7.68E-10	4.0747	0.2547	0.2704	196.2465
127	756.450	529.515	2.1063	1.1828	-0.9719	1.9115	Yes	4.3704	0.0676	375.4299	0.9397	4.6507	0.6372	0.6642	-7.82E-10	4.1154	0.2550	0.2713	196.5178
128	768.410	537.887	2.1229	1.1867	-0.9814	1.9059	Yes	4.4116	0.0673	376.3818	0.9373	4.7065	0.6353	0.6628	-7.97E-10	4.1563	0.2553	0.2724	196.7902
129	780.463	546.324	2.1394	1.1907	-0.9909	1.9002	Yes	4.4529	0.0671	377.3373	0.9350	4.7626	0.6334	0.6613	-8.14E-10	4.1972	0.2557	0.2735	197.0637
130	792.610	554.827	2.1560	1.1947	-1.0005	1.8945	Yes	4.4943	0.0668	378.2966	0.9326	4.8191	0.6315	0.6598	-8.30E-10	4.2383	0.2561	0.2746	197.3382
131	804.851	563.396	2.1726	1.1986	-1.0100	1.8888	Yes	4.5359	0.0666	379.2595	0.9302	4.8761	0.6296	0.6584	-8.48E-10	4.2794	0.2565	0.2757	197.6140
132	817.186	572.030	2.1892	1.2026	-1.0196	1.8830	Yes	4.5777	0.0663	380.2262	0.9279	4.9335	0.6277	0.6569	-8.66E-10	4.3207	0.2570	0.2769	197.8909
133	829.614	580.730	2.2058	1.2065	-1.0291	1.8773	Yes	4.6195	0.0661	381.1965	0.9255	4.9914	0.6258	0.6554	-8.85E-10	4.3621	0.2574	0.2782	198.1691
134	842.136	589.495	2.2224	1.2103	-1.0387	1.8715	Yes	4.6615	0.0658	382.1705	0.9231	5.0496	0.6238	0.6540	-9.05E-10	4.4036	0.2579	0.2794	198.4485
135	854.753	598.327	2.2390	1.2141	-1.0483	1.8657	Yes	4.7037	0.0656	383.1481	0.9208	5.1083	0.6219	0.6525	-9.25E-10	4.4452	0.2585	0.2807	198.7292
136	867.462	607.224	2.2555	1.2179	-1.0579	1.8598	Yes	4.7460	0.0653	384.1293	0.9184	5.1674	0.6199	0.6510	-9.46E-10	4.4870	0.2590	0.2820	199.0112
137	880.266	616.186	2.2721	1.2217	-1.0675	1.8539	Yes	4.7884	0.0651	385.1141	0.9161	5.2269	0.6180	0.6495	-9.68E-10	4.5288	0.2596	0.2833	199.2945
138	893.164	625.215	2.2887	1.2254	-1.0772	1.8480	Yes	4.8309	0.0649	386.1026	0.9137	5.2869	0.6160	0.6480	-9.90E-10	4.5708	0.2601	0.2847	199.5792
139	906.155	634.308	2.3053	1.2291	-1.0868	1.8421	Yes	4.8736	0.0646	387.0946	0.9114	5.3473	0.6140	0.6466	-1.01E-09	4.6129	0.2607	0.2861	199.8652
140	919.240	643.468	2.3219	1.2328	-1.0964	1.8361	Yes	4.9163	0.0644	388.0902	0.9091	5.4081	0.6120	0.6451	-1.04E-09	4.6550	0.2613	0.2874	200.1527
141	932.419	652.693	2.3385	1.2365	-1.1061	1.8302	Yes	4.9593	0.0642	389.0894	0.9067	5.4694	0.6101	0.6436	-1.06E-09	4.6974	0.2619	0.2888	200.4415
142	945.692	661.984	2.3550	1.2401	-1.1157	1.8241	Yes	5.0023	0.0639	390.0921	0.9044	5.5311	0.6080	0.6421	-1.09E-09	4.7398	0.2625	0.2903	200.7318
143	959.058	671.341	2.3716	1.2437	-1.1254	1.8181	Yes	5.0455	0.0637	391.0984	0.9021	5.5932	0.6060	0.6406	-1.11E-09	4.7823	0.2631	0.2917	201.0235
144	972.518	680.763	2.3882	1.2472	-1.1351	1.8120	Yes	5.0887	0.0635	392.1082	0.8998	5.6557	0.6040	0.6391	-1.14E-09	4.8250	0.2638	0.2932	201.3166
145	986.073	690.251	2.4048	1.2508	-1.1448	1.8059	Yes	5.1321	0.0633	393.1215	0.8974	5.7187	0.6020	0.6376	-1.16E-09	4.8677	0.2644	0.2946	201.6113
146	999.720	699.804	2.4214	1.2543	-1.1545	1.7998	Yes	5.1757	0.0631	394.1383	0.8951	5.7821	0.5999	0.6361	-1.19E-09	4.9106	0.2651	0.2961	201.9074
147	1013.462	709.423	2.4380	1.2577	-1.1642	1.7936	Yes	5.2193	0.0628	395.1586	0.8928	5.8459	0.5979	0.6346	-1.22E-09	4.9536	0.2657	0.2976	202.2050
148	1027.298	719.108	2.4546	1.2612	-1.1739	1.7874	Yes	5.2630	0.0626	396.1823	0.8905	5.9102	0.5958	0.6331	-1.25E-09	4.9967	0.2664	0.2991	202.5041
149	1041.227	728.859	2.4711	1.2648	-1.1837	1.7812	Yes	5.3069	0.0624	397.2096	0.8882	5.9749	0.5937	0.6316	-1.28E-09	5.0399	0.2670	0.3006	202.8047
150	1055.250	738.675	2.4877	1.2680	-1.1934	1.7749	Yes	5.3509	0.0622	398.2402	0.8859	6.0401	0.5916	0.6301	-1.30E-09	5.0832	0.2677	0.3022	203.1069
151	1069.367	748.557	2.5043	1.2714	-1.2032	1.7686	Yes	5.3950	0.0620	399.2744	0.8836	6.1056	0.5895	0.6286	-1.34E-09	5.1266	0.2684	0.3037	203.4106
152	1083.578	758.504	2.5209	1.2747	-1.2129	1.7623	Yes	5.4392	0.0618	400.3119	0.8813	6.1717	0.5874	0.6271	-1.37E-09	5.1701	0.2691	0.3053	203.7159
153	1097.882	768.517	2.5375	1.2780	-1.2227	1.7559	Yes	5.4835	0.0616	401.3529	0.8790	6.2381	0.5853	0.6255	-1.40E-09	5.2137	0.2698	0.3069	204.0228
154	1112.280	778.596	2.5541	1.2813	-1.2325	1.7495	Yes	5.5279	0.0614	402.3973	0.8767	6.3050	0.5832	0.6240	-1.43E-09	5.2574	0.2705	0.3085	204.3313
155	1126.773	788.741	2.5707	1.2846	-1.2423	1.7431	Yes	5.5724	0.0612	403.4450	0.8745	6.3723	0.5810	0.6225	-1.46E-09	5.3013	0.2712	0.3101	204.6414
156	1141.358	798.951	2.5872	1.2878	-1.2521	1.7366	Yes	5.6170	0.0610	404.4962	0.8722	6.4401	0.5789	0.6210	-1.50E-09	5.3452	0.2719	0.3117	204.9531
157	1156.038	809.227	2.6038	1.2910	-1.2619	1.7301	Yes	5.6618	0.0608	405.5507	0.8699	6.5083	0.5767	0.6195	-1.53E-09	5.3892	0.2726	0.3133	205.2664
158	1170.812	819.568	2.6204	1.2942	-1.2717	1.7236	Yes	5.7066	0.0606	406.6086	0.8677	6.5769	0.5745	0.6179	-1.56E-09	5.4333	0.2733	0.3150	205.5814
159	1185.679	829.975	2.6370	1.2973	-1.2815	1.7171	Yes	5.7515	0.0604	407.6699	0.8654	6.6460	0.5724	0.6164	-1.60E-09	5.4775	0.2740	0.3167	205.8981
160	1200.640	840.448	2.6536	1.3005	-1.2914	1.7105	Yes	5.7965	0.0602	408.7345	0.8632	6.7155	0.5702	0.6149	-1.64E-09	5.5218	0.2748	0.3183	206.2164

t (s)	$Q = \alpha t^2$ (KW)	Qc (KW)	D (m)	L (m)	Z_o (m)	Z (m)	*IS* ($Z_o > L$) ?	M_{ent} (kg/s)	h_k (KW/mK)	T_g (°K)	$\rho_{U,L}$ (Kg/m^3)	V_{ent} (m^3/s)	D_F Z/H_o	N_F	Equation for N_F	Mass Flow Out (kg/s)	M_{ent} less M_{out} (kg/s)	$V_{remaining\ in\ compt.}$ (m^3/s)	Smoke Volume (m^3)
161	1215.695	850.986	2.8702	1.3038	-1.3012	1.7038	Yes	5.8417	0.0601	409.8024	0.8609	6.7855	0.5679	0.6134	-1.67E-09	5.5861	0.2755	0.3200	206.5364
162	1230.844	861.591	2.8867	1.3067	-1.3111	1.6972	Yes	5.8869	0.0300	440.8833	0.8002	7.3586	0.5657	0.6096	1.60E-09	5.9166	-0.0297	-0.0372	206.4993
163	1246.086	872.260	2.7033	1.3097	-1.3209	1.6979	Yes	5.9498	0.0300	442.0852	0.7980	7.4556	0.5660	0.6097	3.08E-11	5.9228	0.0270	0.0339	206.5331
164	1261.422	882.996	2.7199	1.3128	-1.3308	1.6972	Yes	6.0096	0.0300	443.2896	0.7959	7.5511	0.5657	0.6095	5.28E-10	5.9363	0.0734	0.0922	206.6253
165	1276.853	893.797	2.7365	1.3158	-1.3407	1.6953	Yes	6.0669	0.0300	444.4964	0.7937	7.6437	0.5651	0.6090	-2.01E-11	5.9558	0.1111	0.1400	206.7653
166	1292.376	904.663	2.7531	1.3187	-1.3506	1.6924	Yes	6.1220	0.0300	445.7057	0.7916	7.7342	0.5641	0.6083	-8.47E-11	5.9802	0.1418	0.1791	206.9444
167	1307.994	915.596	2.7697	1.3217	-1.3605	1.6887	Yes	6.1755	0.0300	446.9174	0.7894	7.8229	0.5629	0.6073	-2.05E-10	6.0087	0.1668	0.2112	207.1557
168	1323.706	926.594	2.7863	1.3246	-1.3704	1.6843	Yes	6.2275	0.0300	448.1315	0.7873	7.9103	0.5614	0.6063	-3.75E-10	6.0405	0.1870	0.2376	207.3933
169	1339.511	937.658	2.8028	1.3276	-1.3803	1.6793	Yes	6.2785	0.0300	449.3481	0.7851	7.9967	0.5598	0.6051	-5.80E-10	6.0750	0.2035	0.2592	207.6525
170	1355.410	948.787	2.8194	1.3304	-1.3902	1.6739	Yes	6.3286	0.0300	450.5670	0.7830	8.0823	0.5580	0.6039	-8.03E-10	6.1116	0.2170	0.2771	207.9296
171	1371.403	959.982	2.8360	1.3333	-1.4001	1.6681	Yes	6.3780	0.0300	451.7883	0.7809	8.1675	0.5560	0.6025	-1.03E-09	6.1501	0.2279	0.2918	208.2214
172	1387.490	971.243	2.8526	1.3362	-1.4101	1.6621	Yes	6.4268	0.0300	453.0120	0.7788	8.2523	0.5540	0.6011	-1.25E-09	6.1899	0.2368	0.3041	208.5255
173	1403.670	982.569	2.8692	1.3390	-1.4200	1.6557	Yes	6.4751	0.0300	454.2381	0.7767	8.3369	0.5519	0.5997	-1.47E-09	6.2310	0.2441	0.3143	208.8399
174	1419.944	993.961	2.8858	1.3418	-1.4300	1.6492	Yes	6.5232	0.0300	455.4666	0.7746	8.4214	0.5497	0.5982	-1.66E-09	6.2730	0.2501	0.3229	209.1628
175	1436.313	1005.419	2.9023	1.3445	-1.4399	1.6424	Yes	6.5709	0.0300	456.6974	0.7725	8.5060	0.5475	0.5967	-1.84E-09	6.3158	0.2551	0.3302	209.4930
176	1452.774	1016.942	2.9189	1.3473	-1.4499	1.6356	Yes	6.6185	0.0300	457.9305	0.7704	8.5907	0.5452	0.5951	-2.00E-09	6.3592	0.2592	0.3365	209.8295
177	1469.330	1028.531	2.9355	1.3500	-1.4599	1.6286	Yes	6.6659	0.0300	459.1660	0.7683	8.6756	0.5429	0.5935	-2.15E-09	6.4032	0.2627	0.3419	210.1714

Sample Calculations provided for shaded cells

Appendix C

Sample Calculations For Detector Activation

(Refer Example In Chapter 3-Section 9)

Using a Fast Response Sprinkler With,

User Inputs

RTI=30

T_{act}=93

R_D=1m

This will activate when Temperature of detector exceeds 93°C

This particular scenario activates at 177s, therefore calculations provided here are at t = 177s.

From equations, the solutions to the dimensionless correlations are:

From equation 4.13,

$$A_{H,D} = g / (c_p T_\infty \rho_\infty)$$

$$= 9.81 / (1.05 \times 295 \times 1.2)$$

$$= 0.026392$$

From equation 4.14,

$$t_f^* = 0.954(1 + R_D / H)$$

$$= 0.954(1 + 1/6)$$

$$= 0.1130$$

From equation 4.10,

$$t_2^* = t / (A_{H,D}^{-1/5} \alpha^{-1/5} H^{4/5})$$

$$= 177 / ((0.026392)^{-1/5} (0.0469)^{-1/5} (6)^{4/5})$$

$$= 11.0658$$

From equation 4.8, as $t_2^* > t_f^*$,

$$\Delta T_2^* = \left[\frac{t_2^* - t_f^*}{0.118 + 0.313 R_D / H} \right]^{4/3}$$

$$= \left[\frac{(11.0658 - 1.1130)}{0.118 + 0.313(1/6)} \right]^{4/3}$$

$$= 143.4091$$

From equation 4.9,

$$U_2^* = 0.59 \left(\frac{R_D}{H} \right)^{-0.63} \sqrt{\Delta T_2^*}$$

$$= 0.59 \left(\frac{1}{6} \right)^{-0.63} \sqrt{143.4091}$$

$$= 21.8462$$

From equation 4.12,

$$T = \Delta T_2^* \left[A_{H,D}^{2/5} (T_\infty / g) \alpha^{2/5} H^{-3/5} \right] + T_\infty$$

$$= 143.4091 \left[(0.026392)^{2/5} (295 / 9.81) (0.0469)^{2/5} (6)^{-3/5} \right] + 22$$

$$= 123.1340 \text{ °C}$$

From equation 4.11,

$$U = U_2^*(A_{H,D}{}^{1/5}\alpha^{1/5}H^{1/5})$$

$$= 21.8462((0.026392)^{1/5}(0.0469)^{1/5}(6)^{1/5})$$

$$= 8.1947 \text{ m/s}$$

From equation 4.17,

$$Y = .75\left(\frac{U}{U_2^*}\right)^{1/2}\left(\frac{U_2^*}{\Delta T_2^*}\right)^{1/2}\left(\frac{\Delta T_2^*}{RTI}\right)\left(\frac{t}{t_2^*}\right)(0.188 + 0.313R/H)$$

$$= .75\left(\frac{8.1947}{21.8462}\right)^{1/2}\left(\frac{21.8462}{143.4091}\right)^{1/2}\left(\frac{143.4091}{30}\right)\left(\frac{177}{11.0658}\right)(0.188 + 0.313(1/6))$$

$$= 3.2928$$

From equation 4.16,

$$T_{D,t} = T_\infty + \left(\frac{\Delta T}{\Delta T_2^*}\right)\Delta T_2^*\left[1 - \frac{(1 - e^{-Y})}{Y}\right]$$

$$= 22 + \left(\frac{123.1340 - 22}{143.4091}\right)(143.4091)\left[1 - \frac{(1 - e^{-3.2928})}{3.2928}\right]$$

$$= 93.5613$$

As $T_{D,t} > T_{ACTIVATION}$ the fast response sprinkler will activate.

Detector Activation for a t^2 Fire In a Compartment

Adjustable Variables In Bold Red

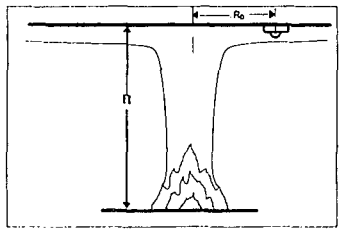

Table 1	
Fire Type	**α**
Slow	0.00293
Medium	0.01172
Fast	0.0469
U Fast	0.1876

Table 2	
Compartment dimensions	
Area (m^2)	**48**
Height (m)	**6**
A_o (m^2)	**12**
H_o (m)	**3**
A_T (m^2)	**252**
δ (m)	**0.016**

Table 3: Thermal Properties	
Material =>	**Gypsum Plaster**
k (KW/mK)	**4.80E-04**
ρ_c (Kg/m^3)	**0.84**
c (KJ/Kg.K)	**1440**

Table 4	
Ambient Conditions	
g (m/s^2)	**9.81**
C_p (KJ/Kg.K)	**1.05**
ρ (Kg/m^3)	**1.2**
T (K)	**295**

Table 5	
Sprinkler Properties	
RTI ((m/s)^.5)	**30**
Tact (°K)	**93**
R_O (m)	**1**

$A_{H,D}$	0.02639225
t_i^*	1.113

Thermal Penetration time (t_p)	161.28

Using α = 0.0469

			FPEtool With Alpert's Correlations					Accounting For Transport Lag, Beyler & Heskestad							
t (s)	$Q = \alpha t^2$ (KW)	h_k (KW/mK)	T_{CJ} (°C)	U_{CJ} (m/s)	τ	$T_{Detector}$ (°C)	Sprinkler Activated ?	t_2^*	ΔT_2^*	U_2^*	T (°C)	U (m/s)	Y	$T_{Detector}$ (°C)	Sprinkler Activated ?
0	0	#DIV/0!	22	0	#DIV/0!	22	No	0	0	0	22	0	#DIV/0!	#DIV/0!	#DIV/0!
1	0.0469	0.76198	22.1109	0.1723	72.28319	22.00152421	No	0.062518544	0	0	22	0	#DIV/0!	#DIV/0!	#DIV/0!
2	0.1876	0.5388	22.2795	0.2734	57.37121	22.00632827	No	0.125037089	0	0	22	0	#DIV/0!	#DIV/0!	#DIV/0!
3	0.4221	0.43993	22.48	0.3583	50.11837	22.01568575	No	0.187555633	0	0	22	0	#DIV/0!	#DIV/0!	#DIV/0!
4	0.7504	0.38099	22.7044	0.4341	45.53556	22.03064601	No	0.250074177	0	0	22	0	#DIV/0!	#DIV/0!	#DIV/0!
5	1.1725	0.34077	22.9485	0.5037	42.27147	22.05210481	No	0.312592722	0	0	22	0	#DIV/0!	#DIV/0!	#DIV/0!
6	1.6884	0.31108	23.2095	0.5688	39.77897	22.08083864	No	0.375111266	0	0	22	0	#DIV/0!	#DIV/0!	#DIV/0!
7	2.2981	0.288	23.4855	0.6303	37.78661	22.11752529	No	0.43762981	0	0	22	0	#DIV/0!	#DIV/0!	#DIV/0!
8	3.0016	0.2694	23.775	0.689	36.1416	22.16275776	No	0.500148355	0	0	22	0	#DIV/0!	#DIV/0!	#DIV/0!
9	3.7989	0.25399	24.0769	0.7453	34.75013	22.21705454	No	0.562666899	0	0	22	0	#DIV/0!	#DIV/0!	#DIV/0!
10	4.69	0.24096	24.3901	0.7995	33.55089	22.28086755	No	0.625185443	0	0	22	0	#DIV/0!	#DIV/0!	#DIV/0!
11	5.6749	0.22974	24.714	0.852	32.50173	22.35458867	No	0.687703988	0	0	22	0	#DIV/0!	#DIV/0!	#DIV/0!
12	6.7536	0.21996	25.0478	0.9029	31.57259	22.43855522	No	0.750222532	0	0	22	0	#DIV/0!	#DIV/0!	#DIV/0!
13	7.9261	0.21133	25.3911	0.9524	30.74135	22.53305472	No	0.812741076	0	0	22	0	#DIV/0!	#DIV/0!	#DIV/0!
14	9.1924	0.20365	25.7433	1.0006	29.99126	22.63832905	No	0.875259621	0	0	22	0	#DIV/0!	#DIV/0!	#DIV/0!
15	10.5525	0.19674	26.104	1.0477	29.3094	22.75457819	No	0.937778165	0	0	22	0	#DIV/0!	#DIV/0!	#DIV/0!
16	12.0064	0.19049	26.4728	1.0937	28.6856	22.88196363	No	1.000296709	0	0	22	0	#DIV/0!	#DIV/0!	#DIV/0!
17	13.5541	0.18481	26.8493	1.1389	28.11174	23.02061146	No	1.062815254	0	0	22	0	#DIV/0!	#DIV/0!	#DIV/0!

Fast Response Sprinkler For Example Of Section 3.9

			FPEtool With Alpert's Correlations					Accounting For Transport Lag, Beyler & Heskestad							
t (s)	$Q = \alpha t^2$ (KW)	h_k (KW/mK)	T_{CJ} (°C)	U_{CJ} (m/s)	τ	$T_{Detector}$ (°C)	Sprinkler Activated ?	t_2^*	ΔT_2^*	U_2^*	T (°C)	U (m/s)	Y	$T_{Detector}$ (°C)	Sprinkler Activated ?
18	15.1956	0.1796	27.2334	1.1831	27.5812	23.17061524	No	1.125333798	0.019088808	0.252044197	22.01346173	0.09454462	0.00407992	22.0000274	No
19	16.9309	0.17481	27.6246	1.2265	27.08857	23.33203862	No	1.187852342	0.211311705	0.838588836	22.14902033	0.31456412	0.02476055	22.0018298	No
20	18.76	0.17038	28.0227	1.2692	26.62936	23.50491782	No	1.250370887	0.474798453	1.257019303	22.33483532	0.4715221	0.04544118	22.0074937	No
21	20.6829	0.16628	28.4275	1.3111	26.19978	23.68926387	No	1.312889431	0.782893707	1.61413071	22.55210894	0.60547861	0.0661218	22.0178575	No
22	22.6996	0.16245	28.8388	1.3524	25.79664	23.88506482	No	1.375407975	1.125345124	1.935219209	22.79361105	0.72592253	0.08680243	22.0334683	No
23	24.8101	0.15888	29.2564	1.3931	25.41722	24.09228768	No	1.43792652	1.496338688	2.231527544	23.05524154	0.83707112	0.10748306	22.0547319	No
24	27.0144	0.15554	29.6801	1.4332	25.05918	24.31088032	No	1.500445064	1.892038065	2.509297963	23.33429495	0.94126594	0.12816369	22.0819653	No
25	29.3125	0.1524	30.1097	1.4727	24.7205	24.54077322	No	1.562963608	2.309685674	2.772450109	23.62882661	1.03997727	0.14884431	22.1154237	No
26	31.7044	0.14944	30.545	1.5118	24.39942	24.78188112	No	1.625482153	2.74718572	3.023648546	23.93735851	1.13420463	0.16952494	22.1553161	No
27	34.1901	0.14664	30.986	1.5503	24.0944	25.03410456	No	1.688000697	3.202881378	3.264808606	24.25872224	1.22466649	0.19020557	22.2018151	No
28	36.7696	0.144	31.4325	1.5883	23.80408	25.29733131	No	1.750519241	3.675423791	3.497365411	24.59196657	1.31190117	0.2108862	22.2550645	No
29	39.4429	0.1415	31.8843	1.6259	23.52726	25.57143776	No	1.813037786	4.163689508	3.722429381	24.93629922	1.3963252	0.23156682	22.3151839	No
30	42.21	0.13912	32.3414	1.6631	23.26289	25.85629015	No	1.87555633	4.666725616	3.940882015	25.29104818	1.47826924	0.25224745	22.3822727	No
31	45.0709	0.13685	32.8035	1.6998	23.01001	26.15174576	No	1.938074874	5.18371173	4.15343789	25.65563491	1.55800135	0.27292808	22.4564132	No
32	48.0256	0.1347	33.2707	1.7362	22.76778	26.45765407	No	2.000593419	5.713932742	4.36068646	26.02955509	1.63574262	0.29360871	22.5376727	No
33	51.0741	0.13264	33.7427	1.7722	22.53544	26.7738577	No	2.063111963	6.256758727	4.563121193	26.4123645	1.71167817	0.31428933	22.6261057	No
34	54.2164	0.13068	34.2195	1.8078	22.3123	27.10019346	No	2.125630508	6.811629783	4.761160449	26.80366828	1.78596492	0.33496996	22.7217554	No
35	57.4525	0.1288	34.7011	1.8431	22.09775	27.4364932	No	2.188149052	7.378044344	4.955162826	27.20311273	1.8587374	0.35565059	22.8246551	No
36	60.7824	0.127	35.1872	1.878	21.89121	27.78258464	No	2.250667596	7.955550019	5.145438654	27.6103788	1.93011201	0.37633122	22.9348291	No
37	64.2061	0.12527	35.6779	1.9127	21.69219	28.13829218	No	2.313186141	8.543736307	5.332258771	28.025177	2.00019034	0.39701184	23.0522939	No
38	67.7236	0.12361	36.173	1.947	21.50021	28.50343758	No	2.375704685	9.14222871	5.515861341	28.44724324	2.06906173	0.41769247	23.177059	No
39	71.3349	0.12201	36.6725	1.981	21.31486	28.87784062	No	2.438223229	9.750683935	5.696457204	28.87633542	2.13680527	0.4383731	23.3091275	No
40	75.04	0.12048	37.1762	2.0147	21.13573	29.26131973	No	2.500741774	10.36878593	5.874234146	29.31223065	2.20349141	0.45905373	23.4484968	No
41	78.8389	0.119	37.6842	2.0481	20.96248	29.65369255	No	2.563260318	10.99624257	6.049360344	29.75472293	2.26918322	0.47973435	23.5951592	No
42	82.7316	0.11758	38.1963	2.0813	20.79478	30.05477643	No	2.625778862	11.63278289	6.221987164	30.20362116	2.33393748	0.50041498	23.7491025	No
43	86.7181	0.1162	38.7125	2.1142	20.63231	30.46438892	No	2.688297407	12.27815477	6.392251461	30.65874754	2.39780554	0.52109561	23.9103101	No
44	90.7984	0.11487	39.2327	2.1469	20.4748	30.88234816	No	2.750815951	12.93212284	6.560277494	31.1199361	2.460834	0.54177624	24.0787618	No
45	94.9725	0.11359	39.7569	2.1793	20.322	31.30847335	No	2.813334495	13.59446686	6.726178516	31.5870315	2.52306534	0.56245686	24.2544337	No
46	99.2404	0.11235	40.2849	2.2114	20.17366	31.742585	No	2.87585304	14.26498013	6.890058114	32.05988799	2.58453842	0.58313749	24.437299	No
47	103.602	0.11115	40.8169	2.2434	20.02956	32.18450534	No	2.938371584	14.9434683	7.052011352	32.5383685	2.64528891	0.60381812	24.6273281	No
48	108.058	0.10998	41.3525	2.2751	19.88949	32.63405858	No	3.000890128	15.62974815	7.212125734	33.02234383	2.70534961	0.62449875	24.8244887	No
49	112.607	0.10885	41.892	2.3066	19.75325	33.09107113	No	3.063408673	16.32364665	7.370482036	33.51169194	2.76475085	0.64517937	25.0287461	No
50	117.25	0.10776	42.4351	2.3378	19.62068	33.55537188	No	3.125927217	17.02500006	7.527155022	34.00629738	2.82352065	0.66586	25.2400638	No
51	121.987	0.1067	42.9818	2.3689	19.49159	34.02679238	No	3.188445761	17.73365317	7.682214064	34.50605068	2.88168504	0.68654063	25.4584031	No
52	126.818	0.10567	43.5322	2.3998	19.36583	34.50516703	No	3.250964306	18.4494586	7.835723679	35.01084791	2.93926823	0.70722126	25.6837237	No
53	131.742	0.10467	44.086	2.4304	19.24326	34.99033321	No	3.31348285	19.1722762	7.987744003	35.52059023	2.99629277	0.72790188	25.9159837	No
54	136.76	0.10369	44.6434	2.4609	19.12374	35.48213143	No	3.376001394	19.90197248	8.138331201	36.03518351	3.05277972	0.74858251	26.1551397	No
55	141.873	0.10274	45.2042	2.4912	19.00713	35.98040544	No	3.438519939	20.63842015	8.287537834	36.55453797	3.10874881	0.76926314	26.4011473	No
56	147.078	0.10182	45.7684	2.5213	18.89331	36.48500234	No	3.501038483	21.38149761	8.435413179	37.07856786	3.16421852	0.78994377	26.6539606	No
57	152.378	0.10093	46.336	2.5512	18.78217	36.99577261	No	3.563557027	22.13108863	8.582003515	37.60719122	3.2192062	0.81062439	26.9135331	No
58	157.772	0.10005	46.9069	2.581	18.6736	37.51257023	No	3.626075572	22.88708193	8.727352378	38.14032957	3.2737282	0.83130502	27.179817	No
59	163.259	0.0992	47.4812	2.6106	18.5675	38.03525267	No	3.688594116	23.64937086	8.871500784	38.67790769	3.32779989	0.85198565	27.452764	No

Fast Response Sprinkler For Example Of Section 3.9

			FPEtool With Alpert's Correlations					Accounting For Transport Lag, Beyler & Heskestad							
t (s)	$Q = \alpha t^2$ (KW)	h_k (KW/mK)	T_{CJ} (°C)	U_{CJ} (m/s)	τ	$T_{Detector}$ (°C)	Sprinkler Activated ?	t_2^*	ΔT_2^*	U_2^*	T (°C)	U (m/s)	Y	$T_{Detector}$ (°C)	Sprinkler Activated ?
60	168.84	0.09837	48.0586	2.64	18.46376	38.56368097	No	3.75111266	24.41785311	9.014487437	39.21985344	3.3814358	0.87266628	27.7323248	No
61	174.515	0.09756	48.6393	2.6692	18.36231	39.09771973	No	3.813631205	25.19243044	9.156348909	39.76609753	3.43464963	0.8933469	28.0184498	No
62	180.284	0.09677	49.2232	2.6983	18.26306	39.63723713	No	3.876149749	25.97300838	9.2971198	40.31657336	3.48745438	0.91402753	28.3110886	No
63	186.146	0.096	49.8102	2.7273	18.16591	40.18210491	No	3.938668293	26.75949607	9.436832895	40.87121683	3.53986233	0.93470816	28.6101904	No
64	192.102	0.09525	50.4003	2.7561	18.0708	40.73219838	No	4.001186838	27.55180601	9.575519288	41.42996624	3.59188516	0.95538879	28.9157042	No
65	198.153	0.09451	50.9935	2.7847	17.97765	41.2873964	No	4.063705382	28.34985386	9.713208509	41.99276211	3.64353394	0.97606941	29.2275784	No
66	204.296	0.09379	51.5898	2.8132	17.88639	41.84758133	No	4.126223926	29.15355827	9.849928635	42.55954708	3.6948192	0.99675004	29.5457613	No
67	210.534	0.09309	52.1891	2.8415	17.79696	42.41263902	No	4.188742471	29.96284071	9.985706385	43.13026577	3.74575096	1.01743067	29.8702008	No
68	216.866	0.0924	52.7913	2.8697	17.70928	42.98245876	No	4.251261015	30.77762533	10.12056722	43.70486468	3.79633878	1.0381113	30.200845	No
69	223.291	0.09173	53.3966	2.8978	17.62332	43.5569332	No	4.313779559	31.59783881	10.25453541	44.2832921	3.84659176	1.05879192	30.5376415	No
70	229.81	0.09107	54.0047	2.9257	17.53899	44.13595838	No	4.376298104	32.42341021	10.38763413	44.86549802	3.89651859	1.07947255	30.880538	No
71	236.423	0.09043	54.6158	2.9535	17.45626	44.71943357	No	4.438816648	33.25427087	10.51988554	45.451434	3.94612758	1.10015318	31.2294823	No
72	243.13	0.0898	55.2297	2.9812	17.37507	45.3072613	No	4.501335192	34.0903543	10.65131079	46.04105316	3.99542667	1.12083381	31.5844219	No
73	249.93	0.08918	55.8465	3.0087	17.29536	45.89934724	No	4.563853737	34.93159603	10.78193015	46.63431004	4.04442347	1.14151443	31.9453047	No
74	256.824	0.08858	56.4661	3.0361	17.2171	46.49560015	No	4.626372281	35.77793358	10.91176304	47.23116057	4.09312525	1.16219506	32.3120785	No
75	263.813	0.08799	57.0885	3.0634	17.14024	47.09593184	No	4.688890825	36.62930631	11.04082806	47.83156199	4.14153899	1.18287569	32.6846912	No
76	270.894	0.0874	57.7137	3.0906	17.06473	47.70025703	No	4.75140937	37.48565536	11.16914305	48.43547279	4.18967139	1.20355632	33.063091	No
77	278.07	0.08684	58.3416	3.1177	16.99054	48.30849336	No	4.813927914	38.34692354	11.29672517	49.04285263	4.23752888	1.22423694	33.4472259	No
78	285.34	0.08628	58.9723	3.1446	16.91761	48.92056128	No	4.876446458	39.2130553	11.42359086	49.65366235	4.28511763	1.24491757	33.8370446	No
79	292.703	0.08573	59.6056	3.1714	16.84593	49.53638394	No	4.938965003	40.08399662	11.54975596	50.26786385	4.33244358	1.2655982	34.2324957	No
80	300.16	0.08519	60.2416	3.1981	16.77544	50.15588719	No	5.001483547	40.95969497	11.67523568	50.88542007	4.37951244	1.28627883	34.6335281	No
81	307.711	0.08466	60.8803	3.2247	16.70612	50.77899944	No	5.064002091	41.8400992	11.80004469	51.50629496	4.4263297	1.30695945	35.040091	No
82	315.356	0.08415	61.5216	3.2512	16.63793	51.40565162	No	5.126520636	42.72515954	11.9241971	52.13045341	4.47290067	1.32764008	35.4521338	No
83	323.094	0.08364	62.1656	3.2776	16.57084	52.03577711	No	5.18903918	43.61482752	12.0477065	52.75786124	4.51923044	1.34832071	35.8696063	No
84	330.926	0.08314	62.8121	3.3039	16.50482	52.66931162	No	5.251557724	44.50905588	12.17058603	53.38848512	4.56532393	1.36900134	36.2924585	No
85	338.853	0.08265	63.4612	3.33	16.43984	53.30619319	No	5.314076269	45.4077986	12.29284833	54.02229259	4.6111859	1.38968196	36.7206409	No
86	346.872	0.08217	64.1128	3.3561	16.37587	53.94636203	No	5.376594813	46.31101075	12.41450561	54.65925199	4.65682092	1.41036259	37.1541042	No
87	354.986	0.08169	64.767	3.3821	16.31289	54.58976054	No	5.439113357	47.21864855	12.5355697	55.29933242	4.70223342	1.43104322	37.5927994	No
88	363.194	0.08123	65.4237	3.4079	16.25086	55.23633316	No	5.501631902	48.13066924	12.65605197	55.94250373	4.74742768	1.45172385	38.036678	No
89	371.495	0.08077	66.0829	3.4337	16.18977	55.88602633	No	5.564150446	49.04703111	12.77596347	56.58873651	4.79240783	1.47240447	38.4856919	No
90	379.89	0.08032	66.7445	3.4594	16.12958	56.53878845	No	5.62666899	49.9676934	12.89531485	57.23800201	4.83717788	1.4930851	38.9397931	No
91	388.379	0.07988	67.4086	3.4849	16.07028	57.19456976	No	5.689187535	50.89261631	13.01411644	57.89027217	4.8817417	1.51376573	39.3989344	No
92	396.962	0.07944	68.0752	3.5104	16.01185	57.85332231	No	5.751706079	51.82176094	13.13237823	58.54551956	4.92610303	1.53444636	39.8630686	No
93	405.638	0.07901	68.7441	3.5358	15.95425	58.51499989	No	5.814224623	52.75508928	13.2501099	59.20371736	4.9702655	1.55512698	40.3321492	No
94	414.408	0.07859	69.4155	3.5611	15.89747	59.17955796	No	5.876743168	53.69256414	13.36732083	59.86483935	5.01423264	1.57580761	40.8061299	No
95	423.273	0.07818	70.0892	3.5863	15.84149	59.84695356	No	5.939261712	54.63414918	13.48402011	60.52885991	5.05800785	1.59648824	41.2849651	No
96	432.23	0.07777	70.7654	3.6115	15.7863	60.51714533	No	6.001780256	55.57980881	13.60021655	61.19575393	5.10159445	1.61716887	41.7686092	No
97	441.282	0.07737	71.4438	3.6365	15.73186	61.19009337	No	6.064298801	56.52950822	13.71591873	61.86549686	5.14499564	1.63784949	42.2570174	No
98	450.428	0.07697	72.1246	3.6614	15.67817	61.8657592	No	6.126817345	57.48321333	13.83113493	62.53806468	5.18821453	1.65853012	42.7501452	No
99	459.667	0.07658	72.8078	3.6863	15.6252	62.54410576	No	6.18933589	58.44089077	13.94587322	63.21343385	5.23125416	1.67921075	43.2479485	No
100	469	0.0762	73.4932	3.7111	15.57294	63.22509728	No	6.251854434	59.40250786	14.06014144	63.89158133	5.27411746	1.69989138	43.7503836	No
101	478.427	0.07582	74.1809	3.7358	15.52138	63.90869927	No	6.314372978	60.36803258	14.1739472	64.57248452	5.31680728	1.720572	44.2574074	No

Fast Response Sprinkler For Example Of Section 3.9

			FPEtool With Alpert's Correlations					Accounting For Transport Lag, Beyler & Heskestad							
t (s)	$Q = \alpha t^2$ (KW)	h_k (KW/mK)	T_{CJ} (°C)	U_{CJ} (m/s)	τ	$T_{Detector}$ (°C)	Sprinkler Activated ?	t_2^*	ΔT_2^*	U_2^*	T (°C)	U (m/s)	Y	$T_{Detector}$ (°C)	Sprinkler Activated ?
102	487.948	0.07545	74.8709	3.7604	15.47049	64.59487846	No	6.376891523	61.33743355	14.28729788	65.25612131	5.3593264	1.74125263	44.768977	No
103	497.562	0.07508	75.5632	3.7849	15.42026	65.28360278	No	6.439410067	62.31068002	14.40020069	65.94247	5.40167751	1.76193326	45.2850501	No
104	507.27	0.07472	76.2576	3.8094	15.37067	65.97484124	No	6.501928611	63.28774184	14.51266263	66.63150933	5.44386325	1.78261389	45.8055848	No
105	517.073	0.07436	76.9544	3.8338	15.32172	66.66856396	No	6.564447156	64.26858944	14.62469048	67.32321846	5.48588616	1.80329451	46.3305398	No
106	526.968	0.07401	77.6533	3.8581	15.27339	67.3647421	No	6.6269657	65.25319381	14.73629089	68.01757693	5.52774873	1.82397514	46.8598739	No
107	536.958	0.07366	78.3545	3.8823	15.22566	68.06334779	No	6.689484244	66.24152652	14.84747031	68.71456467	5.56945338	1.84465577	47.3935466	No
108	547.042	0.07332	79.0578	3.9065	15.17852	68.76435412	No	6.752002789	67.23355963	14.958235	69.414162	5.61100247	1.8653364	47.9315178	No
109	557.219	0.07298	79.7633	3.9305	15.13196	69.46773511	No	6.814521333	68.22926574	15.0685911	70.11634959	5.65239829	1.88601702	48.4737477	No
110	567.49	0.07265	80.4709	3.9545	15.08597	70.17346563	No	6.877039877	69.22861796	15.17854457	70.82110847	5.69364307	1.90669765	49.0201972	No
111	577.855	0.07232	81.1808	3.9785	15.04053	70.8815214	No	6.939558422	70.23158988	15.28810122	71.52842001	5.734739	1.92737828	49.5708275	No
112	588.314	0.072	81.8927	4.0023	14.99563	71.59187895	No	7.002076966	71.23815555	15.39726671	72.23826592	5.77568821	1.94805891	50.1256001	No
113	598.866	0.07168	82.6068	4.0261	14.95126	72.30451556	No	7.06459551	72.24828948	15.50604657	72.95062824	5.81649276	1.96873953	50.6844771	No
114	609.512	0.07137	83.3229	4.0498	14.90742	73.01940925	No	7.127114055	73.26196666	15.6144462	73.6654893	5.85715468	1.98942016	51.247421	No
115	620.253	0.07105	84.0412	4.0735	14.86408	73.73653875	No	7.189632599	74.27916248	15.72247086	74.38283176	5.89767595	2.01010079	51.8143948	No
116	631.086	0.07075	84.7616	4.0971	14.82124	74.45588347	No	7.252151143	75.29985276	15.83012568	75.10263858	5.93805849	2.03078142	52.3853618	No
117	642.014	0.07044	85.484	4.1206	14.7789	75.17742345	No	7.314669688	76.32401373	15.93741567	75.82489298	5.97830417	2.05146204	52.9602857	No
118	653.036	0.07015	86.2085	4.144	14.73703	75.90113936	No	7.377188232	77.35162204	16.04434574	76.5495785	6.01841484	2.07214267	53.5391309	No
119	664.151	0.06985	86.935	4.1674	14.69563	76.62701245	No	7.439706776	78.38265471	16.15092065	77.27667892	6.05839229	2.0928233	54.1218619	No
120	675.36	0.06956	87.6636	4.1907	14.6547	77.35502455	No	7.502225321	79.41708914	16.2571451	78.00617833	6.09823828	2.11350393	54.7084438	No
121	686.663	0.06927	88.3942	4.214	14.61422	78.08515802	No	7.564743865	80.4549031	16.36302363	78.73806103	6.13795451	2.13418455	55.298842	No
122	698.06	0.06899	89.1269	4.2372	14.57418	78.81739574	No	7.627262409	81.49607472	16.46856071	79.4723116	6.17754266	2.15486518	55.8930224	No
123	709.55	0.06871	89.8615	4.2603	14.53457	79.55172109	No	7.689780954	82.5405825	16.5737607	80.20891489	6.21700436	2.17554581	56.4909514	No
124	721.134	0.06843	90.5981	4.2833	14.4954	80.28811792	No	7.752299498	83.58840524	16.67862788	80.94785594	6.25634122	2.19622644	57.0925956	No
125	732.813	0.06815	91.3367	4.3063	14.45664	81.02657053	No	7.814818042	84.6395221	16.78316641	81.68912006	6.2955548	2.21690706	57.6979222	No
126	744.584	0.06788	92.0773	4.3293	14.41829	81.76706367	No	7.877336587	85.69391258	16.88738037	82.43269278	6.33464663	2.23758769	58.3068986	No
127	756.45	0.06761	92.8198	4.3521	14.38035	82.50958248	No	7.939855131	86.75155646	16.99127376	83.17855985	6.37361821	2.25826832	58.9194927	No
128	768.41	0.06735	93.5643	4.375	14.3428	83.25411253	No	8.002373675	87.81243385	17.09485048	83.92670724	6.41247101	2.27894895	59.5356729	No
129	780.463	0.06709	94.3107	4.3977	14.30564	84.00063974	No	8.06489222	88.87652516	17.19811437	84.67712115	6.45120645	2.29962957	60.1554078	No
130	792.61	0.06683	95.0591	4.4204	14.26887	84.74915042	No	8.127410764	89.9438111	17.30106916	85.42978795	6.48982596	2.3203102	60.7786665	No
131	804.851	0.06657	95.8094	4.4431	14.23247	85.4996312	No	8.189929308	91.01427264	17.40371853	86.18469424	6.52833089	2.34099083	61.4054185	No
132	817.186	0.06632	96.5616	4.4656	14.19644	86.25206909	No	8.252447853	92.08789107	17.50606606	86.94182681	6.5667226	2.36167146	62.0356336	No
133	829.614	0.06607	97.3157	4.4882	14.16077	87.00645137	No	8.314966397	93.16464792	17.60811528	87.70117265	6.60500242	2.38235208	62.6692821	No
134	842.136	0.06582	98.0717	4.5106	14.12545	87.76276566	No	8.377484941	94.244525	17.70986964	88.46271892	6.64317162	2.40303271	63.3063345	No
135	854.753	0.06558	98.8295	4.533	14.09049	88.52099986	No	8.440003486	95.32750439	17.8113325	89.22645299	6.68123149	2.42371334	63.9467618	No
136	867.462	0.06534	99.5893	4.5554	14.05587	89.28114215	No	8.50252203	96.41356841	17.9125072	89.9923624	6.71918325	2.44439397	64.5905353	No
137	880.266	0.0651	100.351	4.5777	14.02159	90.043181	No	8.565040574	97.50269964	18.01339696	90.76043484	6.75702814	2.46507459	65.2376267	No
138	893.164	0.06486	101.114	4.6	13.98764	90.8071051	No	8.627559119	98.59488091	18.11400498	91.53065822	6.79476734	2.48575522	65.8880081	No
139	906.155	0.06463	101.88	4.6222	13.95401	91.57290344	No	8.690077663	99.69009526	18.21433437	92.30302058	6.83240203	2.50643585	66.5416518	No
140	919.24	0.0644	102.647	4.6443	13.92071	92.3405652	No	8.752596207	100.788326	18.3143882	93.07751014	6.86993334	2.52711648	67.1985307	No
141	932.419	0.06417	103.416	4.6664	13.88772	93.11007982	Yes	8.815114752	101.8895566	18.41416946	93.85411528	6.90736242	2.5477971	67.8586178	No
142	945.692	0.06394	104.187	4.6884	13.85504	93.88143694	Yes	8.877633296	102.9937709	18.51368112	94.63282454	6.94469036	2.56847773	68.5218865	No
143	959.058	0.06372	104.959	4.7104	13.82267	94.65462643	Yes	8.94015184	104.1009528	18.61292604	95.4136266	6.98191825	2.58915836	69.1883106	No

Fast Response Sprinkler For Example Of Section 3.9

			FPEtool With Alpert's Correlations					Accounting For Transport Lag, Beyler & Heskestad							
t (s)	$Q = \alpha t^2$ (KW)	h_k (KW/mK)	T_{CJ} (°C)	U_{CJ} (m/s)	τ	$T_{Detector}$ (°C)	Sprinkler Activated ?	t_2^*	ΔT_2^*	U_2^*	T (°C)	U (m/s)	Y	$T_{Detector}$ (°C)	Sprinkler Activated ?
144	972.518	0.0635	105.734	4.7323	13.7906	95.42963835	Yes	9.002670385	105.2110865	18.71190708	96.19651031	7.01904715	2.60983899	69.8578643	No
145	986.073	0.06328	106.51	4.7542	13.75882	96.20646294	Yes	9.065188929	106.3241564	18.81062701	96.98146465	7.05607811	2.63051961	70.530522	No
146	999.72	0.06306	107.288	4.7761	13.72734	96.98509067	Yes	9.127707473	107.440147	18.90908858	97.76847876	7.09301216	2.65120024	71.2062584	No
147	1013.46	0.06285	108.068	4.7978	13.69614	97.76551214	Yes	9.190226018	108.5590432	19.00729446	98.55754191	7.12985029	2.67188087	71.8850487	No
148	1027.3	0.06263	108.849	4.8196	13.66522	98.54771816	Yes	9.252744562	109.6808299	19.10524729	99.34864351	7.1665935	2.6925615	72.5668683	No
149	1041.23	0.06242	109.632	4.8413	13.63458	99.33169968	Yes	9.315263106	110.8054923	19.20294965	100.1417731	7.20324275	2.71324212	73.2516928	No
150	1055.25	0.06222	110.417	4.8629	13.60422	100.1174478	Yes	9.377781651	111.9330158	19.3004041	100.9369204	7.23979902	2.73392275	73.9394985	No
151	1069.37	0.06201	111.204	4.8845	13.57412	100.9049539	Yes	9.440300195	113.063386	19.39761312	101.7340752	7.27626321	2.75460338	74.6302615	No
152	1083.58	0.0618	111.993	4.906	13.54429	101.6942093	Yes	9.502818739	114.1965885	19.49457917	102.5332274	7.31263627	2.77528401	75.3239586	No
153	1097.88	0.0616	112.783	4.9275	13.51471	102.4852056	Yes	9.565337284	115.3326094	19.59130466	103.3343672	7.3489191	2.79596463	76.0205667	No
154	1112.28	0.0614	113.575	4.949	13.4854	103.2779345	Yes	9.627855828	116.4714346	19.68779197	104.1374846	7.38511257	2.81664526	76.7200631	No
155	1126.77	0.0612	114.369	4.9704	13.45633	104.0723879	Yes	9.690374372	117.6130504	19.78404341	104.94257	7.42121757	2.83732589	77.4224253	No
156	1141.36	0.06101	115.164	4.9917	13.42752	104.8685577	Yes	9.752892917	118.7574433	19.88006129	105.7496138	7.45723496	2.85800652	78.1276311	No
157	1156.04	0.06081	115.961	5.013	13.39895	105.666436	Yes	9.815411461	119.9045998	19.97584785	106.5586066	7.49316558	2.87868714	78.8356588	No
158	1170.81	0.06062	116.76	5.0343	13.37062	106.466015	Yes	9.877930005	121.0545067	20.0714053	107.369539	7.52901025	2.89936777	79.5464867	No
159	1185.68	0.06043	117.561	5.0555	13.34253	107.2672871	Yes	9.94044855	122.207151	20.16673582	108.1824018	7.5647698	2.9200484	80.2600934	No
160	1200.64	0.06024	118.363	5.0767	13.31468	108.0702447	Yes	10.00296709	123.3625195	20.26184155	108.9971859	7.60044503	2.94072903	80.976458	No
161	1215.69	0.06005	119.167	5.0978	13.28705	108.8748803	Yes	10.06548564	124.5205996	20.35672459	109.8138822	7.63603673	2.96140965	81.6955596	No
162	1230.84	0.03	119.972	5.1189	13.25966	109.6811867	Yes	10.12800418	125.6813787	20.45138703	110.6324818	7.67154568	2.98209028	82.4173778	No
163	1246.09	0.03	120.779	5.14	13.23249	110.4891566	Yes	10.19052273	126.8448442	20.54583088	111.4529759	7.70697263	3.00277091	83.1418924	No
164	1261.42	0.03	121.588	5.161	13.20554	111.2987827	Yes	10.25304127	128.0109838	20.64005817	112.2753559	7.74231835	3.02345154	83.8690834	No
165	1276.85	0.03	122.399	5.1819	13.1788	112.1100582	Yes	10.31555982	129.1797852	20.73407086	113.099613	7.77758357	3.04413216	84.598931	No
166	1292.38	0.03	123.211	5.2028	13.15229	112.922976	Yes	10.37807836	130.3512365	20.82787089	113.9257388	7.81276902	3.06481279	85.3314158	No
167	1307.99	0.03	124.025	5.2237	13.12598	113.7375293	Yes	10.4405969	131.5253256	20.92146018	114.7537249	7.84787542	3.08549342	86.0665186	No
168	1323.71	0.03	124.84	5.2445	13.09989	114.5537113	Yes	10.50311545	132.7020408	21.01484061	115.583563	7.88290347	3.10617405	86.8042204	No
169	1339.51	0.03	125.657	5.2653	13.074	115.3715153	Yes	10.56563399	133.8813704	21.10801402	116.4152447	7.91785386	3.12685467	87.5445026	No
170	1355.41	0.03	126.476	5.2861	13.04831	116.1909347	Yes	10.62815254	135.0633029	21.20098225	117.2487621	7.95272729	3.1475353	88.2873466	No
171	1371.4	0.03	127.296	5.3068	13.02283	117.011963	Yes	10.69067108	136.2478268	21.29374708	118.0841069	7.98752443	3.16821593	89.0327341	No
172	1387.49	0.03	128.118	5.3275	12.99754	117.8345937	Yes	10.75318963	137.4349309	21.38631029	118.9212714	8.02224593	3.18889656	89.7806473	No
173	1403.67	0.03	128.941	5.3481	12.97245	118.6588205	Yes	10.81570817	138.624604	21.47867361	119.7602475	8.05689245	3.20957718	90.5310683	No
174	1419.94	0.03	129.766	5.3687	12.94755	119.484637	Yes	10.87822671	139.816835	21.57083877	120.6010275	8.09146464	3.23025781	91.2839796	No
175	1436.31	0.03	130.593	5.3892	12.92284	120.3120372	Yes	10.94074526	141.011613	21.66280746	121.4436038	8.12596313	3.25093844	92.0393639	No
176	1452.77	0.03	131.421	5.4097	12.89832	121.1410146	Yes	11.0032638	142.2089273	21.75458133	122.2879686	8.16038854	3.27161907	92.7972041	No
177	1469.33	0.03	132.251	5.4302	12.87398	121.9715634	Yes	11.06578235	143.408767	21.84616202	123.1341144	8.19474149	3.29229969	93.5574832	Yes
178	1485.98	0.03	133.082	5.4506	12.84983	122.8036775	Yes	11.12830089	144.6111217	21.93755117	123.9820338	8.22902259	3.31298032	94.3201847	Yes
179	1502.72	0.03	133.915	5.471	12.82585	123.637351	Yes	11.19081944	145.8159808	22.02875034	124.8317193	8.26323243	3.33366095	95.0852921	Yes
180	1519.56	0.03	134.749	5.4914	12.80206	124.4725779	Yes	11.25333798	147.0233339	22.11976113	125.6831637	8.2973716	3.35434158	95.8527891	Yes
181	1536.49	0.03	135.585	5.5117	12.77844	125.3093524	Yes	11.31585653	148.2331709	22.21058507	126.5363598	8.33144068	3.3750222	96.6226598	Yes
182	1553.52	0.03	136.423	5.532	12.75499	126.1476688	Yes	11.37837507	149.4454815	22.30122368	127.3913003	8.36544025	3.39570283	97.3948883	Yes
183	1570.63	0.03	137.262	5.5522	12.73172	126.9875213	Yes	11.44089361	150.6602558	22.39167848	128.2479781	8.39937086	3.41638346	98.1694589	Yes
184	1587.85	0.03	138.102	5.5725	12.70861	127.8289044	Yes	11.50341216	151.8774836	22.48195094	129.1063863	8.43323308	3.43706409	98.9463563	Yes

FIRE ENGINEERING RESEARCH REPORTS

95/1	Full Residential Scale Backdraft	I. B. Bolliger
95/2	A Study of Full Scale Room Fire Experiments	P. A. Enright
95/3	Design of Load-bearing Light Steel Frame Walls for Fire Resistance	J. T. Gerlich
95/4	Full Scale Limited Ventilation Fire Experiments	D. J. Millar
95/5	An Analysis of Domestic Sprinkler Systems for Use in New Zealand	F. Rahmanian
96/1	The Influence of Non-Uniform Electric Fields on Combustion Processes	M. A. Belsham
96/2	Mixing in Fire Induced Doorway Flows	J. M. Clements
96/3	Fire Design of Single Storey Industrial Buildings	B. W. Cosgrove
96/4	Modelling Smoke Flow Using Computational Fluid Dynamics	T. N. Kardos
96/5	Under-Ventilated Compartment Fires - A Precursor to Smoke Explosions	A. R. Parkes
96/6	An Investigation of the Effects of Sprinklers on Compartment Fires	M. W. Radford
97/1	Sprinkler Trade Off Clauses in the Approved Documents	G.J. Barnes
97/2	Risk Ranking of Buildings for Life Safety	J.W. Boyes
97/3	Improving the Waking Effectiveness of Fire Alarms in Residential Areas	T. Grace
97/4	Study of Evacuation Movement through Different Building Components	P. Holmberg
97/5	Domestic Fire Hazard in New Zealand	K.D.J. Irwin
97/6	An Appraisal of Existing Room-Corner Fire Models	D.C. Robertson
97/7	Fire Resistance of Light Timber Framed Walls and Floors	G.C. Thomas
97/8	Uncertainty Analysis of Zone Fire Models	A.M. Walker

School of Engineering
University of Canterbury
Private Bag 4800, Christchurch, New Zealand

Phone 643 366-7001
Fax 643 364-2758